Aus dem Institut für Anatomie I der Heinrich-Heine-Universität Düsseldorf

Direktorin: Univ.-Prof. Dr. med. Dr. rer. pol. Svenja Caspers

Und aus dem Institut für Arbeits- , Sozial- und Umweltmedizin der Heinrich-Heine-Universität Düsseldorf

Direktor: Univ.-Prof. Dr. med. Peter Angerer

Long-Term Air Pollution, Chronic Noise, and Brain Structure

-

Analysis in a Fronto-Parietal Resting State Network

in a Cohort of Older Adults

Dissertation

Zur Erlangung des Grades eines Doktors der Medizin

der Medizinischen Fakultät der Heinrich-Heine-Universität Düsseldorf

vorgelegt von

René Nußbaum

2020

Als Inauguraldissertation gedruckt mit Genehmigung der Medizinischen Fakultät der Heinrich-Heine-Universität Düsseldorf

gez.:

Dekan: Prof. Dr. med Nikolaj Klöcker

Erstgutachterin: Univ.-Prof. Dr. med. Dr. rer. pol. Svenja Caspers

Zweitgutachter: Univ.-Prof. Dr. sc. hum. Oliver Kuß

Own Publications

“Associations between Long-Term Air Pollution, Chronic Noise, and Brain Structure in a Fronto-Parietal Network in a Cohort of Older Adults” – René Nußbaum, Sarah Lucht, Christiane Jockwitz, Susanne Moebus, Miriam Engel, Karl-Heinz Jöckel, Svenja Caspers, Barbara Hoffmann, submitted for publication in Environmental Health Perspectives in 2019

Parts in this dissertation are included from this, my own publication. All content overlapping paragraphs as well as reused tables and figures are marked as such with the citation of my previous publication.

Zusammenfassung

Trotz der Bedeutung für das Verständnis der Zusammenhänge von Luftverschmutzung und Lärmbelastung und dem Verlust neurokognitiver Leistungsfähigkeit sind Studien begrenzt, die diese Expositionen und die Hirnstruktur untersuchen.

Ziel der vorliegenden Studie war es, die Assoziationen zwischen Langzeit-Luftverschmutzung und -Lärmbelastung, neurokognitiver Testleistung und lokaler Hirnatrophie bei älteren Erwachsenen, gemessen mittels des lokalen Gyrifizierungsindex (lGI), zu untersuchen.

Für n = 615 Teilnehmer der bevölkerungsbasierten 1000BRAINS-Studie, die auf der Heinz Nixdorf Recall-Studie basiert, wurde die Exposition gegenüber Feinstaub (PM_{10}, $PM_{2.5}$, $PM_{2.5abs}$), die Partikelanzahl im Akkumulationsmodus (PN_{AM}), Stickoxide (NO_X, NO_2) und die Entfernung zur nächstgelegenen Hauptstraße mithilfe der ESCAPE-Landnutzungsregression und der räumlich-zeitlichen EURopean Air Pollution Dispersion (EURAD) –Transportmodelle bestimmt. Gewichteter 24-Stunden- sowie Nachtlärm wurden gemäß der europäischen Lärmschutzrichtlinie modelliert. Es wurden die Assoziationen zwischen Luftverschmutzung und Lärmbelastung an der Wohnadresse in den Jahren 2006-2008 und der neurokognitiven Testleistung, die von 2011 bis 2015 erfasst wurden, unter Verwendung linearer Regression und unter Berücksichtigung demografischer und persönlicher Merkmale analysiert. Hierdurch wurden Hirnregionen mit potenzieller Relevanz identifiziert. Die lGI-Werte in diesen Regionen wurden mit Magnetresonanztomographie (MRT) (durchgeführt von 2011-2015) erfasst. Mit Hilfe der linearen Regression wurden die Assoziationen zwischen Umweltexpositionen und lGI-Werten (n = 590) unter Berücksichtigung demografischer und Lebensstilvariablen geschätzt.

Luftverschmutzung und Lärmbelastung zeigten eine Assoziation mit der Sprache und dem Kurzzeit- / Arbeitsgedächtnis sowie mit der Gehirnstruktur des Fronto-Parietal-Netzwerks (FPN), einem funktionalen Ruhenetzwerk, das mit diesen kognitiven Prozessen assoziiert ist. Luftverschmutzung war mit niedrigeren lGI-Werten in posterioren Regionen des FPN assoziiert (z. B. -0,02 [95% Konfidenzintervall (CI): -0,04, 0,00] pro 2 ug / m³ PM_{10} im posterioren parietalen Kortex und Precuneus). Im rechten dorsolateralen präfrontalen Kortex waren gewichteter 24-Stunden- sowie Nachtlärm mit höheren lGI-Werten assoziiert (z. B. 0,02 [95% CI: 0,00, 0,04] für 10 dB[A] 24-Stunden-Lärm).

Langzeit-Luftverschmutzung und Lärmexposition waren bei älteren Erwachsenen mit Unterschieden in der Gehirnstruktur des rechtshemisphärischen FPN verbunden, was entsprechend bekannten Theorien zur Gehirnalterung darauf hindeutet, dass Luftverschmutzung und Lärmexposition den Alterungsprozess des Gehirns beeinflussen können.

Abstract

Despite importance for understanding associations of air pollution (AP) and noise exposure with loss of neurocognitive performance, studies investigating these exposures and brain structure are limited.

The objective of this thesis was to estimate associations between long-term AP and noise exposures, neurocognitive test performance, and local Gyrification Indices (lGI), a marker for local brain atrophy, among older adults.

For n=615 participants from the population-based 1000BRAINS study, which is based on the Heinz Nixdorf Recall study, residential exposures to particulate matter (PM10, PM2.5, PM2.5abs), accumulation mode particle number (PNAM), nitrogen oxides (NOX, NO2), and distance to the nearest major road were assessed using the ESCAPE land use regression and spatiotemporal EURopean Air pollution Dispersion (EURAD) chemistry transport models. Weighted 24h and nighttime noise were modeled according to the European noise directive. Associations between AP and noise exposures at the 2006-2008 residential address and neurocognitive test performance were assessed 2011-2015, using linear regression, adjusting for demographic and personal characteristics. Brain regions of potential relevance were identified and lGI values in those regions were quantified using magnetic resonance imaging (MRI) data from 2011-2015. Using linear regression associations between environmental exposures and lGI values (n=590) were estimated, adjusting for demographic and lifestyle variables.

AP and noise exposure were associated with language and short-term/working memory and with brain structure of the fronto-parietal network (FPN), a functional resting-state network associated with these cognitive processes. AP exposure was associated with lower lGI values in posterior regions of the FPN (e.g., -0.02 [95% confidence interval (CI): -0.04, 0.00] per 2 µg/m3 PM10 in the posterior parietal cortex and precuneus). In the right dorsolateral prefrontal cortex, weighted 24h and nighttime noise were associated with higher lGI values (e.g., 0.02 [95% CI: 0.00, 0.04] for 10 dB[A] 24h noise).

Long-term AP and noise exposures were associated with differences in brain structure of the right hemispheric FPN in older adults, indicating AP and noise exposure may influence the physiological aging process of the brain.

Abbreviations

AP	air pollution
ATP	adenosine triphosphate
BC	black carbon
BET	brain extraction
BMI	body mass index
CES-D	Center for Epidemiologic Studies Depression scale
CHD	coronary heart disease
dB[A]	decibel
$Dist_{majroad}$	distance to the nearest major road
DLPFC	dorsolateral prefrontal cortex
EC	elemental carbon
EEG	electroencephalography
EPI	echo planar imaging
ESCAPE	European Study of Cohorts for AP Effects
ETS	environmental tobacco smoke
EURAD	EURopean Air Pollution Dispersion
FMRIB	Functional Magnetic Resonance Imaging of the Brain
FoV	field of view
FPN	fronto-parietal network
FSL	Functional Magnetic Resonance Imaging of the Brain Software Library
FU1	first follow up
(l)GI	(local) gyrification index
GMV	grey matter volume
HNR	Heinz Nixdorf RECALL
IPL	inferior parietal lobule
IQR	interquartile range
ISCED	International Standard Classification of Education
IUTA	Institute of Energy and Environmental Technology
kcal	kilocalories
LANUV	State Office for Nature, Environment and Consumer Protection of North-Rhine-Westphalia
lh	left hemisphere
L_{DEN}	weighted 24h noise
L_{night}	nighttime noise
LUR	land use regression
MELODIC	Multivariate Exploratory Linear Optimized Decomposition into Independent Components
MPRAGE	magnetization-prepared rapid acquisition gradient-echo
(f)MRI	(functional) magnetic resonance imaging
mRNA	messenger ribonucleic acid
NMDA	N-Methyl-D-Aspartat
NO	nitrogen monoxide
NO_2	nitrogen dioxide
NO_X	nitrogen oxides
PASA	posterior-anterior shift in aging theory

PCC/P	posterior cingulate cortex and precuneus
PM	particulate matter
$PM_{2.5}$	particulate matter with an average aerodynamic diameter below 2.5 micrometer
$PM_{2.5\ abs}$	$PM_{2.5}$ absorbance
PM_{10}	particulate matter with an average aerodynamic diameter below 10 micrometer
PN_{AM}	accumulation mode particle number
rh	right hemisphere
ROI	region of interest
SES	socioeconomic status
SPM8	Statistical Parametric Modeling
TNF-α	tumor necrosis factor – alpha
TE	echo time
TR	repetition time
(q)UFP	(quasi) ultra-fine particles
UNESCO	United Nations Educational, Scientific and Cultural Organization
WHO	World Health Organization
WMV	white matter volume

Table of Contents

1 Introduction 1

1.1 Environmental Exposures 1

1.1.1 Air Pollution 1

1.1.2 Noise 2

1.1.3 Traffic-Related Exposures 3

1.2 Neuropsychology, Resting State Networks and Brain Structure 3

1.2.1 Neuropsychological Testing 3

1.2.2 Resting State Networks 3

1.2.3 Local Gyrification Index (lGI) 4

1.3 State of Research 5

1.3.1 Effect of Long-Term Air Pollution and Noise on General Health 5

1.3.2 Effect of Air Pollution and Noise on Neuropsychological Function 6

1.3.3 Effect of Air Pollution and Noise on Brain Structure 7

1.3.4 How Might Air Pollution and Noise Affect The Brain? 8

1.4 Aims of this Dissertation 10

2 Materials and Methods 11

2.1 Study Population 11

2.2 Exposure Assessment 12

2.2.1 Air Pollution 12

2.2.2 Noise Exposure 14

2.2.3 Traffic Indicators 14

2.3 Outcome Data 14

2.3.1 Neuropsychological Assessment 14

2.3.2 Magnetic Resonance Image (MRI) Acquisition 16

2.3.3 Image Processing 17

2.3.3.1 Definition of the FPN Seed Regions in Resting-State fMRI Data 17
2.3.3.2 Surface Reconstruction and local Gyrification Index 17
2.4 Covariates 19
2.5 Statistical Analysis 20
2.5.1 In- and Exclusion Criteria 20
2.5.2 Linear Regression Models 21
2.5.3 Effect Modification 21
2.5.4 Sensitivity Analyses 22
3 Results 22
3.1 Description of Variables 22
3.1.1 Study Population 22
3.1.2 Exposure Variables 24
3.1.3 Neuropsychological Tests 25
3.1.4 local Gyrification Index Values 26
3.2 AP, Noise, and Neuropsychological Tests 27
3.3 AP, Noise, and Brain Structure 31
3.3.1 Right Hemisphere 31
3.3.1 Left Hemisphere 33
3.4 Effect Modification 34
3.4.1 Age 34
3.4.2 Smoking Status 36
3.4.3 Sex and SES 38
3.5 Sensitivity Analysis 42
3.5.1 BMI, CHD, depression, and diabetes 42
3.5.2 Non-working participants only and two-exposure models 44
4 Discussion 46
4.1 Summary of the Results 46

4.2 Interpretation of the Results 46
4.2.1 Main Results 46
4.2.1.1 Right Hemi-Aging Theory 47
4.2.1.2 Posterior-Anterior Shift in Aging Theory 47
4.2.1.3 Special Role of PN_{AM} 49
4.2.1.4 Noise Exposure 50
4.2.1.5 Sex- and Socioeconomic-Independent Effects 52
4.2.2 Sensitivity analysis 52
4.3 Future Studies 53
4.4 Strengths and Limitations of the Study 54
4.5 Conclusion 56
References 57
Supplement 65

1 Introduction

In the course of man-made climate change and increasing environmental pollution ever more people are realizing the devastating consequences of it. Thus evaluating adverse effects of air pollution not only on the environment but also on human health has become gradually more important. Now that current diesel exhaust scandals further the public discussion on the matter, the pressure on politicians continuously rises. So does the demand for stricter limits of various air pollution components. But in order to set those limits to the right level, research needs to be done to show the extent to which actual adverse health effects of air pollution exist. This rationale illustrates the relevance of the following dissertation and the importance of contributing to the consolidation and advancement of the current state of knowledge on adverse health effects of air pollution.

1.1 Environmental Exposures

1.1.1 Air Pollution

The term air pollution (AP) represents different airborne particles (liquid and solid) and gaseous components of different chemical composition. It can be further classified by particle size as well as according to its source of origin (Air Quality Guidelines Global Update 2005, Who, 2006):

One major component of AP is particulate matter (PM). Particles with an average aerodynamic diameter of less than 10 micrometers (µm) are referred to as PM_{10} or coarse particles. Particles with an average aerodynamic diameter below 2.5 µm are called $PM_{2.5}$ or fine particles. The category of ultrafine particles (UFP) includes particles with diameters of less than 100 nanometers (nm). The concentrations of the first two classes of PM are expressed in mass per volume because they make up the majority of all PM mass. Measurement of PM_{10} thereby also includes the whole group of $PM_{2.5}$ and UFP, but $PM_{2.5}$ and UFP only make up a small portion of the total PM_{10} mass. $PM_{2.5}$ can be quantified by filtering out particles over 2.5 µm in diameter. Again, UFPs are contained in this measure but only make up for a very small amount of the total mass of $PM_{2.5}$. Instead, UFP concentrations are usually expressed in number of

particles per volume because UFP make up the majority of all PM in terms of particle numbers. Particle number concentrations for the accumulation mode (PN_{AM}), which reflects particles with diameters between approximately 0.1 and 1.0 µm, are considered a measure of quasi-ultrafine particles (qUFP).

When considering the source of origin, a distinction can be made between anthropogenic and biogenic PM (European Environment Agency, 2013). Anthropogenic PM arises from human activity, e.g. from road traffic, heavy industry, energy production, agriculture, heating, and, mainly in poorer developing countries, from open fires when cooking in closed rooms. Natural phenomena, such as volcanic eruptions, sand storms, forest fires, and sea spray produce PM of biogenic origin. The precise chemical composition of PM depends on its source of origin and can contain anything from shells, pollen, fungal spores or grain granules up to car tire wear, soot, organic carbon particles, nitrates and sulfates from secondary particle formation, or fibrous materials such as asbestos or cotton fibers. (European Environment Agency, 2013)

In addition to PM, various gases are also considered AP. Nitrogen oxides (NO_X) is a collective term for all nitrogen oxide compounds, primarily nitrogen monoxide (NO) and nitrogen dioxide (NO_2) (European Environment Agency, 2013; WHO Regional Office for Europe, 2013). NO makes up the majority of NOx emission and contributes to the formation of ozone and PM. The main sources of anthropogenic NOx emissions are combustion engines and combustion plants for coal, oil, gas, wood and waste. In densely populated metropolitan areas, road traffic is one of the most important sources of NOx, accounting for up to 60% of overall NO_2 emission (European Environment Agency, 2013; WHO Regional Office for Europe, 2013).

1.1.2 Noise

In urban settings, several different sources are responsible for the total noise exposure, including transport (e.g., road, railway, and aircraft traffic) as well as industry or construction work. Additionally, exposure levels can vary over different periods of the day. For example, daytime and nighttime noise can differ

drastically depending on traffic volume, nocturnal flight bans and different working hours in factories or at construction sites.

1.1.3 Traffic-Related Exposures

An important urban source of AP is traffic, which also is a major source of ambient noise. Because they share a common source, AP and traffic noise often occur simultaneously and it is an important task to differentiate between these two exposures when looking at possible independent effects as well as effect modification. Moreover, PM measures do not differentiate by source. Considering the distance people live from the nearest highly trafficked road may add more information about traffic-related AP exposure. Often associated with traffic diesel exhaust in highly urbanized areas, black carbon (BC) or soot may also be of interest. BC is a fraction of $PM_{2.5}$ and is created in fossil fuel burning and combustion engines. The dominating light-absorbing substance elemental carbon (EC) can be quantified as a surrogate measure for BC by measuring the blackness of $PM_{2.5}$ filters. This is oftentimes referred to as $PM_{2.5}$ absorbance ($PM_{2.5\ abs}$, WHO Regional Office for Europe, 2013).

1.2 Neuropsychology, Resting State Networks and Brain Structure

1.2.1 Neuropsychological Testing

Neuropsychological tests are conducted in an effort to quantify the functional intellectual capabilities of individual participants in different cognitive areas and allow comparisons between different participants to be made. Analogous to Jockwitz et al., 2017, these tests can be grouped into the five different neuropsychological domains of Attention, Executive Function, Memory, Working/Short-Term Memory, and Language.

1.2.2 Resting State Networks

The brain consists of a number of Resting State Networks. This term depicts a set of functionally connected brain areas that show simultaneous and spontaneous activation (i.e. fluctuations) when the brain is at rest (Smith et al.,

2009). This state of rest does not refer to a particular state of the brain itself. Instead it denotes any continuous situation in which the participant is not exposed to external stimuli or undergoing a task or activity; it is noteworthy that the state of the eyes is not clearly defined either, so that they may be opened or closed and the view fixed or not (Snyder and Raichle, 2012).

These networks' activity is quantified by means of functional magnetic resonance imaging (fMRI), a method of magnetic resonance imaging (MRI) that measures cerebral blood flow and differences in cerebral blood flow as blood-oxygen-level-dependent (BOLD) imaging (Ogawa et al., 1990). Because cerebral blood flow to and brain activity of the same brain region have shown to be linked, differences in blood flow during task activation and rest corresponds to changes in regional brain activity attributable to the execution of the task and can be used for functional brain imaging (Villringer and Dirnagl, 1995).

One of these networks is the bihemispheric fronto-parietal network (FPN). It includes the dorsolateral prefrontal cortex (DLPFC), posterior cingulate cortex and precuneus (PCC/P), and the inferior parietal lobule (IPL) and has been shown to be active during tasks related to working memory and language function (Smith et al., 2009).

Resting State Networks undergo changes during normal aging and show a high inter-individual variability particularly in older aged participants (Marstaller et al., 2015). This emphasizes the relevance of considering these networks when investigating aging and age related changes in brain morphology and especially brain activity.

1.2.3 Local Gyrification Index (lGI)

As one of the important structural features of the human brain, gyrification refers to the convolution of the cerebral cortex, i.e., the formation in gyri and sulci. Gyrification increases the brains surface and enables it to have more neurons in less space, which leads to higher processing capability and is generally associated with better cognitive performance. The gyrification index (GI) serves as a measure for the degree of gyrification. It is calculated as the ratio of the

total pial surface (including sulci) to the outer pial surface (excluding sulci). Thus, the higher the GI, the stronger the cortical convolution.

When first developed, GI was determined using postmortem brain sections. It was calculated by drawing contour lines corresponding to the sulci and the outer pial surface in the frontal plane, measuring the two lines and taking the ratio. This was a two-dimensional approach for the determination of gyrification as implemented by Zilles et al. in 1988, and was originally done manually.

Extending this approach to the third dimension and improving the measuring accuracy as well as reducing the time spent on the analysis, the local Gyrification Index (lGI) within the Freesurfer software (http://freesurfer.net/) can be used today. This method creates a three-dimensional MRI reconstruction of the brain of a living participant with thousands of vertices. In a particular Region of Interest (ROI), the two surfaces, i.e., the total pial surface and the outer pial surface, are locally calculated and then the ratio is taken. Therefore, it is possible to determine individual lGI values for different ROIs. This method also allows for calculation of the entire brain's gyrification by generating thousands of ROIs all over the brain's surface (Schaer et al., 2008) as a useful and sensitive marker for brain atrophy (e.g. Hogstrom et al., 2013). By comparing different ROIs, it is possible to identify regional differences in lGI and thus in regional cortical atrophy.

1.3 State of Research

1.3.1 Effect of Long-Term Air Pollution and Noise on General Health

In previous studies, long-term AP and noise exposure have been shown to have a negative impact on several different aspects of human health (Kempen et al., 2018; Kim and van den Berg, 2010; Thurston et al., 2017; WHO Regional Office for Europe, 2013). (Nußbaum et al., 2019)

At present, research has focused primarily on the effects of AP on pulmonary disease, cardiovascular diseases, stroke and systemic inflammation. From prior studies, it is known that long-term exposure to PM significantly increases the

risk of lung cancer (Raaschou-Nielsen et al., 2013), having a stroke (Lee et al., 2018; Scheers et al., 2015) or coronary events (Cesaroni et al., 2014).

Long-term studies have shown associations between long-term exposure to NO_2 and mortality (total as well as cardiovascular-, respiratory- and lung cancer-specific) (Cesaroni et al., 2014; Hoek et al., 2013), the frequency of lung cancer (Hamra et al., 2015) and the development of chronic respiratory symptoms (e.g., development of asthma) (Anderson et al., 2013). Additionally, exposure to NO_2 has been linked to impaired lung function (Adam et al., 2014) and type 2 diabetes (Wang et al., 2014).

Several meta-analyses have shown that long-term road traffic noise exposure is significantly associated with hypertension (van Kempen and Babisch, 2012), type 2 diabetes (Dzhambov, 2015), cardiovascular disease (Babisch, 2014), and ischemic heart attack (Kempen et al., 2018).

1.3.2 Effect of Air Pollution and Noise on Neuropsychological Function

Only lately the influence of AP and noise exposure on the brain and on neuropsychological function has gotten into the focus of research. Previous studies have shown associations between exposure to AP and higher incidence of Alzheimer's disease (Jung et al., 2015), depressive symptoms (Lim et al., 2012), and suicide (Bakian et al., 2015). (Nußbaum et al., 2019)

It has also been shown that AP exposure might have an effect on cognitive performance (Tzivian et al., 2016; Xu et al., 2016). Higher levels of PM exposure were associated with a decline in performance for a number of neuropsychological tests, including tasks on working memory with words and numbers, medium-term memory, verbal fluency, spatial and logical thinking, and pattern recognition (Ailshire and Clarke, 2015; Power et al., 2011; Tonne et al., 2014; Tzivian et al., 2016; Weuve et al., 2012). With a doubling in PM concentration (i.e., an increase of 10 micrograms (µg) per m^3), the observed decline in test performance was similar to effects seen in a normally aging brain within a course of approximately two years (Power et al., 2011; Weuve et al., 2012). These results raise the question whether the performance loss in specific

neurocognitive functions is also reflected in structural changes in task-specific brain regions. (Nußbaum et al., 2019)

Effects of long-term ambient noise on cognitive function of adults, so far, have seldom been researched (Nußbaum et al., 2019). Tzivian et al., 2016 found a negative association between long-term noise exposure and neuro-psychological test results regarding memory and executive function. Other studies on traffic noise have looked into short-term effects only and found impaired recall of text, semantic memory, and attention (Hygge et al., 2003) as well as impaired sleep quality (Schapkin et al., 2006).

Furthermore, all of the studies mentioned above, except for Tzivian et al. 2016, looked at either AP or traffic noise. In order to fully understand the effects AP and noise have on neuropsychological function, it is crucial to look at both exposures simultaneously, because they share traffic as their common source in the urban setting.

1.3.3 Effect of Air Pollution and Noise on Brain Structure

In order to explain the decreases in cognitive function that have been seen with increased exposure to AP, several studies have been conducted looking at the association between AP and brain structure. A long-term study observed that higher $PM_{2.5}$ exposure was associated with lower total cerebral brain volume and higher odds of covert brain infarctions (Wilker et al., 2015). Because brain volume can be generally used as marker for age-associated cerebral atrophy, the authors concluded that AP may have serious effects on the structural aging of the brain. In a population of older women, researchers found that $PM_{2.5}$ exposure was associated with decreased white matter volume (WMV) in frontal and temporal regions (Chen et al., 2015). Additionally, it has been shown that $PM_{2.5}$ exposure was associated with reductions in subcortical WMV in the frontal lobe, with smaller clusters in the temporal, parietal, and occipital lobes, and reduced cortical grey matter volume (GMV) in the bilateral superior, middle, and medial frontal gyri (Casanova et al., 2016). One study showed that higher $PM_{2.5}$ and PM_{10} exposure was associated with smaller deep GMV (Power et al., 2018). (Nußbaum et al., 2019)

No studies on the effects of long-term noise exposure on the structure of the brain have been conducted so far. (Nußbaum et al., 2019)

1.3.4 How Might Air Pollution and Noise Affect The Brain?

Before investigating possible associations of AP and noise on brain structure it makes sense to look at possible pathways of how AP and noise might affect the brain. For PM, particle size plays an important role in the possible ways AP affects the body as well as the brain's structure and function. In general, the smaller the particles are, the deeper they can penetrate into the lung and the effective surface area which the particles get in contact with is higher (WHO Regional Office for Europe, 2013). PM_{10} exerts its effect primarily on mucous membranes in the nose and throat or in the lungs and acts systemically via mediators or contaminants, but it cannot pass though the alveolar membrane. $PM_{2.5}$, on the other hand, can enter the alveoli through the lung and cross the alveolar membrane to get into the circulatory system (WHO Regional Office for Europe, 2013). In addition to these pathways, UFP have been shown in animal experiments to be able to pass from the nasal mucosa into the olfactory bulb via neural translocation (Elder et al., 2006; Oberdörster et al., 2004). NO_2 has a low water solubility and thus the pollutant is not bound in the upper airways but penetrates into lower parts of the respiratory tract (bronchioles, alveoli) (WHO Regional Office for Europe, 2013). When in contact with alveolar tissue, the highly oxidative agent can lead to oxidative stress, cell damage, cause inflammatory processes and lead to hyperreactivity of the bronchi (WHO Regional Office for Europe, 2013). (Nußbaum et al., 2019)

On the one hand, AP exposure could lead to atherosclerotic changes in the arteries supplying the brain (Provost et al., 2015). This would result in an increased vascular resistance and reduced cerebral blood flow (Wellenius et al., 2013), which would then favor a loss of function and a decrease in the volume of certain parts of the brain. This would also affect local and overall brain atrophy.

On the other hand, AP exposure could lead to different inflammatory processes in the brain tissue. Mice exposed to acute diesel exhaust gases showed increased activation of microglia, increased lipid peroxidase, neuro-

inflammation in different brain regions, especially in the hippocampus and olfactory bulb, and an impairment of adult neurogenesis (Costa et al., 2015). In addition, rats exposed to similar exhaust gases exhibited a dose-dependent increase in cortical neuronal loss, selective neuronal loss with preserved tissue structure and extracellular matrix, nuclear pyknosis, kariolysis, kariorrhexis, small to moderately large regions with penumbra, and population growth of activated microglia and astrocytes (Ejaz et al., 2014). This indicates that inflammation or oxidative stress to glia or neurons through contact with PM could lead to a loss of function and inflammation-induced alteration and breakdown of brain tissue. The latter could then be measured again as a change in the IGI. At present, it is not clear whether the inflammation necessarily has to occur directly in the brain or whether an inflammation of the olfactory nerve or the lung by nasal or bronchiolar/alveolar contact with PM, respectively, could also be transmitted to the brain via the olfactory nerve or systemic inflammation.

It is also conceivable that inflammation of the blood-brain barrier caused by $PM_{2.5}$ or UFP circulating in the bloodstream may lead to increased permeability of the barrier. In mice, an increased activity of matrix metalloproteinases, a loss of tight junctions at the blood-brain barrier, an increase in tight junction permeability, and an increase in neuroinflammatory markers were observed when exposed to diesel exhaust gases (Oppenheim et al., 2013). An in vitro study (Liu et al., 2015) with human endothelial cells and macrophages has shown that $PM_{2.5}$ affects tight junctions of endothelial cells, increases monocyte trans-migration, and thus possibly also increases the permeability of the blood-brain barrier. At present, it is not fully understood to what extent this increased permeability may allow other pollutants to reach the brain more easily.

Furthermore, Liu et al. (2015) found that glutamate is probably a mediator of the neurotoxic effect of $PM_{2.5}$. Significantly reduced glutaminase could be detected in $PM_{2.5}$-treated macrophages, but this effect was even stronger in extracellular vesicles. In an in-vitro study using astrocytes, the release of glutamate and adenosine triphosphate (ATP) via the activation of connexin and pannexin hemichannels was demonstrated when exposed to BC (Wei et al., 2014). An in-vitro study with rats also showed that ultrafine particle exposure reduced the

synapse function of CA1 neurons (Davis et al., 2013). This was due to a nitrosylation respectively dephosphorylation of various N-Methyl-D-Aspartate (NMDA) receptors and further supports the hypothesis that glutamate may be a mediator of the neurotoxic effect of AP.

It is also possible that AP exposure may lead to hormonal changes in the whole organism or altered gene expression in brain cells, which influence the structure and function of the brain. A study conducted in rats observed that exposure to PM resulted in decreased tumor necrosis factor – alpha (TNF-α) messenger ribonucleic acid (mRNA) levels in the cerebral hemisphere and pituitary gland (Thomson et al., 2007). However, an in-vitro study by Campbell et al., (2014) using human neurons and glia observed an increase of TNF-α in the neurons in both the absence and presence of glia as well as a decrease in reactive oxygen species. These results suggest that human cells may behave differently from animal cells in the presence of PM, at least as far as oxidative stress is concerned; so additional studies in human cells are needed.

As for noise, little work has been done investigating the possible pathways by which it may affect the brain. It has been shown that noise exposure leads to changes in the electroencephalography (EEG) and in autonomic variables that are called arousals or phasic activations (Kim and van den Berg, 2010). Whether this could lead to changes in brain plasticity and structural changes in brain morphology has not been investigated.

1.4 Aims of this Dissertation

In summary, evidence from experimental as well as epidemiological studies supports the hypothesis that AP and noise exposure are adversely associated with general health, cognitive performance and possibly the development of diseases of the brain. Moreover, AP exposure is correlated with a lower total brain volume, with a decrease in cortical and subcortical WMV in association regions, and a reduction of cortical and subcortical GMV. Beyond these solely volumetric findings, there is a lack of further structural correlates in the brain which are associated with AP exposure. Studies on AP and cognitive performance indicate that AP may cause damage to specific brain structures

and functions. For a comprehensive understanding of processes that occur in the brain under AP exposure, it is important to understand which structural brain changes accompany cognitive performance losses. It is likely that different parts of the brain exhibit varying susceptibility to AP-induced changes, but these susceptible regions have not been clearly identified in prior studies. To what extent AP exposure affects the brain's physiological aging process, is not yet completely understood. Thus, it is of interest whether differences in AP and noise exposure are associated with regional differences in the structure of the brain. (Nußbaum et al. 2019)

The aim of this thesis was to first investigate associations of long-term AP and noise exposure and cognitive performance of 615 adult men and women aged 55-85 years from the 1000BRAINS Study. In a second step, resting state networks corresponding to the cognitive performance losses were identified and the degree of local cortical atrophy in these task-specific regions was determined using lGI analyses. Finally, possible associations between AP and noise exposure and local cortical atrophy were explored. So far, there have been studies on AP and volumetric analyses of the brain, but to my knowledge, this is the first study looking at AP and lGI as another important surface-based and thus sensitive structural feature of the brain. Moreover, this is the first study to look at noise exposure in the broader context of brain structure and thus the study is also the first study to look at AP and noise exposure together in this context. (Nußbaum et al. 2019)

Additional effect modification and sensitivity analyses were done to explore ways of further research in the direction of possible mediating and modulating effects demographic and lifestyle characteristics have on the associations between AP and noise and brain structure.

2 Materials and Methods

2.1 Study Population

Data from the successive population-based Heinz Nixdorf Recall (HNR) and 1000BRAINS Studies has been used to carry out the study underlying this

dissertation. The objective of the HNR Study was to investigate risk factors for atherosclerosis, cardiovascular disease, cardiac infarction and death (Schmermund et al., 2002). The objective of the 1000BRAINS Study was the evaluation of the variability of brain structure and function in the course of normal aging (Caspers et al., 2014). The participants from these cohort studies resided in three neighboring cities (Bochum, Essen and Mülheim/Ruhr), which all lie in the urban and industrialized German Ruhr Area (Schmermund et al., 2002). The study area measures about 600 km^2. (Nußbaum et al., 2019)

The random selection process for initial participant acquisition into the HNR Study took place between December 2000 and August 2003 (n=4,814; age range: 45-75 at baseline). After five years (2006-2008) participants were invited to take part in the first follow-up examination (n=4,157). After ten years (2011-2015) a second follow up took place (n=3,089) and participants were asked to additionally participate in the 1000BRAINS Study. Participants without medical contraindications, who were physically able for MRI, also undertook a variety of neuropsychological and motor tests as well as laboratory, genetic and epigenetic analyses (Caspers et al., 2014). Overall, MRI data on 666 participants could be used for the present study. (Nußbaum et al., 2019)

The HNR Study was approved by the ethics committee of the medical faculty of the University of Essen (Ethics votum number: 99-69-1200, date of approval: 12.05.1999). 1000BRAINS was approved by the ethics committee of the medical faculty of the University of Duisburg-Essen (Ethics votum number: 11-4678, date of approval: 05.03.2012). All participants gave their written informed consent. All study procedures complied with the declaration of Helsinki. (Nußbaum et al., 2019)

2.2 Exposure Assessment

2.2.1 Air Pollution

Exposure data on AP was calculated with two different models. On the one hand, the land use regression model (LUR) according to the European Study of Cohorts for AP Effects (ESCAPE) standardized procedure (ESCAPE-LUR) was used to assess PM of varying aerodynamic diameters (≤ 10 µm [PM_{10}] and ≤

2.5 µm [$PM_{2.5}$]) and [$PM_{2.5\ abs}$], a proxy for BC, and nitrogen oxide concentrations (NO_x and NO_2) (for more information see: Beelen et al., 2013 and Eeftens et al., 2012). PM was measured at 20 sites and nitrogen oxide concentrations at 40 sites between October 2008 and October 2009, both in three separate two-week periods to account for different seasons (Beelen et al., 2013). The LUR model was created with the one-year averages of the measured pollutant concentrations from background and traffic-specific monitoring sites and with predictor variables from Europe-wide and local Geographic Information System databases. With the input of each participant's residential address at the first follow-up examination in 2006-2008 the model estimated the 1-year-mean exposure concentration for each participant in the year before the first follow-up examination. (Nußbaum et al., 2019)

On the other hand, the validated, spatio-temporal, three-dimensional EURopean Air Pollution Dispersion (EURAD) chemistry transport model (Büns et al., 2012; Hass et al., 1993; Memmesheimer et al., 2004) was used to assess the accumulation mode particle number concentration (PN_{AM}; between 0.1 and 1.0 µm in aerodynamic diameter, Nonnemacher et al., 2014) for each participant. The multilayer, multigrid EURAD model projects the transport, chemical transformation, and deposition of tropospheric components (Büns et al., 2012). With the input of topographic information from the U.S. Geological Survey database (resolution of approximately 500 m), land use data from the German Tropospheric Research Programme, and both European and local official emission inventories (Memmesheimer et al., 2004) the model estimated the one-year average PN_{AM} concentrations from the 1 km^2 grid cell for each respective residence of the participants for 2006, 2007, and 2008 (Hennig et al., 2016; Nonnemacher et al., 2014). (Nußbaum et al., 2019)

Validation of PN_{AM} estimates was done with measurements taken between January 2011 and December 2014 by the Institute of Energy and Environmental Technology (IUTA) at its measuring station in Mülheim-Styrum using a TSI 3926 scanning mobility particle sizer spectrometer (size range: 0.014-0.750 µm; TSI Incorporation, Shoreview, Minnesota, U.S.A.; for more details, see Birmili et al., 2016).

2.2.2 Noise Exposure

Long-term noise exposure assessment was done in agreement with the European Directive 2002/49/EC (EUR-Lex - 32002L0049 - EN - EUR-Lex, 2002) as weighted 24-hour (L_{DEN}) and nighttime (10pm – 6am; L_{night}) mean noise at facade points. At a height of 4 ± 0.2 m in a 10-m buffer around the residential address, participants were given the maximum noise levels measured. (Nußbaum et al., 2019)

2.2.3 Traffic Indicators

Defined as a street in the upper quintile of traffic density (>26,000 vehicles per day) the distance (m) to the nearest heavily trafficked road ($Dist_{majroad}$) was used to account for traffic-specific exposure. The necessary data was acquired from the State Office for Nature, Environment and Consumer Protection of North-Rhine-Westphalia (LANUV). (Nußbaum et al., 2019)

2.3 Outcome Data

2.3.1 Neuropsychological Assessment

The neuropsychological tests implemented by the 1000BRAINS Study (Caspers et al., 2014) enable the assessment of a variety of cognitive functions. They can be grouped into the five cognitive domains of Attention (Gatterer et al., 1989; Morris et al., 1989), Executive Function (Bäumler, 1985; Morris et al., 1989; Regard et al., 1982; Stroop, 1935; Sturm et al., 1993), Memory (Benton et al., 2009; Lux et al., 2012), Short-Term/Working Memory (Della Sala et al., 1997; Oswald and Fleischmann, 1997; Schellig, 1997), and Language (Aschenbrenner et al., 2000; Schmidt and Metzler, 1992), as earlier described by Jockwitz et al (2017). Table 1 gives an in depth explanation for each test procedure and the assignment into the five domain categories. (Nußbaum et al., 2019)

Table 1. Description of all 19 neuropsychological tests within the five cognitive domains, from Nußbaum et al. 2019

Cognitive function	Domains and Tests	Description
	Attention	
Selective attention	Alter-Konzentrations-test *(Gatterer et al., 1989)*	Time(s) to recognize target figures among distractors
Processing speed	Trail Making test (part A) *(taken from CERAD-Plus; Morris et al., 1989)*	Time(s) to connect randomly arranged digits in ascending order
	Executive Function	
Problem solving	Subtest 3 from "Leistungs-prüfungssystem 50+" *(Sturm et al., 1993)*	Number of correctly identified non-matching figures among geometrical figures
Figural fluency	Fünf-Punkte-test *(Regard et al., 1982)*	Number of different drawn patterns by connecting 5 points in 3 minutes
Concept shifting	Trail Making test (B-A) *(taken from CERAD-Plus; Morris et al., 1989)*	Time(s) to alternately connect letters and numbers in ascending order (TMT B), then calculating: TMT B − TMT A
Susceptibility to interference	Farbe-Wort-Interferenztest *(Jülich version; similar to: Stroop, 1935; Bäumler, 1985)*	Time(s) to name ink color of words with color meaning but printed in a different color (subtracted by the time(s) to read color words)
	Memory	
Figural memory	Benton-test *(Benton et al., 2009)*	Number of errors during free recall of 20 remembered figures
Verbal learning	Verbaler Gedächtnistest *(Lux, S., et al., 2012)*	After learning 15 words in 5 query rounds, number of cumulated free recall and number of delayed recall after 20-30 minutes
	Short Term / Working Memory	
Visual	Visual Pattern test *(Jülich version; similar to: Della Sala et al., 1997)*	Number of memorized patterns presented in a grid of black and white squares
Visual spatial	Block-tapping-test *(Schellig, 1997)*	Number of correctly tap-repeat tapped blocks, forwards and backwards
Verbal	Zahlennachsprechen *(from Nürnberger Alters-Inventar; (Oswald and Fleischmann., 1997)*	Number of correctly repeated digits previously given, forwards and backwards
	Language	
Semantic / phonemic verbal fluency	Regensburger Wortflüssigkeitstest *(Aschenbrenner et al., 2000)*	Number of produced words by category: words beginning with B, alternately beginning with G and R, occupations, and alternately sports and fruits
Vocabulary	Wortschatztest *(Schmidt and Metzler, 1992)*	Number of correctly identified real words among 5 pseudo-words

These tests enable identification of cognitive functions that are differentially affected by aging and assessment of the respective consequences on brain imaging parameters. The resulting neuropsychological profiles allow comparison of intra- and inter-individual strengths and weaknesses. Testing time per participant was approximately 75–105 min, depending on the individual participant's performance. Most neuropsychological tests were designed specifically for the testing of older participants, i.e., 55 years and above.

One to three missing test results per participant were replaced by the age- and sex-stratified median scores. Participants who had more than three missing values were not included in the analysis. Skewed distributions of test results required rank-transformation, mean-centering and scaling of the values for further analysis. With these standard scores, tests were sorted into the five cognitive domain categories and cognitive domain scores were calculated as means of all standard scores for each domain. (Nußbaum et al., 2019)

Early signs of dementia were identified using DemTect (Kalbe et al., 2004). This screening instrument evaluates verbal and working memory, word fluency performance, and intellectual flexibility, and has a high sensitivity for the detection of mild cognitive impairment and early dementia.

2.3.2 Magnetic Resonance Image (MRI) Acquisition

MR Imaging was carried out on a 3T Siemens Tim-TRIO MRI scanner with a 32-channel head coil. For brain function, echo planar imaging (EPI) generated 300 images for each participant at rest and enabled identification of the FPN, with the following parameters of the scans: 36 slices, slice thickness 3.1 mm, TR = 2200 ms, TE = 30 ms, FoV = 200 x 200 mm^2, voxel resolution 3.1 x 3.1 x 3.1 mm^3. For brain structure, 3D high-resolution T1-weighted magnetization-prepared rapid acquisition gradient-echo (MPRAGE) anatomical scans enabled surface reconstruction (Caspers et al., 2014), with the following parameters of the scans: 176 slices, slice thickness= 1mm, repetition time (TR) = 2250 ms, echo time (TE) 3.03 ms, field of view (FoV) = 256 x 256 mm^2, flip angle = 9°, and voxel resolution of 1 x 1 x 1 mm^3. (Nußbaum et al., 2019)

2.3.3 Image Processing

2.3.3.1 Definition of the FPN Seed Regions in Resting-State fMRI Data

How resting state networks can be identified with fMRI data can be read in depth in Jockwitz et al. (2017). As for preprocessing, the Functional Magnetic Resonance Imaging of the Brain (FMRIB) Software Library (FSL) software [FSL - FslWiki; Jenkinson et al., 2012] was used for motion correction (MCFLIRT; Jenkinson et al., 2002), brain extraction (BET; Smith, 2002), high pass temporal filtering (100 ms), linear and nonlinear registration (FLIRT and FNIRT; Jenkinson et al., 2002; Jenkinson and Smith, 2001) to the standard space template (MNI 152), smoothing using a 5-mm FWHM Gaussian kernel, denoisation of the EPI scans using FMRIB's ICA-based Xnoiseifier (FIX), and, finally, correction for motion artifacts (Griffanti et al., 2014; Salimi-Khorshidi et al., 2014). (Nußbaum et al., 2019)

At this stage fMRI scans were suitable for the actual process of identifying the FPN. MELODIC multi-session temporal concatenation (Beckmann et al., 2005) enabled the detection of mutual spatial patterns among participant's resting state scans using probabilistic independent component analysis decomposition of the resting state signals (Beckmann and Smith, 2004). Visual inspection lead to the identification of the best spatial fit to the FPN as stated by (Beckmann and Smith, 2004; Smith et al., 2009). (Nußbaum et al., 2019)

2.3.3.2 Surface Reconstruction and local Gyrification Index

Anatomical scans were preprocessed with Statistical Parametric Modeling (SPM8) and FreeSurfer 5.3.0 [http://freesurfer.net/; Dale et al., 1999; Fischl et al., 1999]. Preprocessing included SPM8 segmentation to construct a reliable brain mask, skull-stripping and going through the cortical reconstruction process as implemented in FreeSurfer 5.3.0 (Dale et al., 1999; Fischl et al., 1999). The single steps consisted of (1) motion correction, (2) intensity normalization, (3) transformation into Talairach space, (4) tessellation of the gray/white matter boundary, (5) correction of topological defects, and (6) expansion of the gray/white matter interface to create the pial surface. (Nußbaum et al., 2019)

At this stage structural MRI scans were suitable for the actual process of lGI value calculation as implemented in FreeSurfer (Schaer et al., 2012, 2008). lGI is defined as the ratio of the total pial surface area (including the contour of each sulcus) to the exterior hull surface area (excluding sulci) in a specific brain region and can be used to assess the amount of cortical folding within the regions of the FPN.

Closely warping the pial surface, i.e. a morphological closing operation with a 15mm sphere closing each sulcus, was used to create the exterior hull surface. LGI values were generated for every vertex of the pial surface (Schaer et al., 2008) as the ratio of the pial surface area (defined as a sphere with the vertex as center and a default 25 mm radius) to the exterior hull surface. This means that higher lGI values indicate a stronger folding of the cortex and decreases in lGI hint at local brain atrophy. lGI was calculated for every region of the FPN (left and right: DLPFC, PCC/P, and IPL) as shown in Figure 1. (Nußbaum et al., 2019)

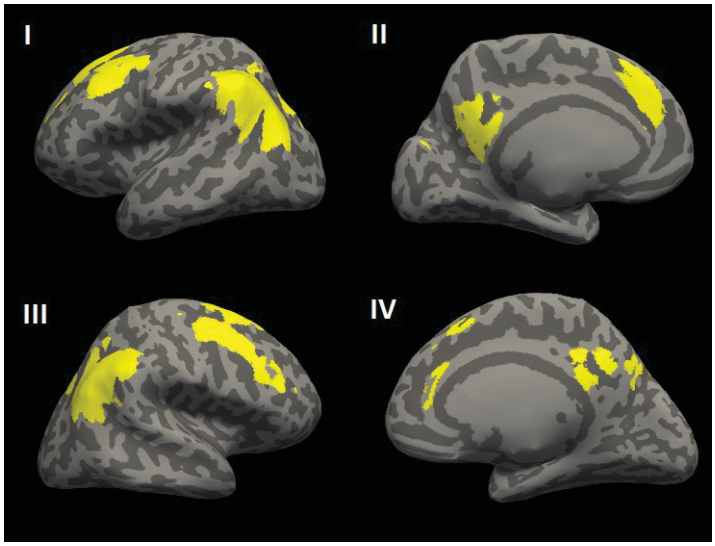

Figure 1. Regions of interest in the fronto-parietal network.
I left hemisphere from lateral: left dorsolateral prefrontal cortex (DLPFC) and left inferior parietal lobule (IPL).
II left hemisphere from medial: left posterior cingulate cortex and precuneus (PCC/P) and left dorsomedial prefrontal cortex.
III right hemisphere from lateral: right dorsolateral prefrontal cortex (DLPFC) and right inferior parietal lobule (IPL).
IV right hemisphere from medial: right posterior cingulate cortex and precuneus (PCC/P) and parts of the right dorsomedial cortex.
From Nußbaum et al., 2019

Surface reconstructions were randomly controlled for the participants. No systematic bias in the current data has been found that would, in turn, bias the results on the lGI measure. Further, all transformations of the FPN onto the individual participants were controlled. Participants for whom the transformations were not satisfactory were excluded from further analysis (n=3).

2.4 Covariates

Within the HNR (Schmermund et al., 2002) and 1000BRAINS (Caspers et al., 2014) Studies, each participant underwent standardized interviews and questionnaires to obtain information on demographic characteristics and lifestyle variables. Demographic characteristics included age in years as continuous variable, sex as dichotomous variable (male and female), and Socioeconomic status (SES) as education level according to the International Standard Classification of Education (ISCED) as total years of formal education, combining school and vocational training (UNESCO (1997)) in four categories: low (≤10 years), medium low (11-13 years), medium high (14-17 years) and high (≥18 years). Additionally, neighborhood unemployment rate, an indicator for neighborhood SES, was obtained from local census authorities for each participant's neighborhood conferring to administrative bounds (median population size of 11,263; collection near baseline; Dragano et al., 2009). Lifestyle variables consisted of alcohol consumption (five categories: 0, 1-3, 4-6, 7-14, and ≥ 14 drinks per week), smoking status (never, former, current), regular exposure to environmental tobacco smoke (ETS; yes/no), cumulative pack-years at baseline (five categories; first group: never-smokers; the rest divided by quartiles), and physical activity (four categories: 0, ≤50, ≤100, and >100 kcal expenditure per week by exercise). Additional covariates for the sensitivity analyses were body mass index (BMI; weight in kilograms divided by squared height in meters [kg/m^2]) and coronary heart disease (CHD; self-reported history of myocardial infarction or coronary intervention at baseline or documented incidence of CHD during follow-up). Type 2 diabetes mellitus (fasting blood glucose >125 mg/dl, blood glucose ≥200 mg/dl or reported use of insulin or oral antihyperglycemic medication in the last 7 days before examination) was likewise included. Depressive symptoms were evaluated with the German version of the Center for Epidemiologic Studies Depression scale (CES-D) short form (Hautzinger, M and Bailer, M, 1993). (Nußbaum et al., 2019)

2.5 Statistical Analysis

2.5.1 In- and Exclusion Criteria

From 3089 participants at the second follow-up examination, 666 finished the first follow-up examination (FU1) and had MRI scans done; with 630 participants also having complete data on AP and noise exposure as well as all covariates at FU1. Only participants with complete or nearly complete neuropsychological testing data were included (≤3 missing values; n=615). (Nußbaum et al., 2019)

Of the 615 participants, 39 had 1 missing value, 13 participants had 2 missing values, and 4 participants had 3 missing values. Additionally, 25 participants were excluded for the IGI analysis if they had defective structural MRI imaging data or imaging data that got corrupted during computational processing. This left a total of N=615 participants with complete data on exposure as well as covariates and neuropsychological test results (neuropsychological tests group) and N=590 participants with additionally usable structural MRI imaging (IGI group; see Figure 2). (Nußbaum et al., 2019)

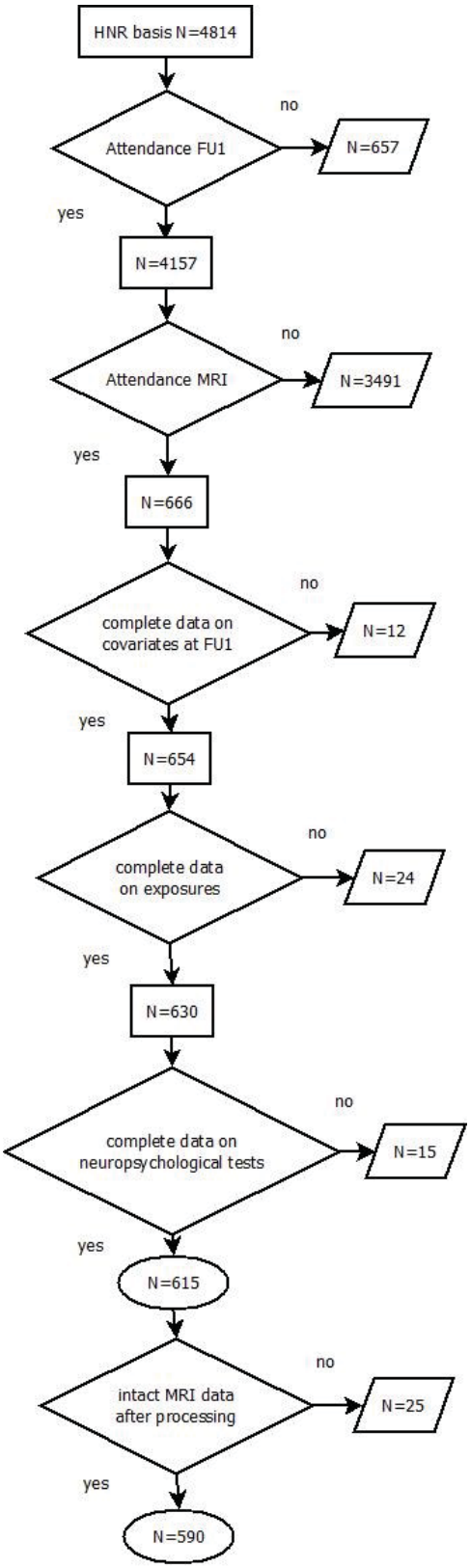

Figure 2. Flowchart on study population selection process. Abbreviations: HNR, Heinz Nixdorf RECALL study; FU1, first Follow-Up in 2006-2008; MRI, magnetic resonance imaging. From Nußbaum et al., 2019

2.5.2 Linear Regression Models

A variety of linear regression models were ran with every AP and noise exposure and the five cognitive domain scores as well as every neuropsychological test separately as outcome variable. The analysis consisted of four steps of adjustment of the models. First and second, an unadjusted model and a discovery model (adjusted for age, individual SES, and sex) were run in an effort to detect any functionally relevant brain regions for a later lGI analysis. Third, in an extended model (additional adjustment for alcohol consumption, smoking status, ETS, cumulative pack-years, and physical activity) possible confounding by lifestyle variables was investigated. The fourth adjustment step consisted of additional adjustment for neighborhood unemployment rate. All residuals were tested for non-normality and non-constant variance of the error terms to address model fit. Because of non-linearity, age was included as mean-centered quadratic and cubic terms. AP exposures were included as continuous variables and model parameters were estimated per interquartile range (IQR) increase in exposure. PN_{AM} was included as the average yearly mean of a three-year span (2006-2008). Noise exposures were included with a threshold at 45 dB[A] for L_{night} and at 50 dB[A] for L_{DEN} and noise values under the set threshold were replaced by the threshold value and values over the threshold were included linearly. Model parameters in noise models were estimated per 10 dB[A] increase. $Dist_{majroad}$ was included as a three categorical variable (<100m, 100m ≤ distance <200m, and ≥200m). The covariates from the discovery and the full model were used to run the base and main models, respectively, in the analysis on brain structure with lGI values of the functionally relevant brain regions as outcome variables. Statistical analyses were conducted in R version 3.4.0 (R Development Core Team, 2008). (Nußbaum et al., 2019)

2.5.3 Effect Modification

To assess possible effect modification by age, sex, smoking status, and SES a product term between the exposure and each respective covariate was added into the main models. Age was dichotomized around the median of 61 years in order to get two groups of the same size and enable better comparability.

Significant improvement of the model was assessed using likelihood ratio tests comparing the product-term model to one without inclusion of a product term (α=0.05).

2.5.4 Sensitivity Analyses

Sensitivity analyses for the main models were performed by adjusting for possible intermediate variables: CHD diagnosis, diabetes mellitus, BMI and degree of depressive symptoms (continuous variable of CES-D score). This was done by including these covariates separately into the models and checking whether the estimates were robust to adjustment for each of the added variables. In order to minimize potential exposure misclassification, additional analyses only among participants who worked less than 15 hours a week were conducted, as the residential-based exposure estimates are expected to be more accurate in this group. I also created two-exposure models to investigate whether pollutants had independent effects. Therefore, $PM_{2.5}$ was included into all other exposure models.

3 Results

3.1 Description of Variables

3.1.1 Study Population

The population for the neuropsychological analysis consisted of 615 participants with 590 of them also being included in the IGI analysis (Figure 2). (Nußbaum et al., 2019)

In general, both study populations were very similar in sociodemographic and lifestyle characteristics (Table 2). The mean age of participants was 61.5 ± 6.7 and 61.3 ± 6.6 years for the neuropsychological and IGI analyses, respectively. 55.9 (54.7) % of the population were men and about 78 % had 11 – 17 years of formal education.

Table 2. Demographic and lifestyle characteristics of the participants of the HNR study at first follow up examination (2006-2008) included in the neuropsychological tests and lGI analyses. From Nußbaum et al., 2019

Variable	Neuropsychological Tests Group (n=615)	IGI Analysis Group (n=590)
	Mean ± SD or *n* (%)	Mean ± SD or *n* (%)
Age (years)	61.5 ± 6.7	61.3 ± 6.6
Sex, female	271 (44.1)	267 (45.3)
Education Level		
≤10 years	29 (4.7)	28 (4.7)
11-13 years	316 (51.4)	307 (52.0)
14-17 years	161 (26.2)	152 (25.8)
≥18 years	109 (17.7)	103 (17.5)
Smoking Status		
Never Smoker	266 (43.3)	257 (43.6)
Former Smoker	258 (42.0)	242 (41.0)
Current Smoker	91 (14.8)	91 (15.4)
Cumulative Smoking (pack-years)[a]	22.1 ± 22.3	21.1 ± 18.4
ETS Exposure, yes	162 (26.3)	157 (26.6)
Alcoholic Drinks per Week		
0	163 (26.5)	155 (26.3)
1-3	136 (22.1)	132 (22.4)
4-6	63 (10.2)	61 (10.3)
7-14	137 (22.3)	132 (22.4)
>14	116 (18.9)	110 (18.6)
Weekly Energy Expenditure through Physical Activity (kilocalories)		
0 (no sports)	205 (33.3)	197 (33.4)
>0≤50	169 (27.5)	160 (27.1)
>50≤100	153 (24.9)	146 (24.7)
>100	88 (14.3)	87 (14.7)
Neighborhood Unemployment (%)	12.0 ± 3.2	12.0 ± 3.2
BMI (kg/m^2)	28.2 ± 4.4	28.2 ± 4.4
CHD, yes	10 (1.6)	8 (1.4)
Diabetes Mellitus, yes	90 (14.6)	85 (14.4)
CES-D Score	7.0 ± 6.0	7.0 ± 5.9

Abbreviations: ETS, environmental tobacco smoke; BMI, body mass index; CHD, coronary heart disease diagnosis; CES-D, Center for Epidemiologic Studies Depression Scale; lGI, local Gyrification Index; HNR, Heinz Nixdorf Recall

[a] Among current and former smokers only

3.1.2 Exposure Variables

Exposure variables were also very similar between the two groups (Table 3). Mean $PM_{2.5}$ (PM_{10}) exposure concentrations were 18.3 ± 1.0 µg/m^3 (27.5 ± 1.8 µg/m^3) for the neuropsychological analysis participants. Mean weighted 24-hour and nighttime noise exposures were 52.9 ± 8.7 dB[A] and 44.0 ± 8.5 dB[A], respectively.

Table 3. Summary statistics for residential long-term exposure levels one year before the first follow-up of the HNR Study (2005-2006) from the EURAD and ESCAPE-LUR exposure models for both study populations. From Nußbaum et al., 2019

	Neuropsychological Tests Group (n=615)			IGI Analysis Group (n=590)		
Exposure	Mean ± SD or n (%)	Range	IQR	Mean ± SD or n (%)	Range	IQR
PM_{10} (µg/m^3)[a]	27.5 ± 1.8	24.1-34.2	2.0	27.5 ± 1.8	24.1-34.2	2.0
$PM_{2.5}$ (µg/m^3)[a]	18.3 ± 1.0	16.1-21.3	1.4	18.2 ± 1.0	16.1-21.3	1.4
PN_{AM} (n/mL)[b]	3,203.6 ± 358.2	2,447.1-4,431.6	497.0	3,202.4 ± 357.0	2,447.1-4,431.6	497.8
NO_X (µg/m^3)[a]	49.3 ± 11.3	24.3-107.7	14.2	49.2 ±11.0	24.3-85.9	14.0
NO_2 (µg/m^3)[a]	29.6 ± 4.7	19.8-62.4	5.3	29.5 ± 4.5	19.8-55.3	5.3
$PM_{2.5abs}$ (10^{-5}/m)[a]	1.5 ± 0.3	1.0-3.4	0.3	1.5 ± 0.3	1.0-3.4	0.3
L_{night} (dB[A])[c]	44.0 ± 8.5	25.2-75.3	12.6	43.9 ± 8.4	25.2-68.5	12.6
L_{DEN} (dB[A])[c]	52.9 ± 8.7	34.3-83.7	12.6	52.8 ± 8.7	34.3-77.6	12.8
$Dist_{majroad}$ (m)[d]						
Absolute Distance	1,098.4 ± 812.0	15.8-4,599.7	1,054.8	1,100.3 ± 805.2	15.8-4,599.7	1046.5
<100	23 (3.7)	-	-	21 (3.6)	-	-
≥100<200	28 (4.6)	-	-	26 (4.4)	-	-
≥200	564 (91.7)	-	-	543 (92.0)	-	-

Abbreviations: HNR, Heinz Nixdorf Recall; EURAD, European Air Pollution Dispersion; ESCAPE-LUR, European Study of Cohorts for Air Pollution Effects - Land Use Regression; LANUV, State Office for Nature, Environment and Consumer Protection of North Rhine-Westphalia; IGI, local Gyrification Index; IQR, interquartile Range; $PM_{2.5}$ (PM_{10}), particulate matter with aerodynamic diameter ≤2.5 µm (≤10 µm); PN_{AM}, accumulation mode particle number; NO_X, any nitrogen oxide; NO_2, nitrogen dioxide; $PM_{2.5abs}$, $PM_{2.5absorbance}$; L_{night}, nighttime mean noise (10pm-6am); L_{DEN}, 24h mean noise; $Dist_{majroad}$, distance to the nearest major road; SD, standard deviation

[a] from ESCAPE-LUR [b] in line with EURAD procedures

[c] modeled according to European Standards [d] from LANUV

AP and noise exposures were right skewed and only discreetly correlated (Spearman correlation coefficient range: 0.17-0.39; Tables 4a and 4b). (Nußbaum et al., 2019)

Table 4a. Spearman correlation coefficients of exposures amongst the neuropsychological tests group (n=615). From Nußbaum et al., 2019

N=615	$PM_{2.5}$	$PM_{2.5abs}$	PN_{AM}	NO_2	NO_X	$Dist_{majroad}$	L_{night}	L_{DEN}
PM_{10}	0.89	0.89	0.50	0.51	0.51	-0.51	0.23	0.22
$PM_{2.5}$		0.89	0.75	0.62	0.62	-0.40	0.22	0.22
$PM_{2.5abs}$			0.56	0.60	0.53	-0.55	0.39	0.39
PN_{AM}				0.55	0.55	-0.14	0.18	0.17
NO_2					0.94	-0.27	0.30	0.30
NO_X						-0.22	0.23	0.23
$Dist_{majroad}$							-0.40	-0.37
L_{night}								0.99

Abbreviations: $PM_{2.5}$, particulate matter with aerodynamic diameter ≤2.5 µm; PM_{10}, particulate matter with aerodynamic diameter ≤2.5 µm; P_{AM}, accumulation mode particle number; NO_X, any nitrogen oxide; NO_2, nitrogen dioxide; $PM_{2.5abs}$, $PM_{2.5}$ absorbance; L_{night}, nighttime mean noise (10pm-6am); L_{DEN}, 24h mean noise; $Dist_{majroad}$, distance to the nearest major road

Table 4b. Spearman correlation coefficients of exposures amongst the lGI group (n=590). From Nußbaum et al., 2019

N=615	$PM_{2.5}$	$PM_{2.5abs}$	PN_{AM}	NO_2	NO_X	$Dist_{majroad}$	L_{night}	L_{DEN}
PM_{10}	0.89	0.89	0.50	0.51	0.50	-0.50	0.24	0.23
$PM_{2.5}$		0.89	0.75	0.62	0.62	-0.39	0.23	0.23
$PM_{2.5abs}$			0.56	0.59	0.52	-0.55	0.40	0.40
PN_{AM}				0.54	0.55	-0.14	0.18	0.17
NO_2					0.94	-0.26	0.30	0.30
NO_X						-0.20	0.22	0.22
$Dist_{majroad}$							-0.39	-0.37
L_{night}								0.99

Abbreviations: lGI, local Gyrification Index; $PM_{2.5}$, particulate matter with aerodynamic diameter ≤2.5 µm; PM_{10}, particulate matter with aerodynamic diameter ≤2.5 µm; P_{AM}, accumulation mode particle number; NO_X, any nitrogen oxide; NO_2, nitrogen dioxide; $PM_{2.5abs}$, $PM_{2.5}$ absorbance; L_{night}, nighttime mean noise (10pm-6am); L_{DEN}, 24h mean noise; $Dist_{majroad}$, distance to the nearest major road

3.1.3 Neuropsychological Tests

The mean results of the neuropsychological tests did not differ much between the group of the neuropsychological test analysis and the slightly smaller lGI analysis group (Table 5).

Table 5. Description of neurocognitive test results by domain. From Nußbaum et al., 2019

Outcome	Neuropsychological Tests Group (n=615)	lGI Analysis Group (n=590)	Range
	Mean ± SD	Mean ± SD	
Attention			
Selective attention, *AKT*[s]	35.3 ± 11.9	35.3 ± 12.0	17-136
Processing speed, *TMT A*[s]	40.9 ± 17.8	40.8 ± 17.9	16-300
Executive Function			
Problem solving, *LPS50*[n]	20.2 ± 5.1	20.2 ± 5.1	5-34

Figural fluency, *FIVE*[n]	26.0 ± 7.5	26.1 ± 7.5	4-57
Concept shifting, *TMT B-A*[s]	56.5 ± 40.1	55.9 ± 40.0	2-372
Susceptibility to interference, *FWI*[s]	44.8 ± 25.7	44.8 ± 25.7	4-307
Memory			
Figural memory, *Benton*[n]	17.3 ± 8.5	17.2 ± 8.5	1-51
Verbal learning, *VGT*[n]	41.4 ± 10.3	41.5 ± 10.2	6-66
Verbal learning, *VGT delayed*[n]	10.6 ± 2.7	10.7 ± 2.6	0-15
Short-Term/Working Memory			
Visual, *VPT*[n]	7.6 ± 1.7	7.6 ± 1.7	4-12
Visual spatial STM, *BTT fw*[n]	6.5 ± 1.8	6.4 ± 1.7	1-12
Visual spatial WM, *BTT bw*[n]	4.8 ± 1.8	4.8 ± 1.8	0-12
Verbal STM, *ZNS fw*[n]	7.7 ± 2.0	7.7 ± 2.1	2-13
Verbal WM, *ZNS bw*[n]	6.8 ± 1.8	6.8 ± 1.8	2-18
Language			
Phonemic verbal fluency, *RWT B words*[n]	18.6 ± 6.5	18.6 ± 6.6	2-39
+ Concept shifting, *RWT G &R words*[n]	18.8 ± 6.2	18.9 ± 6.2	1-40
Semantic verbal fluency, *RWT Occupations*[n]	23.8 ± 6.9	23.7 ± 6.9	5-50
+ *Concept shifting, RWT Sports / Fruits*[n]	19.8 ± 4.8	19.9 ± 4.8	4-37
Vocabulary, WST[n]	30.8 ± 5.2	30.7 ± 5.1	2-41

Abbreviations: AKT, Alter-Konzentrations-test; TMT A, Trail Making test (part A); LPS50, Subtest 3 of "Leistungsprüfungssystem 50+"; FIVE, Fünf-Punkte-test; TMT B-A, Trail Making test part B minus Trail Making Test part A; FWI, Color-Word Interference Test; VGT, Verbaler Gedächtnistest; VPT, Visual-Pattern-test; STM, short-term memory; WM, working memory; BTT, Block-tapping test; fw, forwards; bw, backwards; ZNS, Zahlennachsprechen; RWT, Regensburger Wortflüssigkeitstest; WST, Wortschatztest; SD, standard deviation

[s] measured in seconds

[n] measured in number

3.1.4 local Gyrification Index Values

Mean lGI values were lowest in the DLPFC and highest in the IPL. The right hemisphere showed a broader range of lGI values than the left hemisphere over all regions (Table 6). (Nußbaum et al., 2019)

Table 6. Description of MRI scan local Gyrification Index (lGI) results in the lGI analysis group (n=590). From Nußbaum et al., 2019

Outcome	Mean ± SD	Range
Right Hemisphere		
DLPFC	2.64 ± 0.13	2.28-3.34
PCC/P	2.73 ± 0.17	2.19-3.27
IPL	2.93 ± 0.14	2.46-3.40
Left Hemisphere		
DLPFC	2.50 ± 0.13	2.10-2.92
PCC/P	2.76 ± 0.18	2.27-3.29
IPL	2.98 ± 0.13	2.63-3.40

Abbreviations: MRI, Magnetic Resonance Imaging; lGI, local Gyrification Index; DLPFC, dorsolateral prefrontal cortex; PCC/P, posterior cingulate cortex and precuneus; IPL, inferior parietal lobule

3.2 AP, Noise, and Neuropsychological Tests

The discovery models with domain scores showed negative associations of AP and noise exposure with cognitive function belonging to the Language domain (Figure 3). For other domains, no consistent associations were found. (Nußbaum et al., 2019)

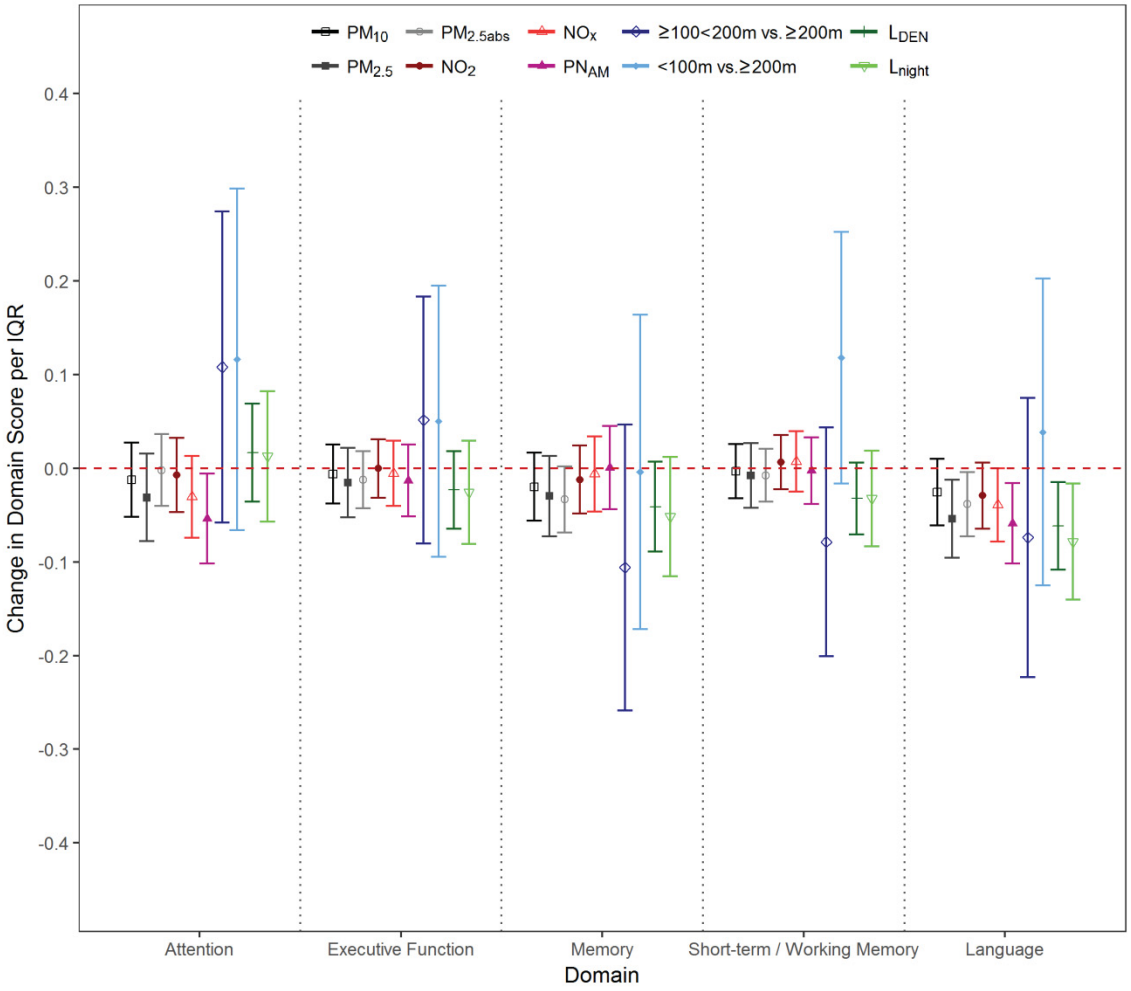

Figure 3. Beta estimates and 95% CI for the associations of AP and noise exposures with cognitive domain scores. N=615. Linear regression models were adjusted for age, sex, and SES (Discovery Model). From Nußbaum et al., 2019

In addition, all separate tests of the Language domain showed similar negative associations (Figure 4). (Nußbaum et al., 2019)

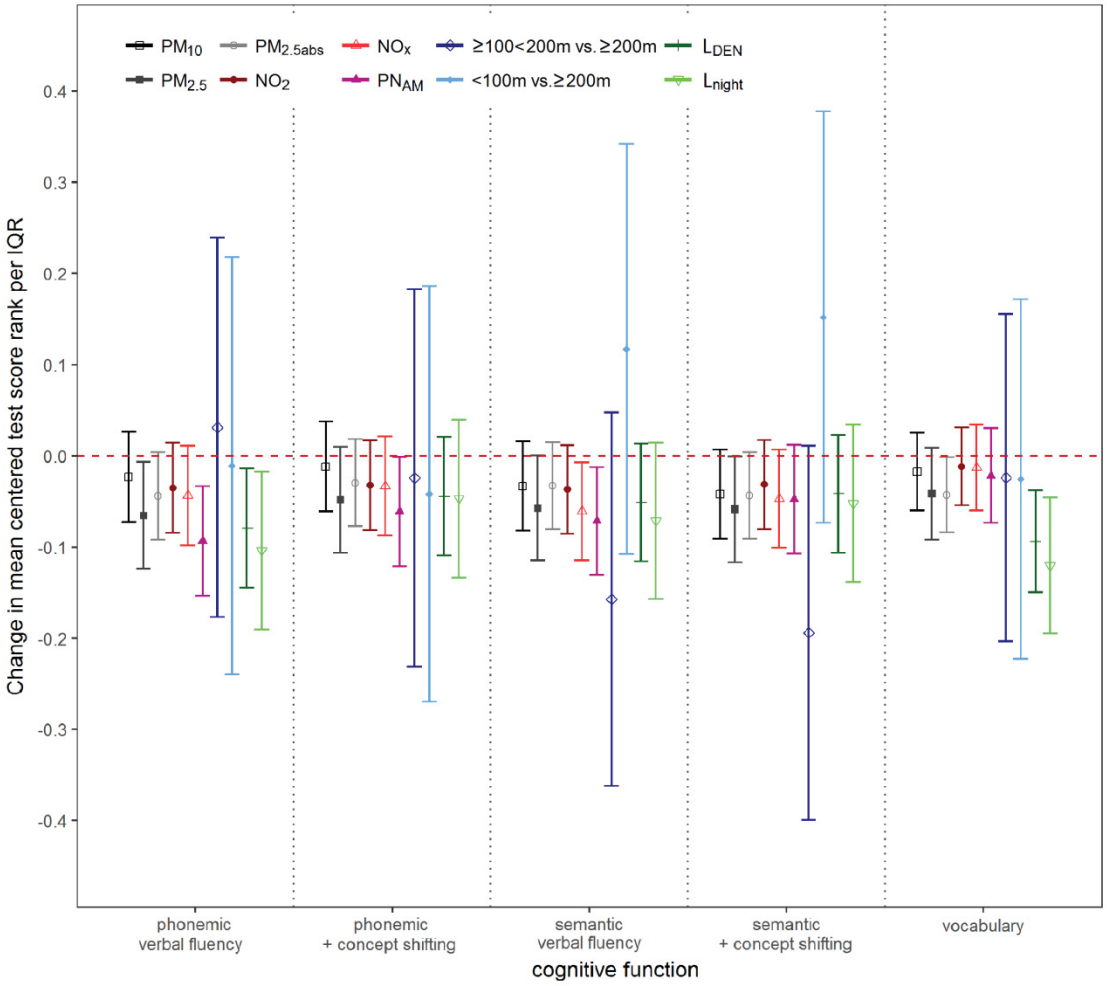

Figure 4. Beta estimates and 95% CI for the associations of AP and noise exposures with neuropsychological test results from the Language Domain. N=615. Linear regression models were adjusted for age, sex, and SES (Discovery Model). From Nußbaum et al., 2019

The individual tests in the Short Term/Working Memory domain showed diverging associations. AP exposure was positively associated with visual spatial short-term memory and negatively with verbal short-term memory (Figure 5). Noise exposure was negatively associated with visual working memory (Figure 5). (Nußbaum et al., 2019)

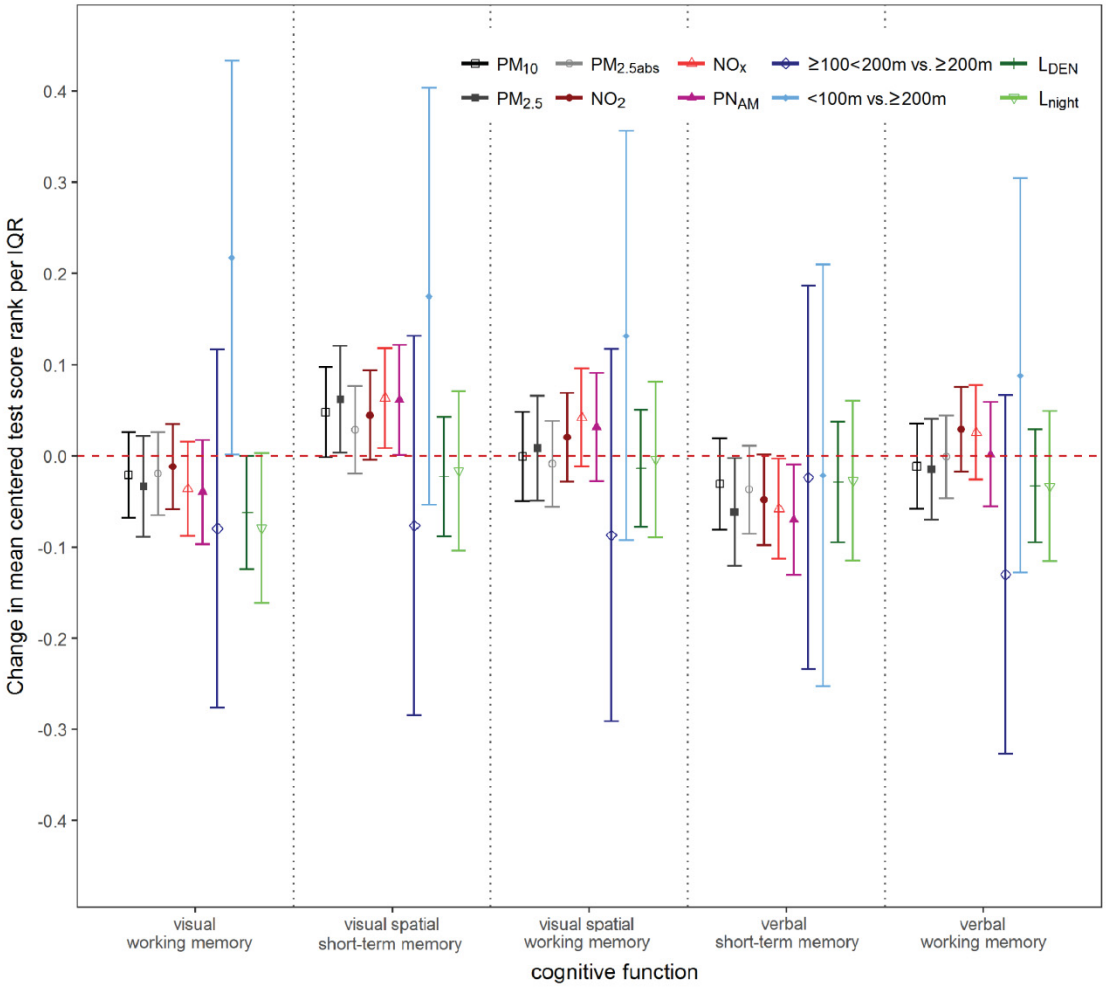

Figure 5. Beta estimates and 95% CI for the associations of AP and noise exposures with neuropsychological test results from the Short-Term/Working Memory Domain. N=615. Linear regression models were adjusted for age, sex, and SES (Discovery Model). From Nußbaum et al., 2019

The separate neuropsychological tests in the three other domains showed no clear pattern of association (Figures 6-8). (Nußbaum et al., 2019)

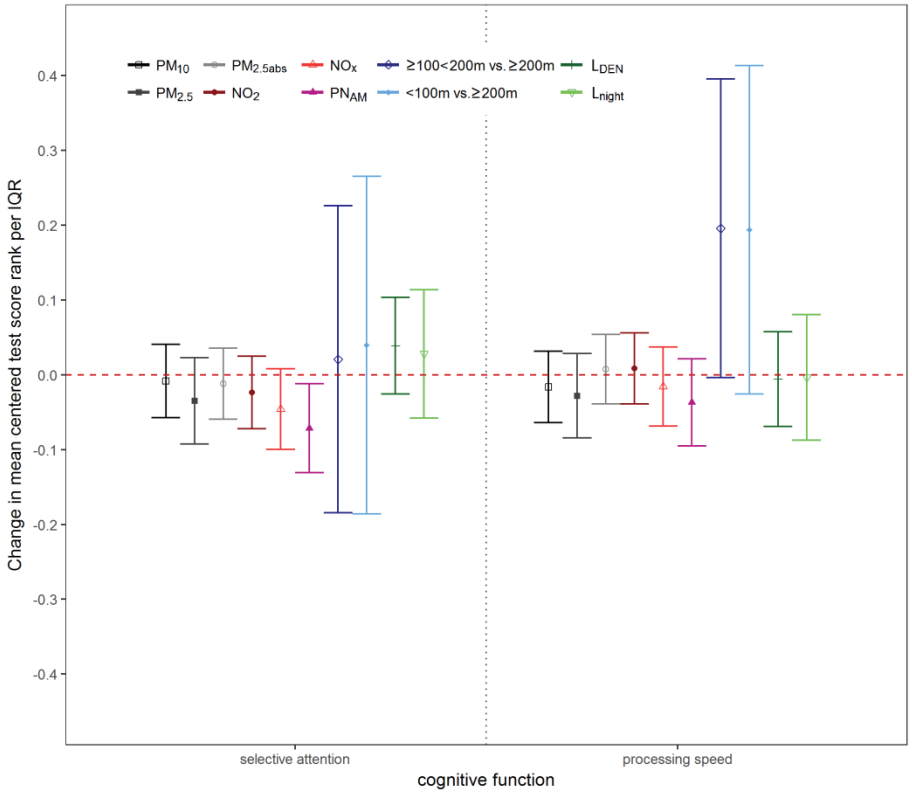

Figure 6. Beta estimates and 95% CI for the associations of AP and noise exposures with neuropsychological test results from the Attention Domain. N=615. Linear regression models were adjusted for age, sex, and SES (Discovery Model). From Nußbaum et al., 2019

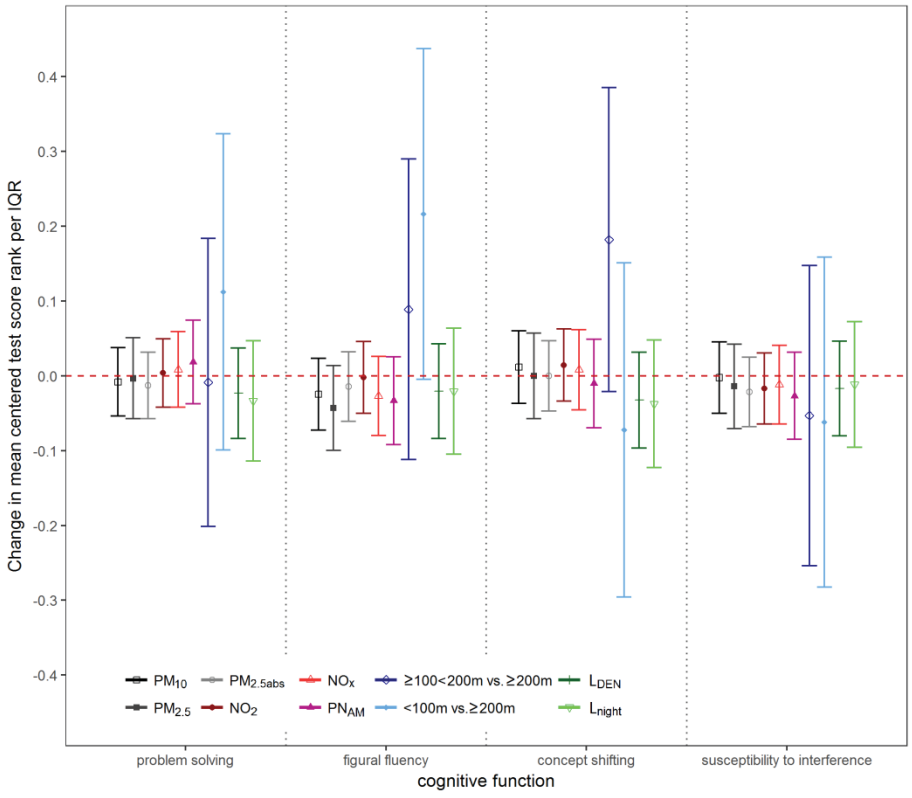

Figure 7. Beta estimates and 95% CI for the associations of AP and noise exposures with neuropsychological test results from the Executive Function Domain. N=615. Linear regression models were adjusted for age, sex, and SES (Discovery Model). From Nußbaum et al., 2019

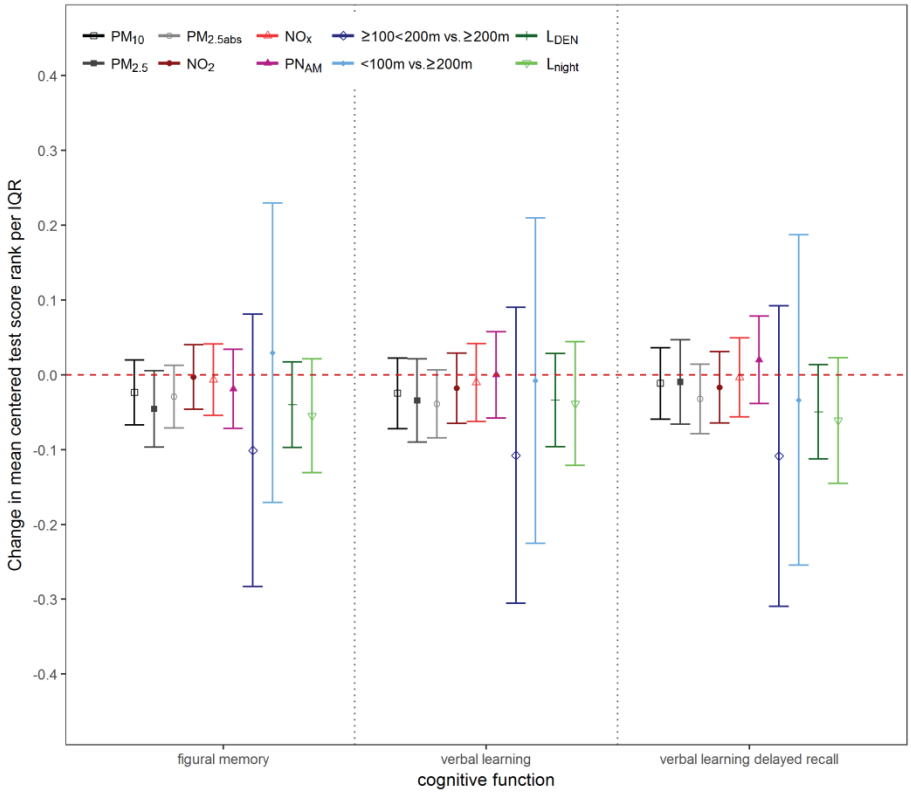

Figure 8. Beta estimates and 95% CI for the associations of AP and noise exposures with neuropsychological test results from the Memory Domain. N=615. Linear regression models were adjusted for age, sex, and SES (Discovery Model). From Nußbaum et al., 2019

Confidence Intervals (CIs) for all models were roughly around the same size, except for models with nighttime noise which CIs were approximately two times wider and models with distance to the nearest road which CIs were three times wider in comparison to the other models.

All estimates were attenuated in the further adjusted models when adding lifestyle variables and especially when adding neighborhood unemployment rate (Tables S1-S5). (Nußbaum et al., 2019)

3.3 AP, Noise, and Brain Structure

3.3.1 Right Hemisphere

The main models showed associations of IQR increases in PM_{10}, $PM_{2.5}$, NO_x, and NO_2 and lower IGI values in the right PCC/P (e.g., -0.02 [95% confidence interval (CI): -0.04, 0.00] per 1.4 µg/m^3 $PM_{2.5}$) and the right IPL (e.g., -0.01 [95% CI: -0.03, 0.00] per 5.3 µg/m^3 NO_2; Figure 9). AP associations in the right DLPFC were less clear, but an IQR increase in PN_{AM} was associated with lower

IGI values (-0.02 [95% CI: -0.04, 0.00]). Contrary, 10 dB[A] increases in L_{night} and in L_{DEN} showed an association with higher IGI values in the DLPFC (e.g., 0.03 [95% CI: 0.00, 0.05] for L_{night}; Figure 9). The two other regions had no associations with noise exposures. Lastly, participants who lived between 100 m and 200 m from a heavily trafficked road had lower IGI values in the right DLPFC (-0.06 [95% CI: -0.12, -0.01]) and in the PCC/P (-0.07 [95% CI: -0.13, 0.00]) than participants who lived 200 m or more from a heavily trafficked road (Figure 9). (Nußbaum et al., 2019)

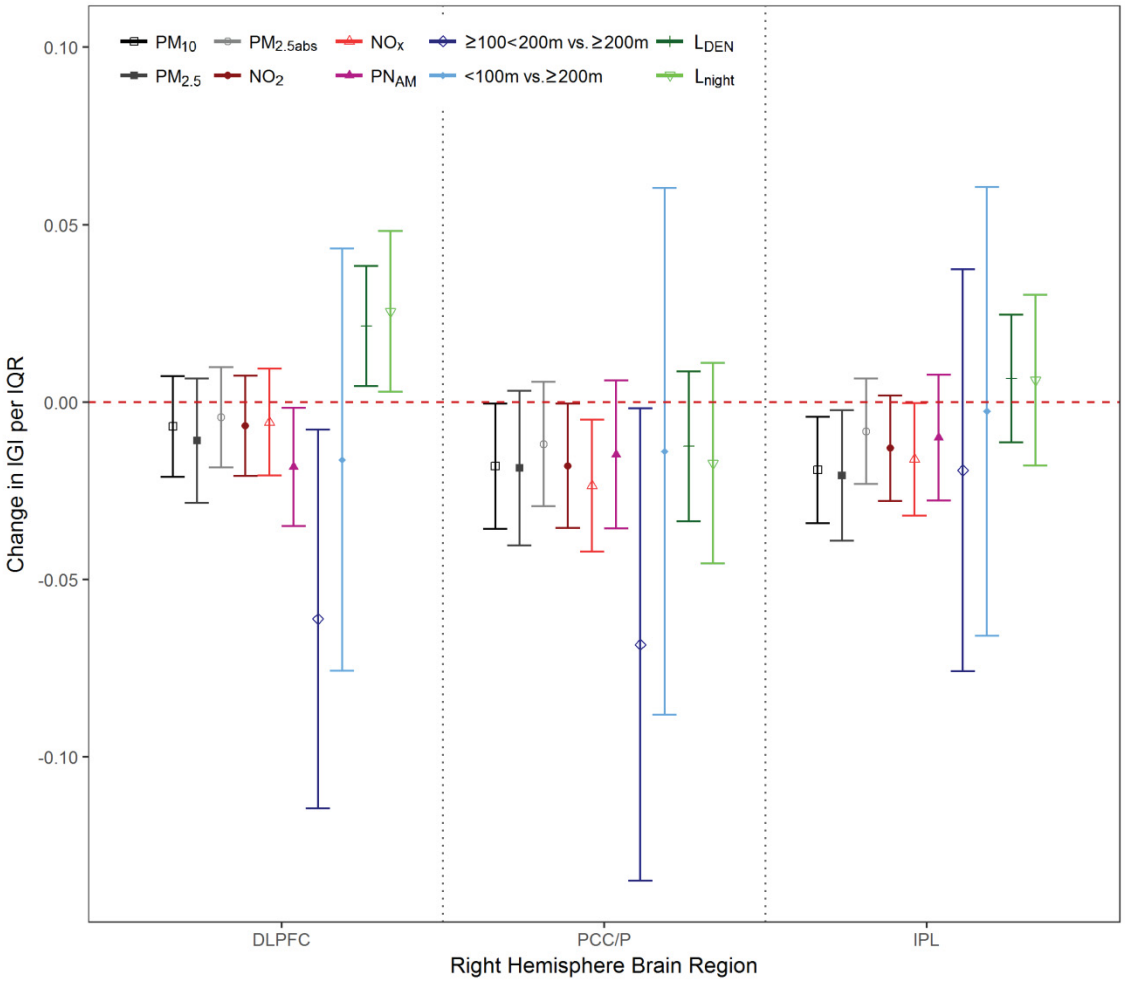

Figure 9. Beta estimates and 95% CI for the associations of AP and noise exposures with IGI in the DLPFC, PCC/P, and IPL of the right hemisphere. N=590. Linear regression models were adjusted for age, sex, SES, alcohol consumption, smoking status, cumulative pack-years, ETS, physical activity, and neighborhood unemployment rate (Main Model). Abbreviations: IGI, local Gyrification Index; DLPFC, dorsolateral prefrontal cortex; PCC/P, posterior cingulate cortex and precuneus; IPL, inferior parietal lobule. From Nußbaum et al., 2019

3.3.1 Left Hemisphere

No stringent pattern of associations was found between the left hemispheric lGI values and AP or noise exposures (Figure 10). (Nußbaum et al., 2019)

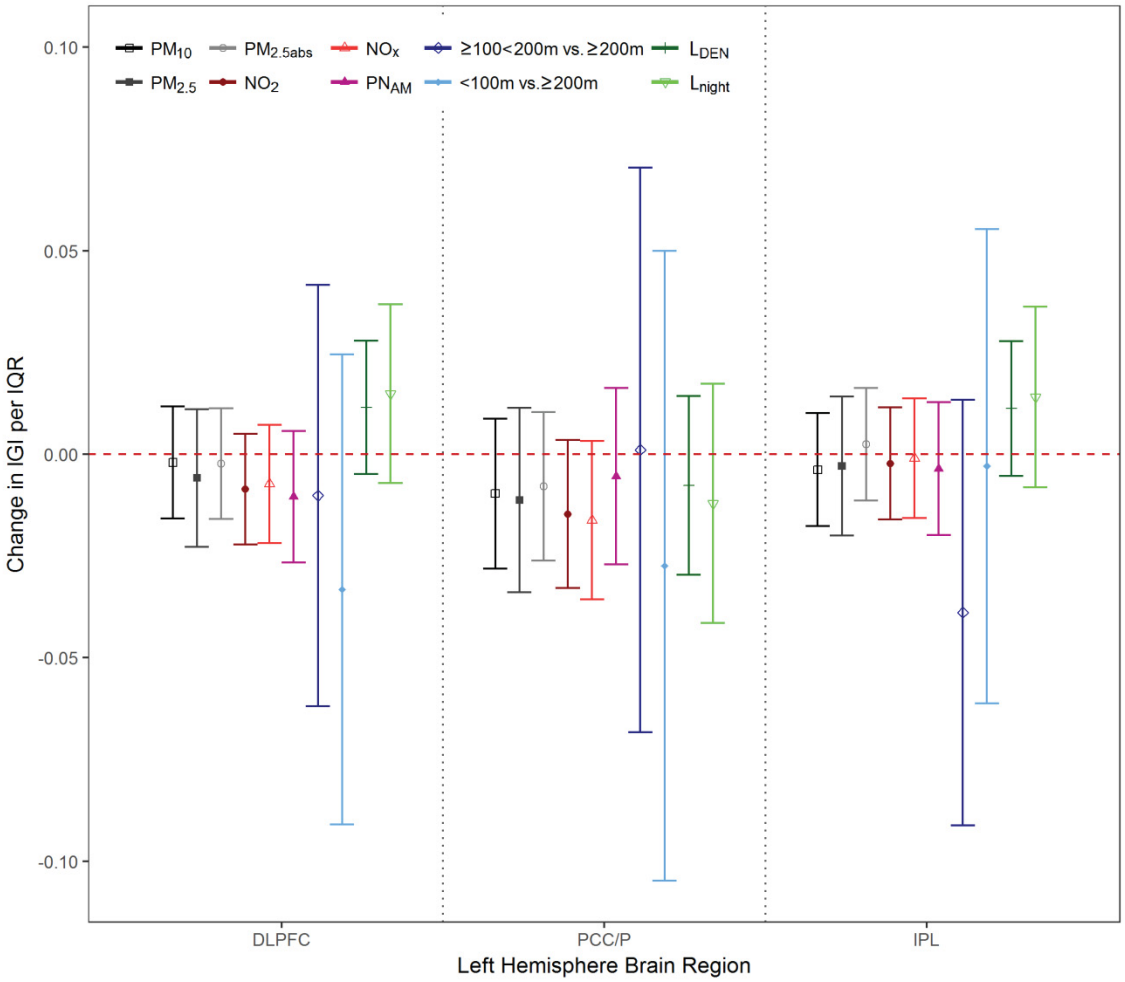

Figure 10. Beta estimates and 95% CI for the associations of AP and noise exposures with lGI in the DLPFC, PCC/P, and IPL of the left hemisphere. N=590. Linear regression models were adjusted for age, sex, SES, alcohol consumption, smoking status, cumulative pack-years, ETS, physical activity, and neighborhood unemployment rate (Main Model). Abbreviations: lGI, local Gyrification Index; DLPFC, dorsolateral prefrontal cortex; PCC/P, posterior cingulate cortex and precuneus; IPL, inferior parietal lobule. From Nußbaum et al., 2019

The estimates for all crude, base and main models for both hemispheres can be seen in Table S6. (Nußbaum et al., 2019)

3.4 Effect Modification

3.4.1 Age

In the right PCC/P, the effect modification analysis for age showed lower IGI values in association to PN_{AM} exposure for participants 61 years or older compared with participants younger than 61 (lr-test: 0.02; Figure 11, d); also subgroup 'Young' showed lower IGI values in association to weighted 24h (lr-test: 0.04) and nighttime (lr-test: 0.03) noise exposure than subgroup 'Old' (Figure 12, e-f). In the left DLPFC, subgroup 'Old' showed higher IGI values in association to weighted 24h (lr-test: 0.04) and nighttime (lr-test: 0.02) noise exposure than subgroup 'Young' (Figure 12, e-f). For other AP/noise exposures and brain regions, no effect modification by age was found (Figure 11, a-c, and Figure 12, a-d).

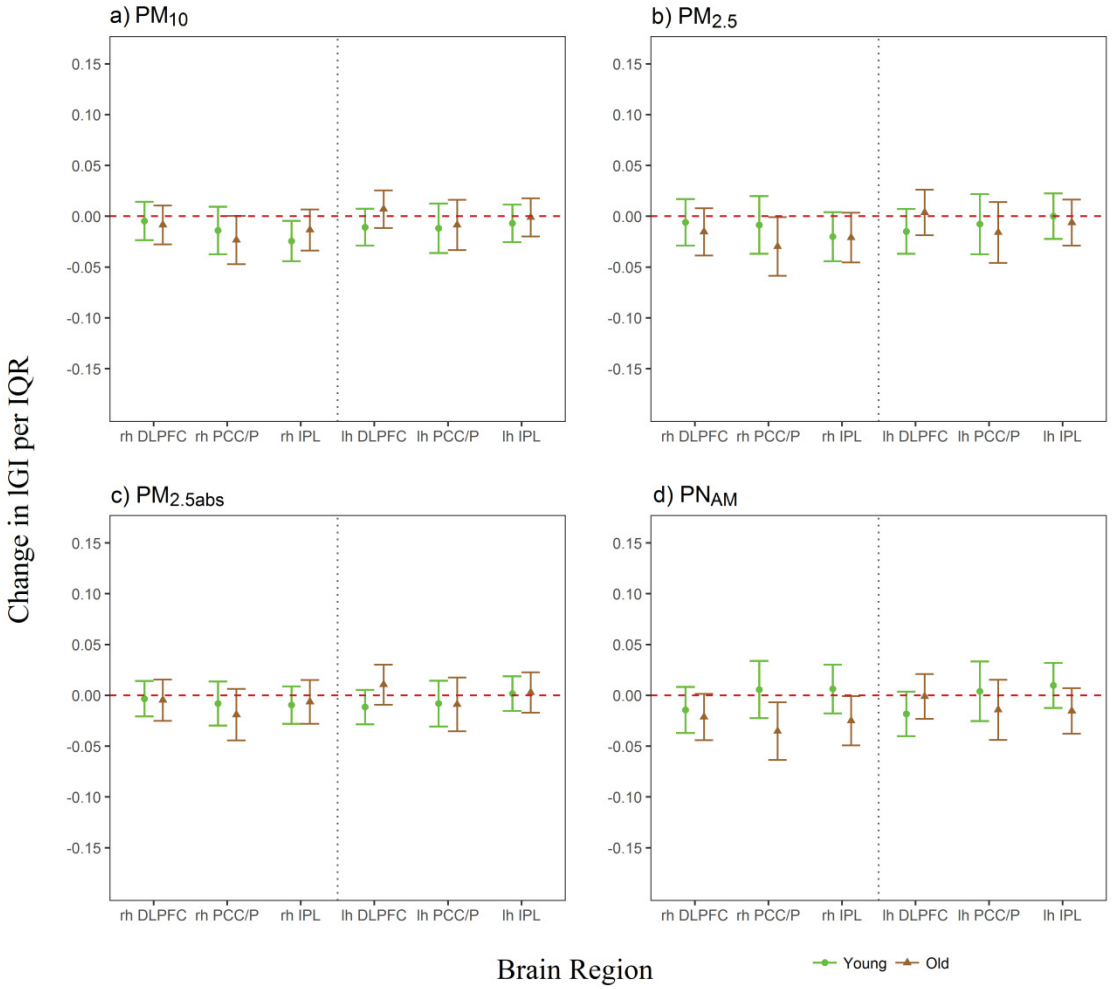

Figure 11. Beta estimates and 95% CI for the associations of particulate matter and IGI values in all brain regions by age (<61 years [Young] and ≥61 years [Old]). N=590. Linear regression models were adjusted for age (dichotomized at the median of 61), sex, SES, alcohol consumption, smoking status, cumulative pack-years, ETS, physical activity, and neighborhood unemployment rate. Age was also included as product term. Abbreviations: IGI, local

Gyrification Index; IQR, interquartile range; rh, right hemisphere; lh, left hemisphere; DLPFC, dorsolateral prefrontal cortex; PCC/P, posterior cingulate cortex and precuneus; IPL, inferior parietal lobule.

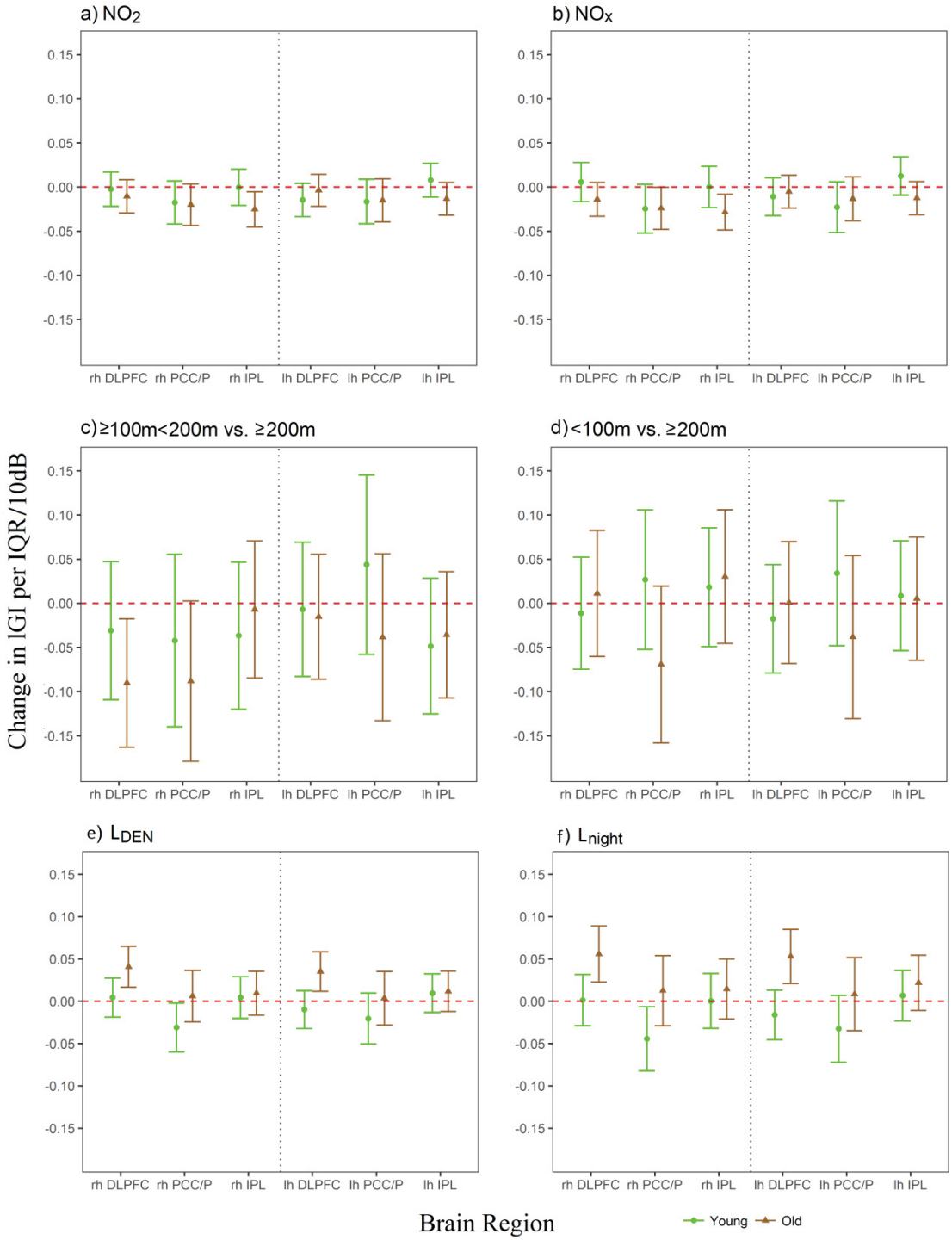

Figure 12. Beta estimates and 95% CI for the associations of nitrogen oxides, distance to the nearest major road, noise exposure and lGI values in all brain regions by age (<61 years [Young] and ≥61 years [Old]). N=590. Linear regression models were adjusted for age (dichotomized at the median of 61), sex, SES, alcohol consumption, smoking status, cumulative pack-years, ETS, physical activity, and neighborhood unemployment rate. Age was also included as product term. Abbreviations: lGI, local Gyrification Index; IQR, interquartile range; rh, right hemisphere; lh, left hemisphere; DLPFC, dorsolateral prefrontal cortex; PCC/P, posterior cingulate cortex and precuneus; IPL, inferior parietal lobule.

3.4.2 Smoking Status

In the left PCC/P, the effect modification analysis for smoking status showed higher lGI values in association to PN_{AM} exposure for current smokers in comparison to never smokers and ex- smokers (lr-test: 0.004; Figure 13, d). For other AP and noise exposures and brain regions, no effect modification by smoking status was found (Figure 13, a-c, and Figure 14).

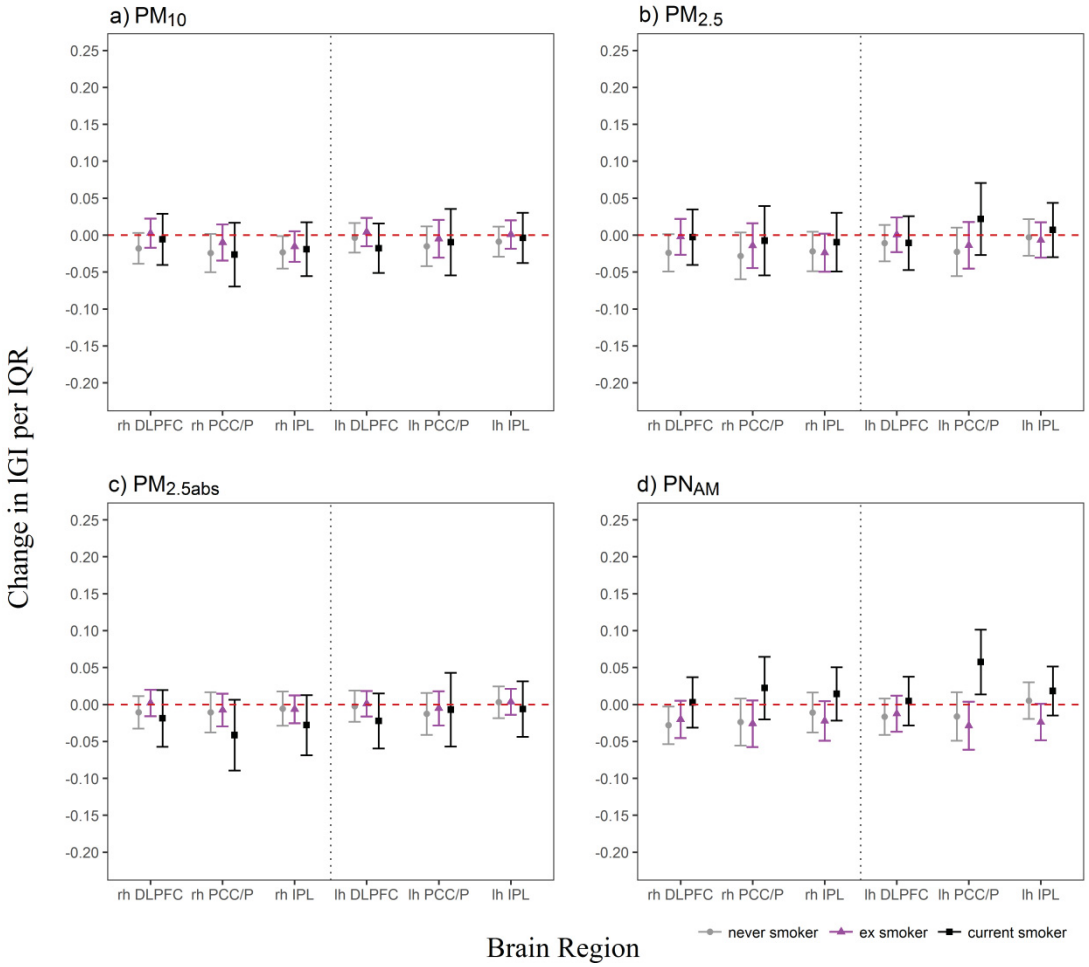

Figure 13. Beta estimates and 95% CI for the associations of particulate matter and lGI values in all brain regions by smoking status (never smoker, ex-smoker, and current smoker). N=590. Linear regression models were adjusted for age, sex, SES, alcohol consumption, smoking status, cumulative pack-years, ETS, physical activity, and neighborhood unemployment rate. Smoking status was also included as product term. Abbreviations: lGI, local Gyrification Index; IQR, interquartile range; rh, right hemisphere; lh, left hemisphere; DLPFC, dorsolateral prefrontal cortex; PCC/P, posterior cingulate cortex and precuneus; IPL, inferior parietal lobule.

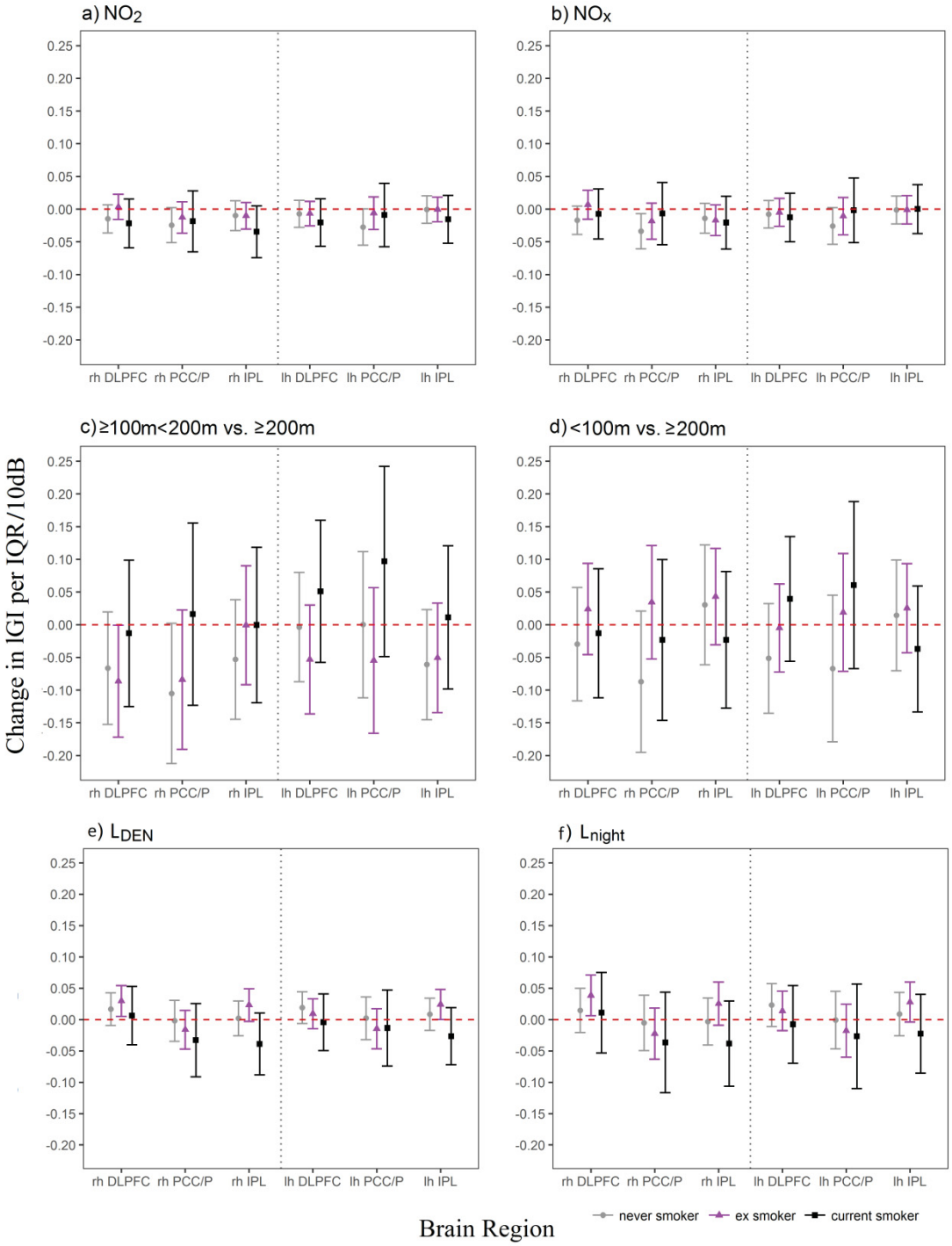

Figure 14. Beta estimates and 95% CI for the associations of nitrogen oxides, distance to the nearest major road, noise exposure and lGI values in all brain regions by smoking status (never smoker, ex-smoker, and current smoker). N=590. Linear regression models were adjusted for age, sex, SES, alcohol consumption, smoking status, cumulative pack-years, ETS, physical activity, and neighborhood unemployment rate. Smoking status was also included as product term. Abbreviations: lGI, local Gyrification Index; IQR, interquartile range; rh, right hemisphere; lh, left hemisphere; DLPFC, dorsolateral prefrontal cortex; PCC/P, posterior cingulate cortex and precuneus; IPL, inferior parietal lobule.

3.4.3 Sex and SES

No effect modification by sex or SES was found (Figures 15-18).

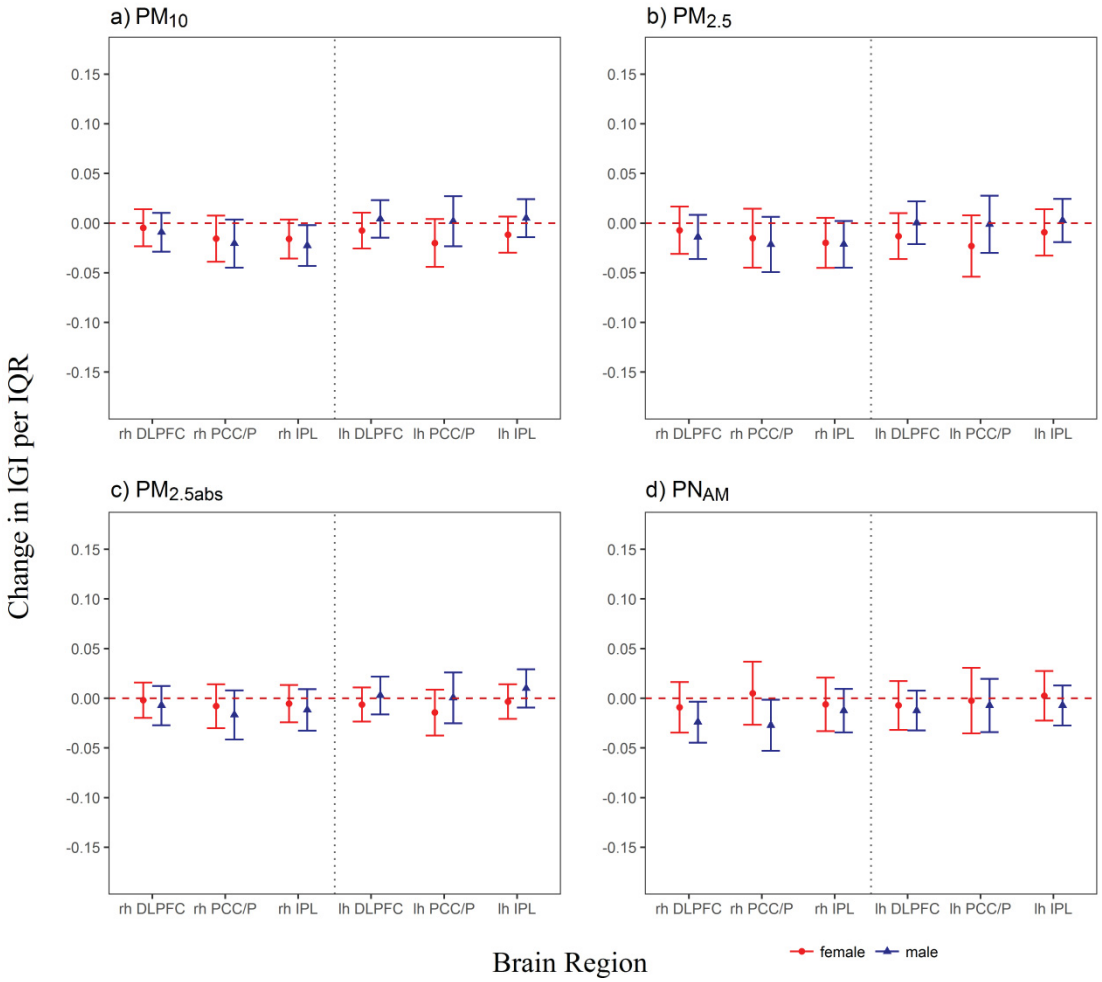

Figure 15. Beta estimates and 95% CI for the associations of particulate matter and lGI values in all brain regions by sex. N=590. Linear regression models were adjusted for age, sex, SES, alcohol consumption, smoking status, cumulative pack-years, ETS, physical activity, and neighborhood unemployment rate. Sex was also included as product term. Abbreviations: lGI, local Gyrification Index; IQR, interquartile range; rh, right hemisphere; lh, left hemisphere; DLPFC, dorsolateral prefrontal cortex; PCC/P, posterior cingulate cortex and precuneus; IPL, inferior parietal lobule.

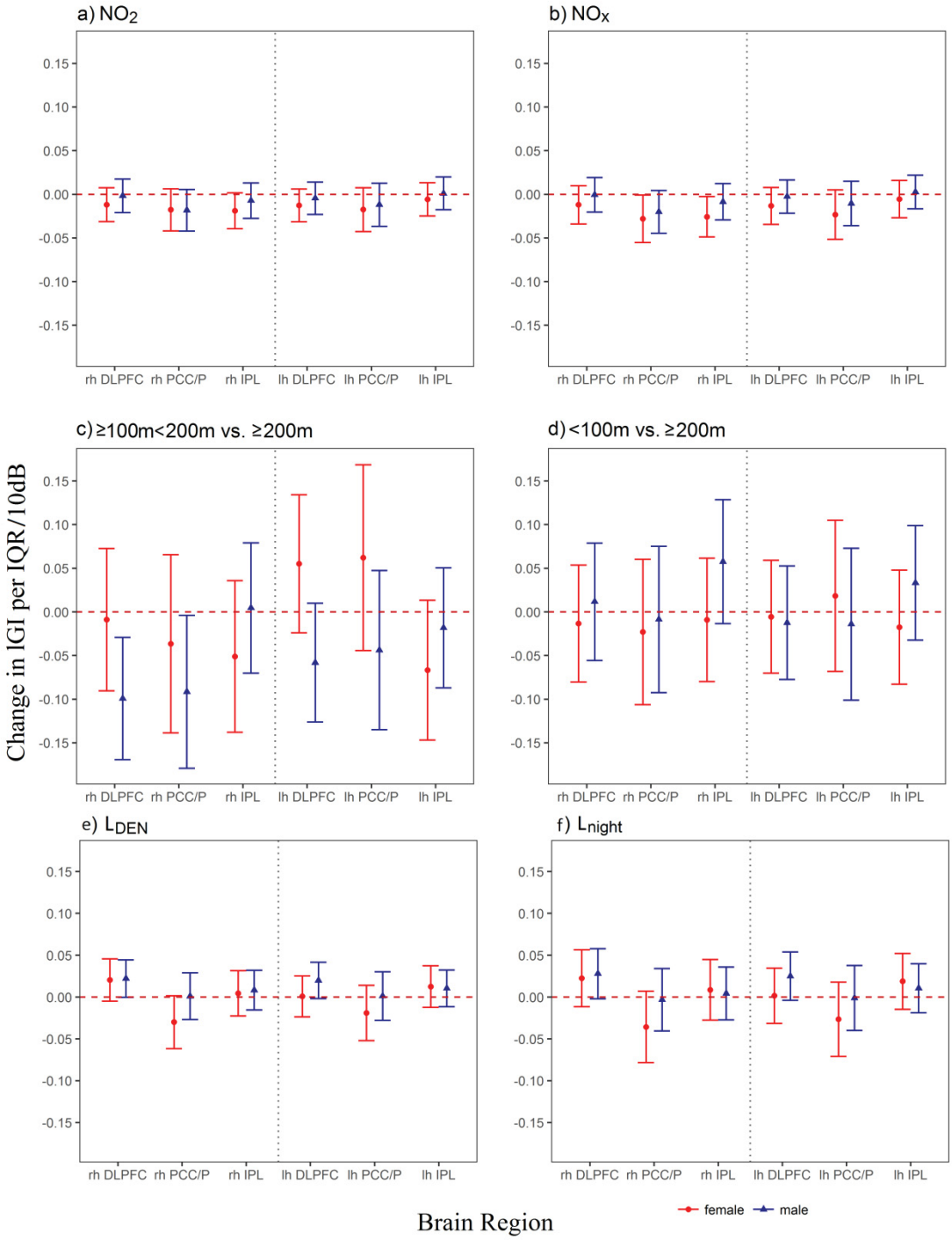

Figure 16. Beta estimates and 95% CI for the associations of nitrogen oxides, distance to the nearest major road, noise exposure and IGI values in all brain regions by sex. N=590. Linear regression models were adjusted for age, sex, SES, alcohol consumption, smoking status, cumulative pack-years, ETS, physical activity, and neighborhood unemployment rate. Sex was also included as product term. Abbreviations: IGI, local Gyrification Index; IQR, interquartile range; rh, right hemisphere; lh, left hemisphere; DLPFC, dorsolateral prefrontal cortex; PCC/P, posterior cingulate cortex and precuneus; IPL, inferior parietal lobule.

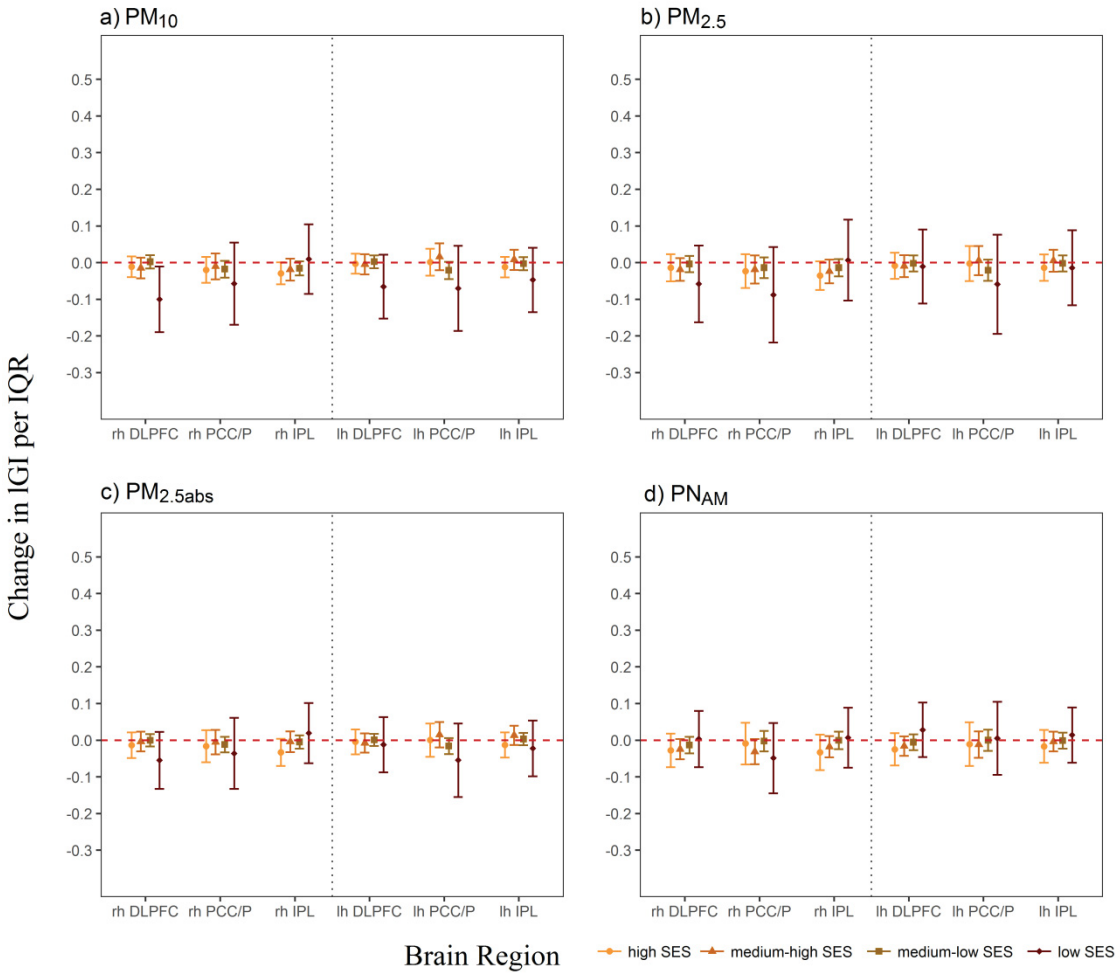

Figure 17. Beta estimates and 95% CI for the associations of particulate matter and lGI values in all brain regions by SES (high, medium-high, medium-low, and low). N=590. Linear regression models were adjusted for age, sex, SES, alcohol consumption, smoking status, cumulative pack-years, ETS, physical activity, and neighborhood unemployment rate. SES was also included as product term. Abbreviations: lGI, local Gyrification Index; IQR, interquartile range; rh, right hemisphere; lh, left hemisphere; DLPFC, dorsolateral prefrontal cortex; PCC/P, posterior cingulate cortex and precuneus; IPL, inferior parietal lobule.

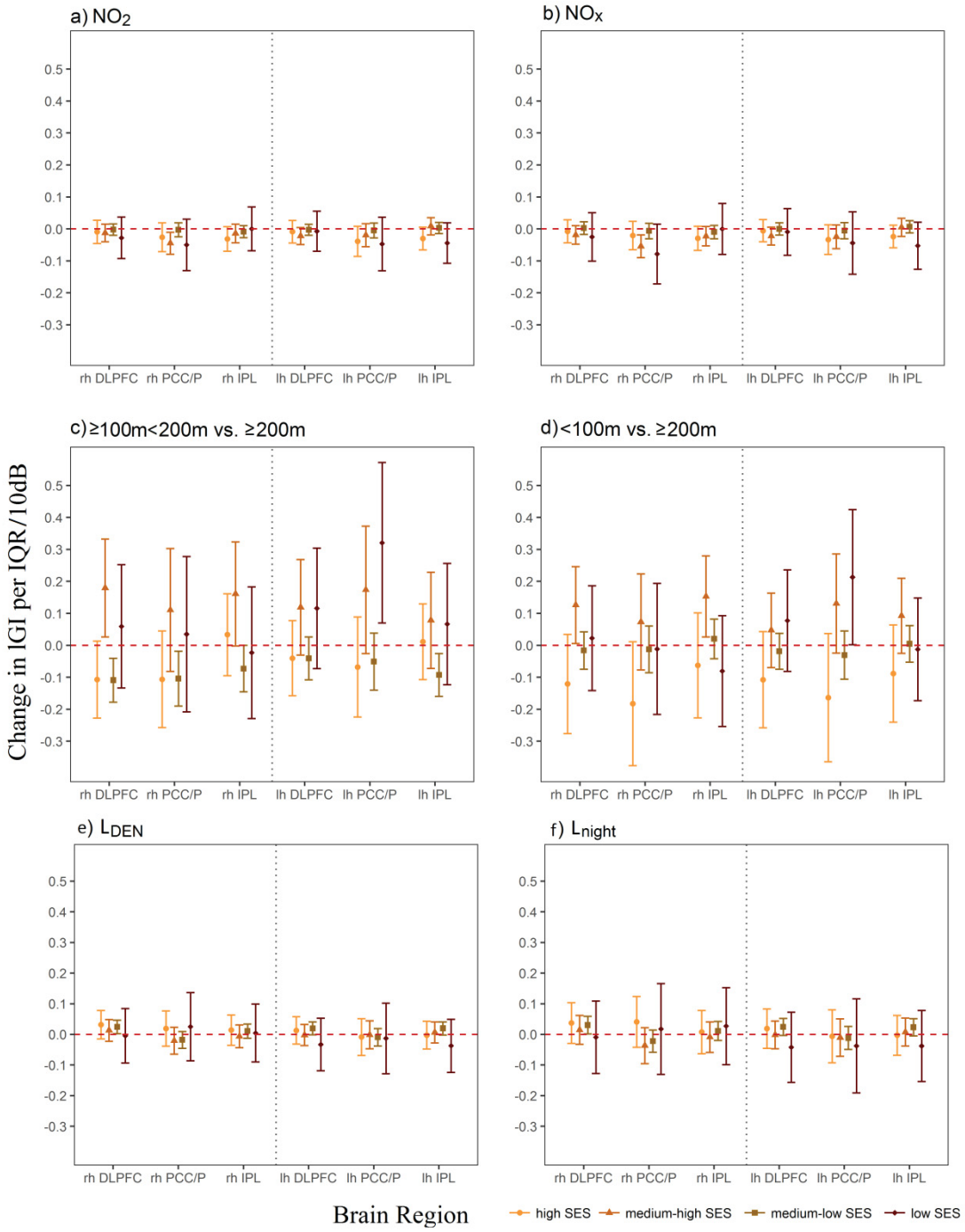

Figure 18. Beta estimates and 95% CI for the associations of nitrogen oxides, distance to the nearest major road, noise exposure and IGI values in all brain regions by SES (high, medium-high, medium-low, and low). N=590. Linear regression models were adjusted for age, sex, SES, alcohol consumption, smoking status, cumulative pack-years, ETS, physical activity, and neighborhood unemployment rate. SES was also included as product term. Abbreviations: IGI, local Gyrification Index; IQR, interquartile range; rh, right hemisphere; lh, left hemisphere; DLPFC, dorsolateral prefrontal cortex; PCC/P, posterior cingulate cortex and precuneus; IPL, inferior parietal lobule.

3.5 Sensitivity Analysis

3.5.1 BMI, CHD, depression, and diabetes

The individual addition of BMI, CHD, depression, and diabetes in the sensitivity analyses did not change the results of the main model (Figures 19-20). (Nußbaum et al., 2019)

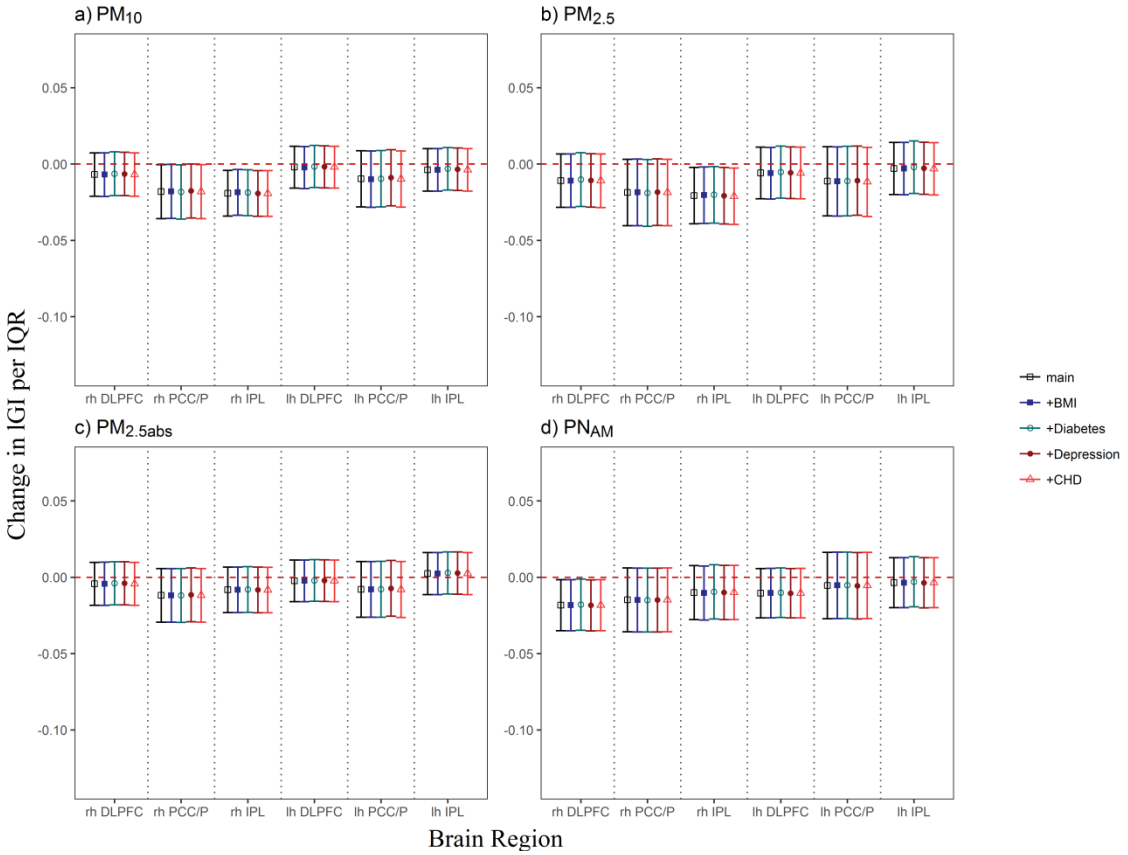

Figure 19. Beta estimates and 95% CI for the associations of particulate matter and IGI values in all brain regions. N=590. The Main model was adjusted for age, sex, SES, alcohol consumption, smoking status, cumulative pack-years, ETS, physical activity, and neighborhood unemployment rate. Sensitivity models separately included BMI, Diabetes, Depression, and CHD in addition to the main model. Abbreviations: IGI, local Gyrification Index; IQR, interquartile range; DLPFC, dorsolateral prefrontal cortex; PCC/P, posterior cingulate cortex and precuneus; IPL, inferior parietal lobule; CHD, coronary heart disease diagnosis; lh, left hemisphere; rh, right hemisphere. From Nußbaum et al., 2019

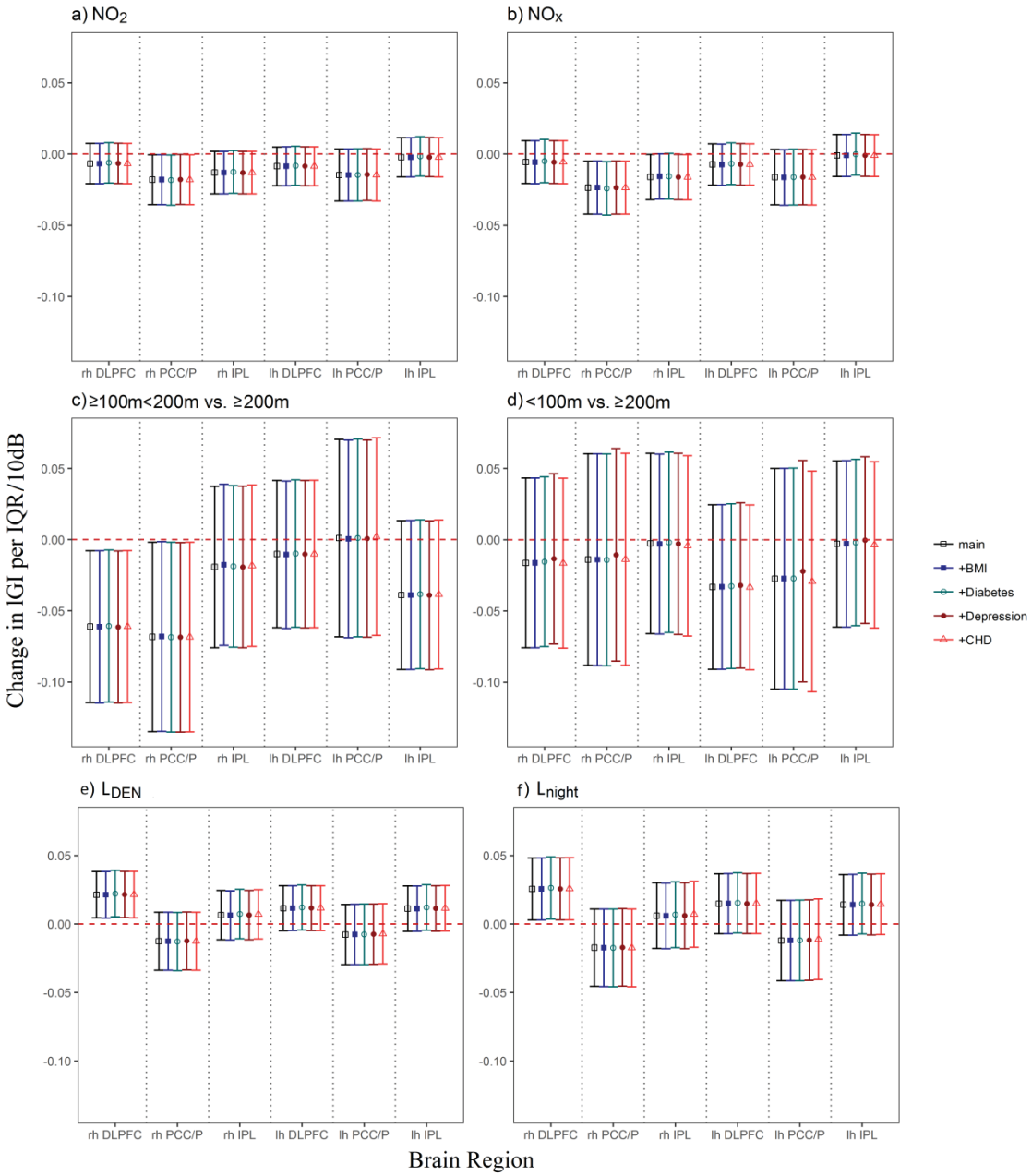

Figure 20. Beta estimates and 95% CI for the associations of nitrogen oxides, distance to the nearest major road, noise exposure and IGI values in all brain regions. N=590. The Main model was adjusted for age, sex, SES, alcohol consumption, smoking status, cumulative pack-years, ETS, physical activity, and neighborhood unemployment rate. Sensitivity models separately included BMI, Diabetes, Depression, and CHD in addition to the main model. Abbreviations: IGI, local Gyrification Index; IQR, interquartile range; DLPFC, dorsolateral prefrontal cortex; PCC/P, posterior cingulate cortex and precuneus; IPL, inferior parietal lobule; CHD, coronary heart disease diagnosis; lh, left hemisphere; rh, right hemisphere. Modified from Nußbaum et al., 2019

3.5.2 Non-working participants only and two-exposure models

Generally, CIs got wider in the non-working and two-exposure analyses and associations between AP exposure and lGI values were attenuated (Figure 21 and Figure 22, a-d). Associations between noise exposures and lGI values were robust to sensitivity analysis among non-working people only and with double exposure models (Figure 22, e-f).

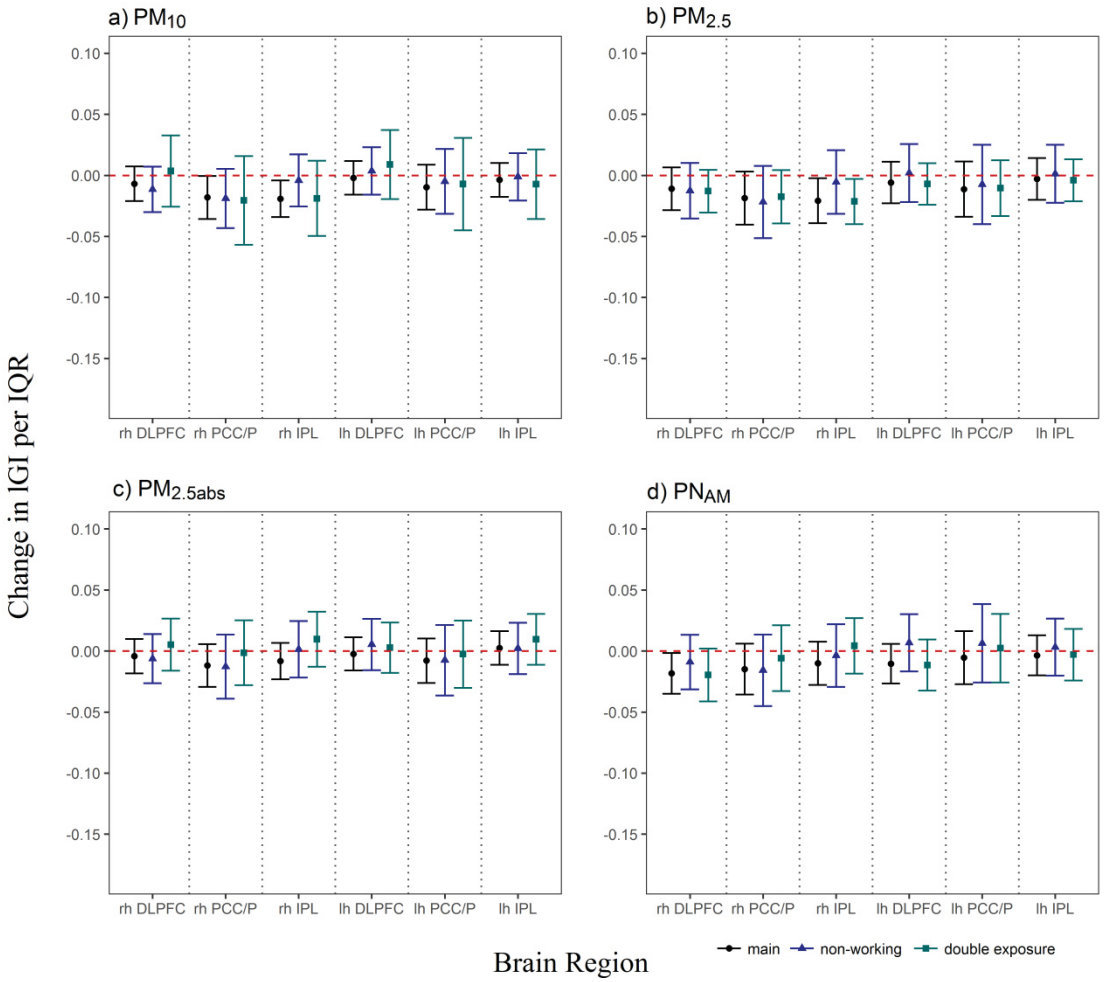

Figure 21. Beta estimates and 95% CI for the associations of particulate matter and lGI values in all brain regions. N=590. The Main model was adjusted for age, sex, SES, alcohol consumption, smoking status, cumulative pack-years, ETS, physical activity, and neighborhood unemployment rate. Sensitivity models included running the analysis among non-working people only (n=310) and adding $PM_{2.5}$ to the main model (L_{night} to the $PM_{2.5}$ model) for the double exposure analysis. Abbreviations: lGI, local Gyrification Index; IQR, interquartile range; DLPFC, dorsolateral prefrontal cortex; PCC/P, posterior cingulate cortex and precuneus; IPL, inferior parietal lobule; lh, left hemisphere; rh, right hemisphere

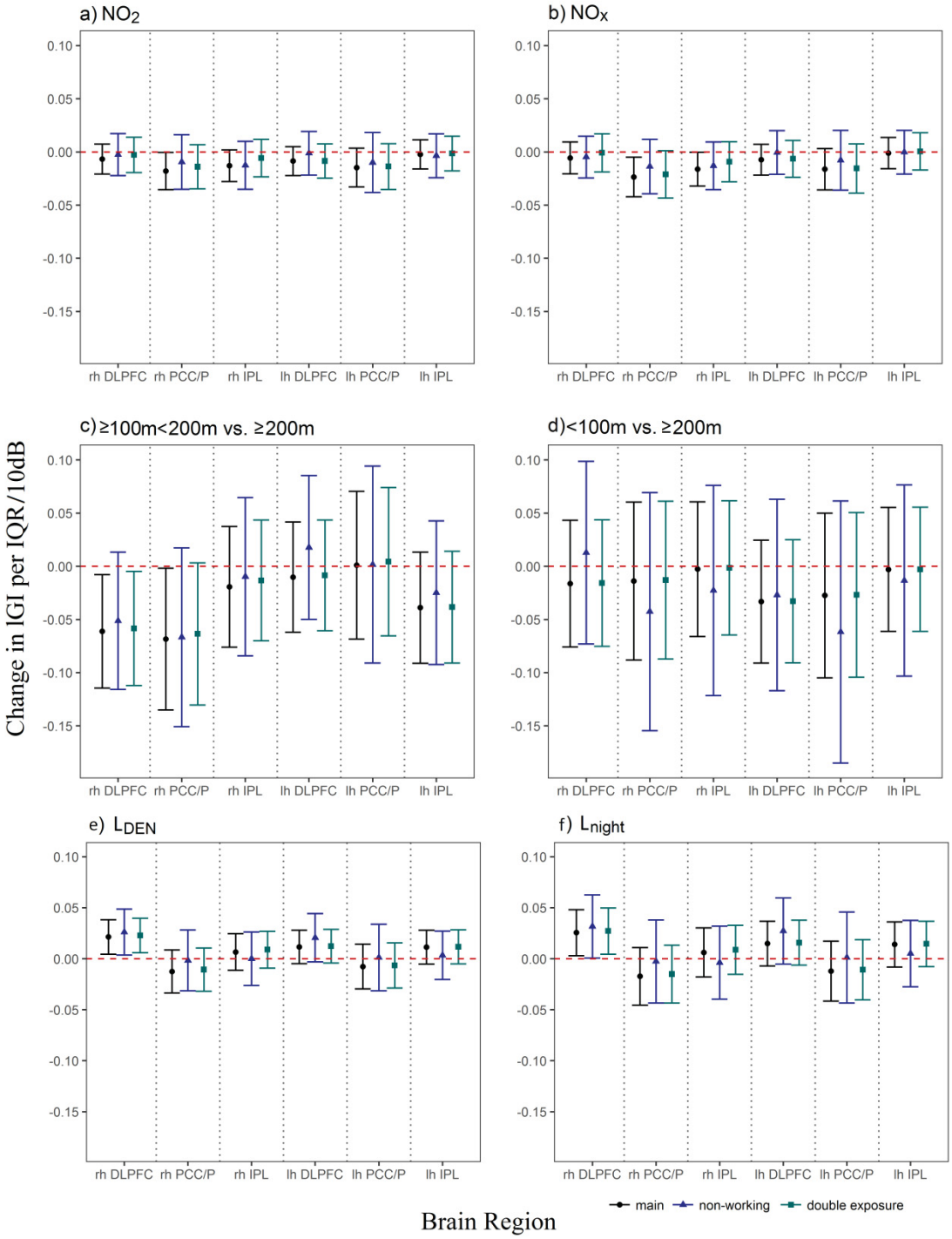

Figure 22. Beta estimates and 95% CI for the associations of nitrogen oxides and distance to the nearest major road and lGI values in all brain regions. N=590. The Main model was adjusted for age, sex, SES, alcohol consumption, smoking status, cumulative pack-years, ETS, physical activity, and neighborhood unemployment rate Sensitivity models included running the analysis among non-working people only (n=310) and adding $PM_{2.5}$ to the main model (L_{night} to the $PM_{2.5}$ model) for the double exposure analysis.. Abbreviations: lGI, local Gyrification Index; IQR, interquartile range; DLPFC, dorsolateral prefrontal cortex; PCC/P, posterior cingulate cortex and precuneus; IPL, inferior parietal lobule; lh, left hemisphere; rh, right hemisphere

4 Discussion

4.1 Summary of the Results

Long-term AP and noise exposure showed associations with neurocognitive test performance that can be assigned to the domains of Short-Term/Working Memory and Language. On this foundation, further structural MRI analyses focused on the functionally relevant FPN. (Nußbaum et al. 2019)

AP exposures showed negative associations with right hemispheric lGI values over all three regions of the FPN. Noise exposures showed a positive association in the frontal region. In the left hemisphere, no associations between exposures and lGI could be seen. (Nußbaum et al., 2019)

In addition, some suggestive evidence for effect modification by age and by smoking status was found, but none for sex and SES. Sensitivity analysis showed robustness of all models to separately adding BMI, diabetes, depression, and CHD. AP models were attenuated by analysis among non-working participants only and double exposure analysis with noise models being also robust to these.

4.2 Interpretation of the Results

4.2.1 Main Results

The aim of this thesis was to research associations between long-term AP and noise exposure and local structural changes in the brain coinciding with cognitive performance losses. As structural feature for investigation the local gyrification index was chosen, as it is a marker of regional brain atrophy in the aging brain. (Nußbaum et al., 2019)

In addition, effect modification and sensitivity analysis were meant to open up ways of further research in the directions of possible mediating and modulating effects by demographic and lifestyle variables.

Prior studies featured associations between $PM_{2.5}$, PM_{10}, and $Dist_{majroad}$ and lower total, grey and white matter volumes as markers for brain structure (Casanova et al., 2016; Chen et al., 2015; Power et al., 2018; Wilker et al.,

2015). These studies along with the findings in this thesis of regional alteration of brain structure, further the possibility of the presence of an association between AP and brain atrophy in function-specific regions during the physiological aging process. (Nußbaum et al., 2019)

4.2.1.1 Right Hemi-Aging Theory

Only the lGI values of the right hemispheric DLPFC, PPC/P, and IPL showed a negative association with AP exposure. (Nußbaum et al., 2019)

The right hemi-aging theory (Albert and Moss, 1988; Brown and Jaffe, 1975; Dolcos et al., 2002; Goldstein and Shelly, 1981; Grady et al., 1994) delivers an explanation for the solely right hemispheric effect. The right hemi-aging theory is based on the observation that functional alterations during physiological aging occur earlier in the right hemisphere than in the left hemisphere of the brain. It is suggested that the right hemisphere might age faster and accumulate changes attributable to aging to a greater extend. Although at first only supported by neuropsychological test data and thus driven by brain function, present literature also shows support for the theory when looking at brain structure (e.g. Jockwitz et al., 2017; Kovalev et al., 2003) and functional connectivity (e.g. Lu et al., 2011). This leads to the conclusion that AP exposure might speed up normal aging related changes in the brain, also leading to a higher adverseness of endogenous or exogenous risk factors for damaging processes in the brain. (Nußbaum et al., 2019)

A slightly different, but in terms of patho-mechanisms also relevant, explanation to consider might be that AP already makes up for a portion of the physiological aging process of the brain which everyone experiences in his or her lifetime and which has been investigated so far without special consideration of AP. The current analysis might have been able to deduct and damask that there might actually be a portion of the physiological aging process that is attributable to AP exposure.

4.2.1.2 Posterior-Anterior Shift in Aging Theory

Overall, $PM_{2.5}$, PM_{10}, NO_X, and NO_2 had similar effects on local brain structure of the three observed brain areas of the right hemisphere. The right DLPFC was

not associated with these pollutants, whereas the right PCC/P and IPL showed decreases in lGI values with higher levels of exposure. (Nußbaum et al., 2019)

The posterior-anterior shift in aging theory (PASA; Davis et al., 2008) delivers an explanation for the missing effect on frontal brain areas. The PASA theory is based on the observation that, in aging participants, frontal brain areas showed more activation where posterior ones were less activated. It is suggested that this resembles compensational processes for a loss of functioning in the posterior areas. Although at first only supported by data on brain function, present literature also delivers support for the theory when looking at brain structure (e.g. Jockwitz et al., 2017). The theory indicates that functional damage in posterior areas might be compensated by higher levels of activation in frontal regions, perhaps triggering processes of brain plasticity, regional hypertrophy and higher lGI values in these more active regions. (Nußbaum et al., 2019)

PASA, as mentioned above, could explain why there was no effect on the frontal brain regions. Because of the compensatory processes, an adverse effect of $PM_{2.5}$, PM_{10}, NO_X, and NO_2 on the DLPFC could have been masked by opposing effects of hypertrophy. (Nußbaum et al., 2019)

As current mechanistic pathways for the effects of PM, NO_2, and NOx direct and indirect effects on the body via inhalation through the lungs are assumed (WHO Regional Office for Europe, 2013). They might also have an impact on the brain via indirect triggering of systemic and local inflammation. These would be processes that could affect all of the observed brain regions via the cerebral arteries (Block and Calderón-Garcidueñas, 2009; Jayaraj et al., 2017). (Nußbaum et al., 2019)

In this context, it is of interest whether differences in hemodynamics and overall blood flow between different brain areas contribute to a different accessibility of AP effects to the brain tissue. If, in frontal brain regions, the higher blood flow – as implied by PASA - and thus different hemodynamic behavior is accompanied by a lower accessibility of AP effects to the brain tissue, this would be a rivaling effect for the hypothesis of hypertrophy. On the other hand, a higher blood flow could also lead to a higher local exposure to AP effects, which would then

question the current findings. Therefore, this relationship between blood flow to a specific brain region and accessibility of adverse effects due to AP on the local brain tissue in question needs to be further investigated.

4.2.1.3 Special Role of PN_{AM}

PN_{AM} showed a single negative association with lGI values of the right hemispheric DLPFC. (Nußbaum et al., 2019)

The mechanistic pathway for PM, NO_2, and NOx, as mentioned above, is thought to be mainly via the cerebral arteries. PN_{AM}, on the other hand, is suggested to additionally impact the brain through another way. Following nasal intake, very small particles or small particle-induced inflammatory processes might be transported to frontal brain areas via axons from the olfactory nerve and the olfactory bulb (Elder et al., 2006; Oberdörster et al., 2004). The possibly resulting relatively high concentrations of PN_{AM} in frontal brain regions together with the right-hemi aging theory might be the reason for the solitary adverse association of PN_{AM} exposure and the right DLPFC. (Nußbaum et al., 2019)

Notably, PASA would indicate that aging related structural changes would be only seen later in the DLPFC in the context of brain aging. Especially this region seems to be affected by PN_{AM} in the present study, indicating a high adverseness of PN_{AM} or PN_{AM} related damaging processes in a region known to have a relatively high capability of preserving its function and structure into old age. One possible explanation might be that PN_{AM} might reach frontal brain areas faster, earlier and in higher quantities via the olfactory transport mechanism than other AP exposures can. (Nußbaum et al., 2019)

The effect modification analysis for age showed a negative association between PN_{AM} exposure and lGI values in posterior regions of the right hemisphere in the subgroup ‘Old’. This association was neither present in the subgroup ‘Young’ nor in the frontal region of the right hemisphere. This indicates that during the aging process the vulnerability of posterior regions to PN_{AM} might be enhanced. If the proposed mechanistic pathway of nasal intake and axonal transport holds true, the findings of this thesis would align well in suggesting a spread of damaging processes due to PN_{AM} from frontal to posterior areas in the course

of aging. Again, these processes could be either inflammatory or further axonal transport. Because there is a lack of negative association between PN_{AM} and IGI values in the frontal region, this would also mean that there is a limit for the damaging capability of PN_{AM} in the DLPFC.

The effect modification analysis for smoking status showed higher IGI values in association to PN_{AM} in the left PCC/P for current smokers in comparison to non-smokers and ex-smokers. Though smoking could possibly induce atrophy of the olfactory nerve as it is associated with olfactory impairment (Frye et al., 1990; Katotomichelakis et al., 2007) and thus might lead to lower sensitivity to PN_{AM} via the proposed olfactory axonal transport mechanism, this theory cannot explain the observed positive association and possibly protective effect. Another aspect of smoking to consider is the effect nicotine has on the brain. Studies have shown that nicotine might have a neuroprotective effect in the domains of attention, working memory, and executive function (Swan and Lessov-Schlaggar, 2007). One major way nicotine affects the brain is via up-regulation of nicotinic acetylcholine receptors and involvement in neurotransmitter pathways in the brain (Sabbagh et al., 2002; Swan and Lessov-Schlaggar, 2007). How AP might intervene in these processes is not clear and needs to be investigated. In this context, special attention should be given to inter-individual genetic variability, because it has already been shown that the effect of nicotine on the brain is modulated by inter-individual genetic variation (Jacobsen et al., 2006).

4.2.1.4 Noise Exposure

Higher 24h mean weighted noise and nighttime noise exposures showed positive associations with IGI values in the right DLPFC but no associations at all in the IGI values of the other regions of the FPN. On the one hand, this could hint at the possibility that there is actually no adverse effect of noise exposure on brain structure; maybe there is even a positive effect on the DLPFC. On the other hand, in the analysis, outdoor facade noise values were considered as real noise exposure for each participant. In reality, this might not always hold true, as oftentimes more exposed people display stronger protective behavior. This protective behavior might include closing windows more often and for

longer periods of the day or the installment of sound-proof windows. The systematic differences in protective behaviors might have confounded the analysis and might have led to misclassification of actual, i.e. indoor, noise exposure. Therefore, future studies need to include indoor noise exposure as a supposedly better assessment of real noise exposure levels. (Nußbaum et al., 2019)

Conversely, if future studies confirm these counter-intuitive results, PASA might deliver another explanation. The effects noise might have on the brain could be rather diffuse than locally confined. Firstly, noise is made up of energy-carrying sound waves, which might affect the whole brain fairly equally distributed through physical interaction. This would result in minor damage to brain cells all over the brain. Secondly, annoyance because of noise exposure might trigger stress-related processes in the brain which again would lead to diffuse brain damage. Thirdly, bad sleep quality due to nightly noise exposure (Schapkin et al., 2006) might inhibit nightly reorganization processes during sleep that are needed to prevent diffuse brain damage. This proposed diffuse damage could have not been detected via our locally confined lGI analysis. Either every single of these diffuse damage spots was still too small to be detected or they were in regions outside the FPN as regions this analysis did not include. Nevertheless, this diffuse minor structural damage might have a cumulative negative effect on overall brain function leading to brain plasticity and possibly hypertrophy in frontal brain regions in the sense of PASA compensational processes. The analysis on cognitive test data supports a possibly damaging effect of noise exposure on higher cognitive functioning. The most adversely effects were found in verbal fluency and vocabulary test performance. (Nußbaum et al., 2019)

In addition, the effect modification analysis found that the higher lGI values in frontal regions of the FPN were driven by the ‘Old’ subgroup. This indicates that an effect of noise on the brain might increase or accumulate over years of aging. Alternatively, the damage compensating processes according to PASA theory might only set in later in life or the threshold of noise induced damage might be reached later. Interestingly, the subgroup ‘Young’ shows a negative association between noise and lGI values in the PCC/P. This association is not

present for the subgroup ‘Old’ and could be explained by the theory that younger participants might have more brain tissue to lose. In older participants this region might have already taken an amount of damage that cannot be increased further. Both associations together indicate that young participants might over years of aging accumulate damage in posterior areas which then leads to cognitive performance losses and PASA compensatory processes and hyper-plasticity in frontal regions.

Although indicative results on cognitive functioning have been found, the analysis on brain structure does not deliver a cohesive picture. In summary, further studies are needed to investigate possible associations between long-term noise exposure and brain atrophy.

4.2.1.5 Sex- and Socioeconomic-Independent Effects

Overall, no effect modification for sex and SES was found. This indicates that AP and noise exposures show associations independent of sex and SES, which emphasizes the impact of environmental exposures on both men and women and people of every socioeconomic / educational status. It furthers the population-wide importance of the matter and highlights the significance of implementing protective measures that reach all of those population groups equally.

4.2.2 Sensitivity analysis

The stability of the models under sensitivity analysis adjustment for BMI, diabetes, depression, and CHD speaks for the robustness of the models and suggests no underlying confounding by these variables.

The analysis among working people showed a widening of CIs which is expected when reducing the sample size from N=590 to N=310. It also showed a slight attenuation of estimates for AP models which could be explained by exposure misclassification being present in the study or the sample size being too small to detect the small effects these exposures might have, which seems plausible as most CIs are still nearly fully overlapping between the main models and the working people only models. Another reason might be that the results

are driven by working people. As work supposedly stimulates brain plasticity and leads to better preserved brain structure overall, they might have more brain tissue and capacity at risk. Not including working people might mean not including the actual population at risk.

The double exposure models with AP had also wider CIs and slight attenuation of the estimates. Considering the high correlation between $PM_{2.5}$ and the other AP exposures this result seems plausible. Also as $PM_{2.5}$ is part of PM_{10} indicates, that the association seen in the PM_{10} analysis might actually be driven by the $PM_{2.5}$ fraction.

Noise models were robust to analysis among working people only and double exposure models, indicating good model fit and absence of exposure misclassification.

4.3 Future Studies

Future studies should consider investigating functional connectivity of the FPN in the context of AP and noise exposure. This would show whether the given interpretations on PASA and right hemi-aging theories can be upheld when also considering functional network reorganization. Moreover, we still need more basic experimental research with animal and human brain tissue and brain imaging studies on local differences in association to AP to further develop pathways and mechanisms. For a complete understanding of AP effects on the brain, we need to research the crossing or circumvention of the blood-brain-barrier by AP and further investigate additional indirect AP effects without direct contact with brain tissue. Additionally, it would be of interest to know which particles reach which brain regions in what quantities. (Nußbaum et al., 2019)

With noise, so far there have been no basic studies on mechanisms by which it might affect the brain. Consequently, work needs to be done on AP effects on activation and deactivation of brain regions via auditory input and channeling through the auditory system and whether these changes in activation levels impact brain plasticity and brain structure and function at all. (Nußbaum et al., 2019)

Moreover, it would be of interest to evaluate whether noise exposure interacts directly with the brain via the physical properties of sound waves, which carry a significant amount of energy and could possibly damage the brain tissue.

At present, there is a debate amongst scientists which structural feature is suited best for investigating the structure of the aging brain. On the one hand, lGI is suited to investigate even small changes in the cortical surface and corresponds directly to cortical neuron numbers and the brain's processing capabilities. On the other hand, it has limits when considering brain volume and is not the only marker for brain atrophy. (Nußbaum et al., 2019) For a greater understanding of the whole research topic and better comparability to other studies on brain structure, further markers should be also considered (e.g. total brain volume, volume of gray and white matter, or cortical thickness).

For clarifying the different effects AP and noise might have at different ages and identifying the population most at risk, it might be of interest to look at populations of different ages and possibly also conduct a prospective longitudinal cohort study with several follow up examinations, multiple lGI analyses and repeated assessment of exposure levels over several years.

As smoking seems to be able to modulate the association between PN_{AM} and brain structure, further research needs to be done in order to confirm or dismiss the seemingly positive effect of smoking. In this context, especially the effect on olfactory axonal transport mechanisms and possible mechanistic interactions of AP and nicotine seem to be of interest.

4.4 Strengths and Limitations of the Study

One strength of this thesis was the inclusion of participants over a large age span (55-85 years at FU1), so the analysis could very well handle the research topic considering the aging brain. Where Casanova et al. (2016) and Chen et al. (2015) only included women into their studies, the present study was able to include a fairly balanced population of 45.3% women and 54.7% men. (Nußbaum et al., 2019)

This thesis benefitted from the broad individual-level assessment within the Heinz Nixdorf Recall and the 1000BRAINS study, as these studies generated extensive data on exposures and covariates as possible confounding variables. Especially notable is the data on neuropsychological testing and MRI from the 1000BRAINS study, as both of these together are seldom available in one cohort study. (Nußbaum et al., 2019)

Furthermore, the approach of investigating differences in task-specific, fronto-parietal regions, and not only global differences in brain structure, directly connects this work to preceding studies on cognitive function and AP and noise exposure. Although there already have been studies on brain structure and AP with volumetric measures, this seems to be the first work to include lGI as another important structural feature of the brain. In addition, this is also the first study to investigate noise and brain structure and thus it is the first study to investigate AP, noise exposure and brain structure altogether. As previous studies only used $PM_{2.5}$ (Casanova et al., 2016; Chen et al., 2015), $PM_{2.5}$ and PM_{10} (Power et al., 2018), or $PM_{2.5}$ and $Dist_{majroad}$ (Wilker et al., 2015), this thesis also included a wider range of exposures. (Nußbaum et al., 2019)

In the sensitivity analysis possible further confounders were examined which solidified the quality of the models. Extensive effect modification analysis showed the varying relevance of age, smoking status, sex, and SES for AP and noise exposure effects on the brain.

One of the limitations of this thesis was the lower number of participants (n=590) when compared to preceding studies of this kind. Although the implemented exposure models are well established and validated for epidemiological research, exposure misclassification can be expected to have occurred, especially for participants who spent much time away from their home address. As for noise exposure, possibility of protective behavior in high exposed individuals was not considered. (Nußbaum et al., 2019)

Moreover, neuropsychological test models were attenuated under addition of lifestyle and neighborhood variables, particularly the neighborhood unemployment rate. As over time, the development of cognitive capabilities relates to the environment in which people get their cognitive stimuli,

investigation of the effect neighborhood variables have on cognition in studies concerning AP and noise exposure seems to be important.

The role of smoking in possibly altering or modulating the mechanisms by which AP, especially PN_{AM}, affects the brain needs to be further investigated. Thus, a comparing study of current smokers, former smokers and ex-smokers could be done as in the present study population size for smokers was only N=91.

In the working people only analysis just a smaller population size of N=310 could be used. In order to solidify the results that seemingly were driven by working people mainly, the number of participants could be increased in following works.

4.5 Conclusion

This thesis contributes to the body of evidence for the existence of structural changes in the brain due to long-term AP and noise exposure coinciding with cognitive performance losses. The observation of associations between AP and local brain structure for only the right hemisphere stands in agreement with the right hemi-aging theory and implicates an involvement of AP exposure in the physiological aging process. Likewise, the predominance of associations for posterior brain regions aligns well with the PASA theory on brain aging. Upcoming works should focus on the combination of brain structure with structural as well as functional connectivity and consider age, smoking status, employment status, and neighborhood variables as possible modifiers of long-term AP and noise exposure effects. (Nußbaum et al., 2019)

References

Adam, M., Schikowski, T., Carsin, A.E., Cai, Y., Jacquemin, B., Sanchez, M., Vierkötter, A., Marcon, A., Keidel, D., Sugiri, D., Kanani, Z.A., Nadif, R., Siroux, V., Hardy, R., Kuh, D., Rochat, T., Bridevaux, P.-O., Eeftens, M., Tsai, M.-Y., Villani, S., Phuleria, H.C., Birk, M., Cyrys, J., Cirach, M., Nazelle, A. de, Nieuwenhuijsen, M.J., Forsberg, B., Hoogh, K. de, Declerq, C., Bono, R., Piccioni, P., Quass, U., Heinrich, J., Jarvis, D., Pin, I., Beelen, R., Hoek, G., Brunekreef, B., Schindler, C., Sunyer, J., Krämer, U., Kauffmann, F., Hansell, A.L., Künzli, N., Probst-Hensch, N., 2014. Adult lung function and long-term air pollution exposure. ESCAPE: a multicentre cohort study and meta-analysis. Eur. Respir. J. erj01300-2014. https://doi.org/10.1183/09031936.00130014

Ailshire, J.A., Clarke, P., 2015. Fine Particulate Matter Air Pollution and Cognitive Function Among U.S. Older Adults. J. Gerontol. B. Psychol. Sci. Soc. Sci. 70, 322–328. https://doi.org/10.1093/geronb/gbu064

Albert, M. S., & Moss, M. B., 1988. Geriatric neuropsychology [WWW Document]. URL http://psycnet.apa.org/record/1988-98391-000 (accessed 5.5.18).

Anderson, H.R., Favarato, G., Atkinson, R.W., 2013. Long-term exposure to air pollution and the incidence of asthma: meta-analysis of cohort studies. Air Qual. Atmosphere Health 6, 47–56. https://doi.org/10.1007/s11869-011-0144-5

Aschenbrenner, Steffen, Oliver Tucha, and Klaus W. Lange., 2000. “RWT.” Regensburger Wortflüssigkeits-Test. Gött. Hogrefe.

Babisch, 2014 [WWW Document], n.d. URL http://www.noiseandhealth.org/article.asp?issn=1463-1741;year=2014;volume=16;issue=68;spage=1;epage=9;aulast=Babisch (accessed 6.11.18).

Bakian, A.V., Huber, R.S., Coon, H., Gray, D., Wilson, P., McMahon, W.M., Renshaw, P.F., 2015. Acute air pollution exposure and risk of suicide completion. Am. J. Epidemiol. 181, 295–303. https://doi.org/10.1093/aje/kwu341

Bäumler, Günther, and J. R. Stroop, 1985. Farbe-Wort-Interferenztest nach JR Stroop (FWIT). Hogrefe Verl. Für Psychol.

Beckmann, C.F., DeLuca, M., Devlin, J.T., Smith, S.M., 2005. Investigations into resting-state connectivity using independent component analysis. Philos. Trans. R. Soc. B Biol. Sci. 360, 1001–1013. https://doi.org/10.1098/rstb.2005.1634

Beckmann, C.F., Smith, S.M., 2004. Probabilistic independent component analysis for functional magnetic resonance imaging. IEEE Trans. Med. Imaging 23, 137–152. https://doi.org/10.1109/TMI.2003.822821

Beelen, R., Hoek, G., Vienneau, D., Eeftens, M., Dimakopoulou, K., Pedeli, X., Tsai, M.-Y., Künzli, N., Schikowski, T., Marcon, A., Eriksen, K.T., Raaschou-Nielsen, O., Stephanou, E., Patelarou, E., Lanki, T., Yli-Tuomi, T., Declercq, C., Falq, G., Stempfelet, M., Birk, M., Cyrys, J., von Klot, S., Nádor, G., Varró, M.J., Dėdelė, A., Gražulevičienė, R., Mölter, A., Lindley, S., Madsen, C., Cesaroni, G., Ranzi, A., Badaloni, C., Hoffmann, B., Nonnemacher, M., Krämer, U., Kuhlbusch, T., Cirach, M., de Nazelle, A., Nieuwenhuijsen, M., Bellander, T., Korek, M., Olsson, D., Strömgren, M., Dons, E., Jerrett, M., Fischer, P., Wang, M., Brunekreef, B., de Hoogh, K., 2013. Development of NO2 and NOx land use regression models for estimating air pollution exposure in 36 study areas in Europe – The ESCAPE project. Atmos. Environ. 72, 10–23. https://doi.org/10.1016/j.atmosenv.2013.02.037

Benton, A. L., et al., 2009. Der Benton-Test Huber. Hogrefe.

Birmili, W., Weinhold, K., Rasch, F., Sonntag, A., Sun, J., Merkel, M., Wiedensohler, A., Bastian, S., Schladitz, A., Löschau, G., Cyrys, J., Pitz, M., Gu, J., Kusch, T., Flentje, H., Quass, U., Kaminski, H., Kuhlbusch, T.A.J., Meinhardt, F., Schwerin, A., Bath, O., Ries, L., Wirtz, K., Fiebig, M., 2016. Long-term

observations of tropospheric particle number size distributions and equivalent black carbon mass concentrations in the German Ultrafine Aerosol Network (GUAN). Earth Syst. Sci. Data 8, 355–382. https://doi.org/10.5194/essd-8-355-2016

Block, M.L., Calderón-Garcidueñas, L., 2009. Air Pollution: Mechanisms of Neuroinflammation & CNS Disease. Trends Neurosci. 32, 506–516. https://doi.org/10.1016/j.tins.2009.05.009

Brown, J.W., Jaffe, J., 1975. Hypothesis on cerebral dominance. Neuropsychologia 13, 107–110. https://doi.org/10.1016/0028-3932(75)90054-8

Büns, C., Klemm, O., Wurzler, S., Hebbinghaus, H., Steckelbach, I., Friesel, J., Ebel, A., Friese, E., Jakobs, H., Memmesheimer, M., 2012. Comparison of four years of air pollution data with a mesoscale model. Atmospheric Res. 118, 404–417. https://doi.org/10.1016/j.atmosres.2012.07.009

Campbell, A., Daher, N., Solaimani, P., Mendoza, K., Sioutas, C., 2014. Human brain derived cells respond in a type-specific manner after exposure to urban particulate matter (PM). Toxicol. Vitro Int. J. Publ. Assoc. BIBRA 28, 1290–1295. https://doi.org/10.1016/j.tiv.2014.06.015

Casanova, R., Wang, X., Reyes, J., Akita, Y., Serre, M.L., Vizuete, W., Chui, H.C., Driscoll, I., Resnick, S.M., Espeland, M.A., Chen, J.-C., 2016. A Voxel-Based Morphometry Study Reveals Local Brain Structural Alterations Associated with Ambient Fine Particles in Older Women. Front. Hum. Neurosci. 10, 495. https://doi.org/10.3389/fnhum.2016.00495

Caspers, S., Moebus, S., Lux, S., Pundt, N., Schütz, H., Mühleisen, T.W., Gras, V., Eickhoff, S.B., Romanzetti, S., Stöcker, T., Stirnberg, R., Kirlangic, M.E., Minnerop, M., Pieperhoff, P., Mödder, U., Das, S., Evans, A.C., Jöckel, K.-H., Erbel, R., Cichon, S., Nöthen, M.M., Sturma, D., Bauer, A., Jon Shah, N., Zilles, K., Amunts, K., 2014. Studying variability in human brain aging in a population-based German cohort-rationale and design of 1000BRAINS. Front. Aging Neurosci. 6, 149. https://doi.org/10.3389/fnagi.2014.00149

Cesaroni, G., Forastiere, F., Stafoggia, M., Andersen, Z.J., Badaloni, C., Beelen, R., Caracciolo, B., Faire, U. de, Erbel, R., Eriksen, K.T., Fratiglioni, L., Galassi, C., Hampel, R., Heier, M., Hennig, F., Hilding, A., Hoffmann, B., Houthuijs, D., Jöckel, K.-H., Korek, M., Lanki, T., Leander, K., Magnusson, P.K.E., Migliore, E., Ostenson, C.-G., Overvad, K., Pedersen, N.L., J, J.P., Penell, J., Pershagen, G., Pyko, A., Raaschou-Nielsen, O., Ranzi, A., Ricceri, F., Sacerdote, C., Salomaa, V., Swart, W., Turunen, A.W., Vineis, P., Weinmayr, G., Wolf, K., Hoogh, K. de, Hoek, G., Brunekreef, B., Peters, A., 2014. Long term exposure to ambient air pollution and incidence of acute coronary events: prospective cohort study and meta-analysis in 11 European cohorts from the ESCAPE Project. BMJ 348, f7412. https://doi.org/10.1136/bmj.f7412

Chen, J.-C., Wang, X., Wellenius, G.A., Serre, M.L., Driscoll, I., Casanova, R., McArdle, J.J., Manson, J.E., Chui, H.C., Espeland, M.A., 2015. Ambient air pollution and neurotoxicity on brain structure: Evidence from women's health initiative memory study. Ann. Neurol. 78, 466–476. https://doi.org/10.1002/ana.24460

Costa, L.G., Cole, T.B., Coburn, J., Chang, Y.-C., Dao, K., Roqué, P.J., 2015. Neurotoxicity of traffic-related air pollution. Neurotoxicology. https://doi.org/10.1016/j.neuro.2015.11.008

Dale, A.M., Fischl, B., Sereno, M.I., 1999. Cortical surface-based analysis. I. Segmentation and surface reconstruction. NeuroImage 9, 179–194. https://doi.org/10.1006/nimg.1998.0395

Davis, D.A., Akopian, G., Walsh, J.P., Sioutas, C., Morgan, T.E., Finch, C.E., 2013. Urban air pollutants reduce synaptic function of CA1 neurons via an NMDA/NȮ pathway in vitro. J. Neurochem. 127, 509–519. https://doi.org/10.1111/jnc.12395

Davis, S.W., Dennis, N.A., Daselaar, S.M., Fleck, M.S., Cabeza, R., 2008. Qué PASA? The Posterior-Anterior Shift in Aging. Cereb. Cortex N. Y. N 1991 18, 1201–1209. https://doi.org/10.1093/cercor/bhm155

Della Sala, S., et al., 1997. The Visual Patterns Test: A new test of short-term visual recall. Suffolk Thames Val. Test Co.

Dolcos, F., Rice, H.J., Cabeza, R., 2002. Hemispheric asymmetry and aging: right hemisphere decline or asymmetry reduction. Neurosci. Biobehav. Rev. 26, 819–825.

Dragano, N., Hoffmann, B., Stang, A., Moebus, S., Verde, P.E., Weyers, S., Möhlenkamp, S., Schmermund, A., Mann, K., Jöckel, K.-H., Erbel, R., Siegrist, J., Group, H.N.R.S.I., 2009. Subclinical coronary atherosclerosis and neighbourhood deprivation in an urban region. Eur. J. Epidemiol. 24, 25–35. https://doi.org/10.1007/s10654-008-9292-9

Dzhambov, A.M., 2015. Long-term noise exposure and the risk for type 2 diabetes: A meta-analysis. Noise Health 17, 23–33. https://doi.org/10.4103/1463-1741.149571

Eeftens, M., Beelen, R., de Hoogh, K., Bellander, T., Cesaroni, G., Cirach, M., Declercq, C., Dėdelė, A., Dons, E., de Nazelle, A., Dimakopoulou, K., Eriksen, K., Falq, G., Fischer, P., Galassi, C., Gražulevičienė, R., Heinrich, J., Hoffmann, B., Jerrett, M., Keidel, D., Korek, M., Lanki, T., Lindley, S., Madsen, C., Mölter, A., Nádor, G., Nieuwenhuijsen, M., Nonnemacher, M., Pedeli, X., Raaschou-Nielsen, O., Patelarou, E., Quass, U., Ranzi, A., Schindler, C., Stempfelet, M., Stephanou, E., Sugiri, D., Tsai, M.-Y., Yli-Tuomi, T., Varró, M.J., Vienneau, D., Klot, S. von, Wolf, K., Brunekreef, B., Hoek, G., 2012. Development of Land Use Regression models for PM(2.5), PM(2.5) absorbance, PM(10) and PM(coarse) in 20 European study areas; results of the ESCAPE project. Environ. Sci. Technol. 46, 11195–11205. https://doi.org/10.1021/es301948k

Ejaz, S., Anwar, K., Ashraf, M., 2014. MRI and neuropathological validations of the involvement of air pollutants in cortical selective neuronal loss. Environ. Sci. Pollut. Res. Int. 21, 3351–3362. https://doi.org/10.1007/s11356-013-2294-5

Elder, A., Gelein, R., Silva, V., Feikert, T., Opanashuk, L., Carter, J., Potter, R., Maynard, A., Ito, Y., Finkelstein, J., Oberdörster, G., 2006. Translocation of Inhaled Ultrafine Manganese Oxide Particles to the Central Nervous System. Environ. Health Perspect. 114, 1172–1178. https://doi.org/10.1289/ehp.9030

EUR-Lex - 32002L0049 - EN - EUR-Lex [WWW Document], n.d. URL http://eur-lex.europa.eu/legal-content/DE/TXT/?uri=celex%3A32002L0049 (accessed 3.24.17).

European Environment Agency, 2013. Air pollution fact sheet 2013- Germany.

Fischl, B., Sereno, M.I., Dale, A.M., 1999. Cortical surface-based analysis. II: Inflation, flattening, and a surface-based coordinate system. NeuroImage 9, 195–207. https://doi.org/10.1006/nimg.1998.0396

Frye, R.E., Schwartz, B.S., Doty, R.L., 1990. Dose-Related Effects of Cigarette Smoking on Olfactory Function. JAMA 263, 1233–1236. https://doi.org/10.1001/jama.1990.03440090067028

FSL - FslWiki [WWW Document], n.d. URL https://fsl.fmrib.ox.ac.uk/fsl/fslwiki (accessed 3.24.17).

Gatterer G, Fischer P, Simanyi M, Danielczyk W, 1989. The A-K-T (‘“Alters-Konzentrations-Test”’) a new psychometric test for geriatric patients. Funct Neurol 4(3):273–276.

Goldstein, G., Shelly, C., 1981. Does the right hemisphere age more rapidly than the left? J. Clin. Neuropsychol. 3, 65–78. https://doi.org/10.1080/01688638108403114

Grady, C.L., Maisog, J.M., Horwitz, B., Ungerleider, L.G., Mentis, M.J., Salerno, J.A., Pietrini, P., Wagner, E., Haxby, J.V., 1994. Age-related changes in cortical

blood flow activation during visual processing of faces and location. J. Neurosci. Off. J. Soc. Neurosci. 14, 1450–1462.
Griffanti, L., Salimi-Khorshidi, G., Beckmann, C.F., Auerbach, E.J., Douaud, G., Sexton, C.E., Zsoldos, E., Ebmeier, K.P., Filippini, N., Mackay, C.E., Moeller, S., Xu, J., Yacoub, E., Baselli, G., Ugurbil, K., Miller, K.L., Smith, S.M., 2014. ICA-based artefact removal and accelerated fMRI acquisition for improved resting state network imaging. NeuroImage 95, 232–247. https://doi.org/10.1016/j.neuroimage.2014.03.034
Hamra, G.B., Laden, F., Cohen, A.J., Raaschou-Nielsen, O., Brauer, M., Loomis, D., 2015. Lung Cancer and Exposure to Nitrogen Dioxide and Traffic: A Systematic Review and Meta-Analysis. Environ. Health Perspect. 123, 1107–1112. https://doi.org/10.1289/ehp.1408882
Hass, H., Ebel, A., Feldmann, H., Jakobs, H.J., Memmesheimer, M., 1993. Evaluation studies with a regional chemical transport model (EURAD) using air quality data from the EMEP monitoring network. Atmospheric Environ. Part Gen. Top., European Monitoring and Evaluation Program Workshop on the Combined Analysis of Measurements and Model Results with Special Emphasis on NO/VOC/Oxidants 27, 867–887. https://doi.org/10.1016/0960-1686(93)90007-L
Hautzinger, M, Bailer, M, 1993. Allgemeine Depressions Skala – ADS [in German]. Weinheim:Beltz.
Hennig, F., Sugiri, D., Tzivian, L., Fuks, K., Moebus, S., Jöckel, K.-H., Vienneau, D., Kuhlbusch, T., de Hoogh, K., Memmesheimer, M., Jakobs, H., Quass, U., Hoffmann, B., Hennig, F., Sugiri, D., Tzivian, L., Fuks, K., Moebus, S., Jöckel, K.-H., Vienneau, D., Kuhlbusch, T.A.J., de Hoogh, K., Memmesheimer, M., Jakobs, H., Quass, U., Hoffmann, B., 2016. Comparison of Land-Use Regression Modeling with Dispersion and Chemistry Transport Modeling to Assign Air Pollution Concentrations within the Ruhr Area. Atmosphere 7, 48. https://doi.org/10.3390/atmos7030048
Hoek, G., Krishnan, R.M., Beelen, R., Peters, A., Ostro, B., Brunekreef, B., Kaufman, J.D., 2013. Long-term air pollution exposure and cardio- respiratory mortality: a review. Environ. Health 12, 43. https://doi.org/10.1186/1476-069X-12-43
Hogstrom, L.J., Westlye, L.T., Walhovd, K.B., Fjell, A.M., 2013. The structure of the cerebral cortex across adult life: age-related patterns of surface area, thickness, and gyrification. Cereb. Cortex N. Y. N 1991 23, 2521–2530. https://doi.org/10.1093/cercor/bhs231
Hygge, S., Boman, E., Enmarker, I., 2003. The effects of road traffic noise and meaningful irrelevant speech on different memory systems. Scand. J. Psychol. 44, 13–21.
Jacobsen, L.K., Pugh, K.R., Mencl, W.E., Gelernter, J., 2006. C957T polymorphism of the dopamine D2 receptor gene modulates the effect of nicotine on working memory performance and cortical processing efficiency. Psychopharmacology (Berl.) 188, 530–540. https://doi.org/10.1007/s00213-006-0469-1
Jayaraj, R.L., Rodriguez, E.A., Wang, Y., Block, M.L., 2017. Outdoor Ambient Air Pollution and Neurodegenerative Diseases: the Neuroinflammation Hypothesis. Curr. Environ. Health Rep. 4, 166–179. https://doi.org/10.1007/s40572-017-0142-3
Jenkinson, M., Bannister, P., Brady, M., Smith, S., 2002. Improved optimization for the robust and accurate linear registration and motion correction of brain images. NeuroImage 17, 825–841.
Jenkinson, M., Beckmann, C.F., Behrens, T.E.J., Woolrich, M.W., Smith, S.M., 2012. FSL. NeuroImage 62, 782–790. https://doi.org/10.1016/j.neuroimage.2011.09.015
Jenkinson, M., Smith, S., 2001. A global optimisation method for robust affine registration of brain images. Med. Image Anal. 5, 143–156.

Jockwitz, C., Caspers, S., Lux, S., Jütten, K., Schleicher, A., Eickhoff, S.B., Amunts, K., Zilles, K., 2017. Age- and function-related regional changes in cortical folding of the default mode network in older adults. Brain Struct. Funct. 222, 83–99. https://doi.org/10.1007/s00429-016-1202-4

Jung, C.-R., Lin, Y.-T., Hwang, B.-F., 2015. Ozone, Particulate Matter, and Newly Diagnosed Alzheimer's Disease: A Population-Based Cohort Study in Taiwan. J. Alzheimers Dis. 44, 573–584. https://doi.org/10.3233/JAD-140855

Kalbe, E., Kessler, J., Calabrese, P., Smith, R., Passmore, A.P., Brand, M., Bullock, R., 2004. DemTect: a new, sensitive cognitive screening test to support the diagnosis of mild cognitive impairment and early dementia. Int. J. Geriatr. Psychiatry 19, 136–143. https://doi.org/10.1002/gps.1042

Katotomichelakis, M., Balatsouras, D., Tripsianis, G., Davris, S., Maroudias, N., Danielides, V., Simopoulos, C., 2007. The effect of smoking on the olfactory function. Rhinology 45, 273–280.

Kempen, E. van, Casas, M., Pershagen, G., Foraster, M., 2018. WHO Environmental Noise Guidelines for the European Region: A Systematic Review on Environmental Noise and Cardiovascular and Metabolic Effects: A Summary. Int. J. Environ. Res. Public. Health 15. https://doi.org/10.3390/ijerph15020379

Kim, R., van den Berg, M., 2010. Night Noise Guidelines for Europe. Noise Health 12, 61–3. https://doi.org/10.4103/1463-1741.63204

Kovalev, V.A., Kruggel, F., von Cramon, D.Y., 2003. Gender and age effects in structural brain asymmetry as measured by MRI texture analysis. NeuroImage 19, 895–905. https://doi.org/10.1016/S1053-8119(03)00140-X

Lee, K.K., Miller, M.R., Shah, A.S.V., 2018. Air Pollution and Stroke. J. Stroke 20, 2–11. https://doi.org/10.5853/jos.2017.02894

Lim, Y.-H., Kim, H., Kim, J.H., Bae, S., Park, H.Y., Hong, Y.-C., 2012. Air pollution and symptoms of depression in elderly adults. Environ. Health Perspect. 120, 1023–1028. https://doi.org/10.1289/ehp.1104100

Liu, F., Huang, Y., Zhang, F., Chen, Q., Wu, B., Rui, W., Zheng, J.C., Ding, W., 2015. Macrophages treated with particulate matter PM2.5 induce selective neurotoxicity through glutaminase-mediated glutamate generation. J. Neurochem. 134, 315–326. https://doi.org/10.1111/jnc.13135

Lu, H., Xu, F., Rodrigue, K.M., Kennedy, K.M., Cheng, Y., Flicker, B., Hebrank, A.C., Uh, J., Park, D.C., 2011. Alterations in Cerebral Metabolic Rate and Blood Supply across the Adult Lifespan. Cereb. Cortex N. Y. NY 21, 1426–1434. https://doi.org/10.1093/cercor/bhq224

Lux, S., et al., 2012. VGT: Verbaler Gedächtnistest: Bielefelder Kategorielle Wortlisten. Gött. Verl. Hans Huber.

Marstaller, L., Williams, M., Rich, A., Savage, G., Burianová, H., 2015. Aging and large-scale functional networks: White matter integrity, gray matter volume, and functional connectivity in the resting state. Neuroscience 290, 369–378. https://doi.org/10.1016/j.neuroscience.2015.01.049

Memmesheimer, M., Friese, E., Ebel, A., Jakobs, H. j., Feldmann, H., Kessler, C., Piekorz, G., 2004. Long-term simulations of particulate matter in Europe on different scales using sequential nesting of a regional model. Int. J. Environ. Pollut. 22, 108–132. https://doi.org/10.1504/IJEP.2004.005530

Morris, J.C., Heyman, A., Mohs, R.C., Hughes, J.P., van Belle, G., Fillenbaum, G., Mellits, E.D., Clark, C., 1989. The consortium to establish a registry for Alzheimer's disease (CERAD): I. Clinical and neuropsychological assessment of Alzheimer's disease. Neurology 39, 1159–1165. https://doi.org/10.1212/WNL.39.9.1159

Nonnemacher, M., Jakobs, H., Viehmann, A., Vanberg, I., Kessler, C., Moebus, S., Möhlenkamp, S., Erbel, R., Hoffmann, B., Memmesheimer, M., 2014. Spatio-temporal modelling of residential exposure to particulate matter and gaseous

pollutants for the Heinz Nixdorf Recall Cohort. Atmos. Environ. 91, 15–23. https://doi.org/10.1016/j.atmosenv.2014.03.052
Oberdörster, G., Sharp, Z., Atudorei, V., Elder, A., Gelein, R., Kreyling, W., Cox, C., 2004. Translocation of Inhaled Ultrafine Particles to the Brain. Inhal. Toxicol. 16, 437–445. https://doi.org/10.1080/08958370490439597
Ogawa, S., Lee, T.M., Kay, A.R., Tank, D.W., 1990. Brain magnetic resonance imaging with contrast dependent on blood oxygenation. Proc. Natl. Acad. Sci. 87, 9868–9872. https://doi.org/10.1073/pnas.87.24.9868
Oppenheim, H.A., Lucero, J., Guyot, A.-C., Herbert, L.M., McDonald, J.D., Mabondzo, A., Lund, A.K., 2013. Exposure to vehicle emissions results in altered blood brain barrier permeability and expression of matrix metalloproteinases and tight junction proteins in mice. Part. Fibre Toxicol. 10, 62. https://doi.org/10.1186/1743-8977-10-62
Oswald, W. D., and U. M. Fleischmann., 1997. Das Nürnberger-Alters-Inventar (NAI). Hogrefe Gött.
Power, M.C., Lamichhane, A.P., Liao, D., Xu, X., Jack, C.R., Gottesman, R.F., Mosley, T., Stewart, J.D., Yanosky, J.D., Whitsel, E.A., 2018. The Association of Long-Term Exposure to Particulate Matter Air Pollution with Brain MRI Findings: The ARIC Study. Environ. Health Perspect. 126, 027009. https://doi.org/10.1289/EHP2152
Power, M.C., Weisskopf, M.G., Alexeeff, S.E., Coull, B.A., Spiro, A., Schwartz, J., 2011. Traffic-Related Air Pollution and Cognitive Function in a Cohort of Older Men. Environ. Health Perspect. 119, 682–687. https://doi.org/10.1289/ehp.1002767
Provost, E.B., Madhloum, N., Panis, L.I., Boever, P.D., Nawrot, T.S., 2015. Carotid Intima-Media Thickness, a Marker of Subclinical Atherosclerosis, and Particulate Air Pollution Exposure: the Meta-Analytical Evidence. PLOS ONE 10, e0127014. https://doi.org/10.1371/journal.pone.0127014
R Development Core Team, 2008. R Development Core Team (2008). R: A language and environment for statistical computing. R Foundation for Statistical Computing, Vienna, Austria. ISBN 3-900051-07-0, URL http://www.R-project.org.
Raaschou-Nielsen, O., Andersen, Z.J., Beelen, R., Samoli, E., Stafoggia, M., Weinmayr, G., Hoffmann, B., Fischer, P., Nieuwenhuijsen, M.J., Brunekreef, B., Xun, W.W., Katsouyanni, K., Dimakopoulou, K., Sommar, J., Forsberg, B., Modig, L., Oudin, A., Oftedal, B., Schwarze, P.E., Nafstad, P., De Faire, U., Pedersen, N.L., Östenson, C.-G., Fratiglioni, L., Penell, J., Korek, M., Pershagen, G., Eriksen, K.T., Sørensen, M., Tjønneland, A., Ellermann, T., Eeftens, M., Peeters, P.H., Meliefste, K., Wang, M., Bueno-de-Mesquita, B., Key, T.J., de Hoogh, K., Concin, H., Nagel, G., Vilier, A., Grioni, S., Krogh, V., Tsai, M.-Y., Ricceri, F., Sacerdote, C., Galassi, C., Migliore, E., Ranzi, A., Cesaroni, G., Badaloni, C., Forastiere, F., Tamayo, I., Amiano, P., Dorronsoro, M., Trichopoulou, A., Bamia, C., Vineis, P., Hoek, G., 2013. Air pollution and lung cancer incidence in 17 European cohorts: prospective analyses from the European Study of Cohorts for Air Pollution Effects (ESCAPE). Lancet Oncol. 14, 813–822. https://doi.org/10.1016/S1470-2045(13)70279-1
Regard, M., Strauss, E., Knapp, P., 1982. Children's Production on Verbal and Non-Verbal Fluency Tasks. Percept. Mot. Skills 55, 839–844. https://doi.org/10.2466/pms.1982.55.3.839
Sabbagh, M.N., Lukas, R.J., Sparks, D.L., Reid, R.T., 2002. The nicotinic acetylcholine receptor, smoking, and Alzheimer's disease. J. Alzheimers Dis. JAD 4, 317–325.
Salimi-Khorshidi, G., Douaud, G., Beckmann, C.F., Glasser, M.F., Griffanti, L., Smith, S.M., 2014. Automatic denoising of functional MRI data: combining independent

component analysis and hierarchical fusion of classifiers. NeuroImage 90, 449–468. https://doi.org/10.1016/j.neuroimage.2013.11.046
Schaer, M., Cuadra, M.B., Schmansky, N., Fischl, B., Thiran, J.-P., Eliez, S., 2012. How to Measure Cortical Folding from MR Images: a Step-by-Step Tutorial to Compute Local Gyrification Index. JoVE J. Vis. Exp. e3417–e3417. https://doi.org/10.3791/3417
Schaer, M., Cuadra, M.B., Tamarit, L., Lazeyras, F., Eliez, S., Thiran, J.-P., 2008. A surface-based approach to quantify local cortical gyrification. IEEE Trans. Med. Imaging 27, 161–170. https://doi.org/10.1109/TMI.2007.903576
Schapkin, S.A., Falkenstein, M., Marks, A., Griefahn, B., 2006. Executive brain functions after exposure to nocturnal traffic noise: effects of task difficulty and sleep quality. Eur. J. Appl. Physiol. 96, 693–702. https://doi.org/10.1007/s00421-005-0049-9
Scheers, H., Jacobs, L., Casas, L., Nemery, B., Nawrot, T.S., 2015. Long-Term Exposure to Particulate Matter Air Pollution Is a Risk Factor for Stroke: Meta-Analytical Evidence. Stroke 46, 3058–3066. https://doi.org/10.1161/STROKEAHA.115.009913
Schellig, Dieter, 1997. Block-tapping-test. FrankfurtMain Ger. Swets Test Serv.
Schmermund, A., Möhlenkamp, S., Stang, A., Grönemeyer, D., Seibel, R., Hirche, H., Mann, K., Siffert, W., Lauterbach, K., Siegrist, J., Jöckel, K.-H., Erbel, R., 2002. Assessment of clinically silent atherosclerotic disease and established and novel risk factors for predicting myocardial infarction and cardiac death in healthy middle-aged subjects: rationale and design of the Heinz Nixdorf RECALL Study. Risk Factors, Evaluation of Coronary Calcium and Lifestyle. Am. Heart J. 144, 212–218.
Schmidt, Karl-Heinz, and Peter Metzler., 1992. Wortschatztest: WST. Beltz.
Smith, S.M., 2002. Fast robust automated brain extraction. Hum. Brain Mapp. 17, 143–155. https://doi.org/10.1002/hbm.10062
Smith, S.M., Fox, P.T., Miller, K.L., Glahn, D.C., Fox, P.M., Mackay, C.E., Filippini, N., Watkins, K.E., Toro, R., Laird, A.R., Beckmann, C.F., 2009. Correspondence of the brain's functional architecture during activation and rest. Proc. Natl. Acad. Sci. U. S. A. 106, 13040–13045. https://doi.org/10.1073/pnas.0905267106
Snyder, A.Z., Raichle, M.E., 2012. A brief history of the resting state: The Washington University perspective. NeuroImage, 20 YEARS OF fMRI 62, 902–910. https://doi.org/10.1016/j.neuroimage.2012.01.044
Stroop, J.R., 1935. Studies of interference in serial verbal reactions. J. Exp. Psychol. 18, 643–662. https://doi.org/10.1037/h0054651
Sturm W, Willmes K, Horn W, 1993. Leistungspru¨fungssystem fu¨r 50–90ja¨hrige. Handanweisung,. Hogrefe Gött.
Swan, G.E., Lessov-Schlaggar, C.N., 2007. The Effects of Tobacco Smoke and Nicotine on Cognition and the Brain. Neuropsychol. Rev. 17, 259–273. https://doi.org/10.1007/s11065-007-9035-9
Thomson, E.M., Kumarathasan, P., Calderón-Garcidueñas, L., Vincent, R., 2007. Air pollution alters brain and pituitary endothelin-1 and inducible nitric oxide synthase gene expression. Environ. Res. 105, 224–233. https://doi.org/10.1016/j.envres.2007.06.005
Thurston, G.D., Kipen, H., Annesi-Maesano, I., Balmes, J., Brook, R.D., Cromar, K., De Matteis, S., Forastiere, F., Forsberg, B., Frampton, M.W., Grigg, J., Heederik, D., Kelly, F.J., Kuenzli, N., Laumbach, R., Peters, A., Rajagopalan, S.T., Rich, D., Ritz, B., Samet, J.M., Sandstrom, T., Sigsgaard, T., Sunyer, J., Brunekreef, B., 2017. A joint ERS/ATS policy statement: what constitutes an adverse health effect of air pollution? An analytical framework. Eur. Respir. J. 49. https://doi.org/10.1183/13993003.00419-2016

Tonne, C., Elbaz, A., Beevers, S., Singh-Manoux, A., 2014. Traffic-related Air Pollution in Relation to Cognitive Function in Older Adults. Epidemiol. Camb. Mass 25, 674–681. https://doi.org/10.1097/EDE.0000000000000144

Tzivian, L., Dlugaj, M., Winkler, A., Hennig, F., Fuks, K., Sugiri, D., Schikowski, T., Jakobs, H., Erbel, R., Jöckel, K.-H., Moebus, S., Hoffmann, B., Weimar, C., Heinz Nixdorf Recall Study Investigative Group, 2016. Long-term air pollution and traffic noise exposures and cognitive function:A cross-sectional analysis of the Heinz Nixdorf Recall study. J. Toxicol. Environ. Health A 79, 1057–1069. https://doi.org/10.1080/15287394.2016.1219570

van Kempen, E., Babisch, W., 2012. The quantitative relationship between road traffic noise and hypertension: a meta-analysis. J. Hypertens. 30, 1075. https://doi.org/10.1097/HJH.0b013e328352ac54

Villringer, A., Dirnagl, U., 1995. Coupling of brain activity and cerebral blood flow: basis of functional neuroimaging. Cerebrovasc. Brain Metab. Rev. 7, 240–276.

Wang, B., Xu, D., Jing, Z., Liu, D., Yan, S., Wang, Y., 2014. MECHANISMS IN ENDOCRINOLOGY: Effect of long-term exposure to air pollution on type 2 diabetes mellitus risk: a systemic review and meta-analysis of cohort studies. Eur. J. Endocrinol. 171, R173–R182. https://doi.org/10.1530/EJE-14-0365

Wei, H., Deng, F., Chen, Y., Qin, Y., Hao, Y., Guo, X., 2014. Ultrafine carbon black induces glutamate and ATP release by activating connexin and pannexin hemichannels in cultured astrocytes. Toxicology 323, 32–41. https://doi.org/10.1016/j.tox.2014.06.005

Wellenius, G.A., Boyle, L.D., Wilker, E.H., Sorond, F.A., Coull, B.A., Koutrakis, P., Mittleman, M.A., Lipsitz, L.A., 2013. Ambient Fine Particulate Matter Alters Cerebral Hemodynamics in the Elderly. Stroke 44, 1532–1536. https://doi.org/10.1161/STROKEAHA.111.000395

Weuve, J., Puett, R.C., Schwartz, J., Yanosky, J.D., Laden, F., Grodstein, F., 2012. Exposure to Particulate Air Pollution and Cognitive Decline in Older Women. Arch. Intern. Med. 172, 219–227. https://doi.org/10.1001/archinternmed.2011.683

Who, Organization, W.H., UNAIDS, Europe, W.R.O. for, 2006. Air Quality Guidelines: Global Update 2005. World Health Organization.

WHO Regional Office for Europe, 2013. Review of evidence on health aspects of air pollution – REVIHAAP Project: Technical Report. WHO Regional Office for Europe, Copenhagen.

Wilker, E.H., Preis, S.R., Beiser, A.S., Wolf, P.A., Au, R., Kloog, I., Li, W., Schwartz, J., Koutrakis, P., DeCarli, C., Seshadri, S., Mittleman, M.A., 2015. Long-term exposure to fine particulate matter, residential proximity to major roads and measures of brain structure. Stroke 46, 1161–1166. https://doi.org/10.1161/STROKEAHA.114.008348

Xu, X., Ha, S.U., Basnet, R., 2016. A Review of Epidemiological Research on Adverse Neurological Effects of Exposure to Ambient Air Pollution. Front. Public Health 4. https://doi.org/10.3389/fpubh.2016.00157

Zilles, K., Armstrong, E., Schleicher, A., Kretschmann, H.-J., 1988. The human pattern of gyrification in the cerebral cortex. Anat. Embryol. (Berl.) 179, 173–179. https://doi.org/10.1007/BF00304699

Supplement

Table S1. Estimates of the cognitive domain models per IQR increase in mean exposure levels with increasing model adjustment among the Neuropsychological Tests group (n=615) of the 1000BRAINS study. From Nußbaum et al., 2019

Exposure / Adjustment Model	Cognitive Domain				
	Attention	Executive Function	Memory	Short Term/Working Memory	Language
PM_{10}($\mu g/m^3$)					
Discovery[a]	-0.01 (-0.05; 0.03)	-0.01 (-0.04; 0.03)	-0.02 (-0.06; 0.02)	0.00 (-0.03; 0.03)	-0.03 (-0.06; 0.01)
Extended[b]	-0.01 (-0.05; 0.03)	0.00 (-0.03; 0.03)	-0.01 (-0.05; 0.03)	0.00 (-0.03; 0.03)	-0.02 (-0.05; 0.02)
Extended-Plus[c]	-0.01 (-0.05; 0.04)	0.01 (-0.03; 0.05)	0,00 (-0.04; 0.04)	0.00 (-0.03; 0.04)	0.00 (-0.04; 0.04)
$PM_{2.5}$ ($\mu g/m^3$)					
Discovery[a]	-0.03 (-0.08; 0.02)	-0.02 (-0.05; 0.02)	-0.03 (-0.07; 0.01)	-0.01 (-0.04; 0.03)	-0.05 (-0.10; -0.01)
Extended[b]	-0.02 (-0.07; 0.02)	-0.01 (-0.04; 0.03)	-0.01 (-0.06; 0.03)	0.00 (-0.04; 0.03)	-0.04 (-0.08; 0.01)
Extended-Plus[c]	-0.02 (-0.08; 0.03)	0.01 (-0.03; 0.05)	-0.01 (-0.06; 0.04)	0.01 (-0.03; 0.05)	-0.02 (-0.07; 0.03)
$PM_{2.5abs}$ (10^{-5}/m)					
Discovery[a]	0.00 (-0.04; 0.04)	-0.01 (-0.04; 0.02)	-0.03 (-0.07; 0.00)	-0.01 (-0.04; 0.02)	-0.04 (-0.07; 0.00)
Extended[b]	0.00 (-0.03; 0.04)	-0.01 (-0.04; 0.02)	-0.02 (-0.06; 0.02)	-0.01 (-0.04; 0.02)	-0.02 (-0.06; 0.01)
Extended-Plus[c]	0.01 (-0.03; 0.06)	0.01 (-0.03; 0.04)	-0.02 (-0.06; 0.02)	0.00 (-0.03; 0.03)	-0.01 (-0.05; 0.03)
PN_{AM} (n/mL)					
Discovery[a]	-0.05 (-0.10; -0.01)	-0.01 (-0.05; 0.03)	0.00 (-0.04; 0.04)	0.00 (-0.04; 0.03)	-0.06 (-0.10; -0.02)
Extended[b]	-0.05 (-0.09; 0.00)	0.00 (-0.04; 0.04)	0.01 (-0.03; 0.06)	0.01 (-0.03; 0.04)	-0.04 (-0.08; 0.00)
Extended-Plus[c]	-0.05 (-0.10; 0.00)	0.01 (-0.03; 0.05)	0.02 (-0.03; 0.07)	0.02 (-0.02; 0.06)	-0.03 (-0.08; 0.01)
NO_2 ($\mu g/m^3$)					
Discovery[a]	-0.01 (-0.05; 0.03)	0.00 (-0.03; 0.03)	-0.01 (-0.05; 0.02)	0.01 (-0.02; 0.04)	-0.03 (-0.06; 0.01)
Extended[b]	0.00 (-0.04; 0.04)	0.01 (-0.03; 0.04)	0.01 (-0.03; 0.04)	0.01 (-0.02; 0.04)	-0.02 (-0.05; 0.02)
Extended-Plus[c]	0.01 (-0.04; 0.05)	0.02 (-0.02; 0.05)	0.01 (-0.03; 0.05)	0.02 (-0.01; 0.05)	0.00 (-0.04; 0.03)
NO_X ($\mu g/m^3$)					

Discovery[a]	-0.03 (-0.07; 0.01)	-0.01 (-0.04; 0.03)	-0.01 (-0.05; 0.03)	0.01 (-0.02; 0.04)	-0.04 (-0.08; 0.00)
Extended[b]	-0.02 (-0.07; 0.02)	0.00 (-0.03; 0.04)	0.01 (-0.03; 0.05)	0.01 (-0.02; 0.04)	-0.02 (-0.06; 0.01)
Extended-Plus[c]	-0.02 (-0.07; 0.03)	0.01 (-0.03; 0.05)	0.02 (-0.02; 0.06)	0.02 (-0.02; 0.05)	-0.01 (-0.05; 0.03)
$Dist_{majroad}$ (m) ≥100<200 vs ≥200					
Discovery[a]	0.11 (-0.06; 0.27)	0.05 (-0.08; 0.18)	-0.11 (-0.26; 0.05)	-0.08 (-0.20; 0.04)	-0.07 (-0.22; 0.08)
Extended[b]	0.12 (-0.05; 0.29)	0.06 (-0.07; 0.19)	-0.08 (-0.23; 0.08)	-0.07 (-0.20; 0.05)	-0.06 (-0.20; 0.09)
Extended-Plus[c]	0.12 (-0.04; 0.29)	0.07 (-0.07; 0.20)	-0.07 (-0.23; 0.08)	-0.07 (-0.19; 0.05)	-0.05 (-0.20; 0.09)
$Dist_{majroad}$ (m) <100 vs ≥200					
Discovery[a]	0.12 (-0.07; 0.30)	0.05 (-0.09; 0.20)	0.00 (-0.17; 0.16)	0.12 (-0.02; 0.25)	0.04 (-0.13; 0.20)
Extended[b]	0.11 (-0.07; 0.30)	0.05 (-0.10; 0.20)	0.01 (-0.15; 0.18)	0.11 (-0.03; 0.25)	0.02 (-0.14; 0.18)
Extended-Plus[c]	0.12 (-0.06; 0.30)	0.06 (-0.09; 0.20)	0.02 (-0.15; 0.19)	0.12 (-0.02; 0.25)	0.03 (-0.13; 0.19)
L_{night} (dB[A])					
Discovery[a]	0.01 (-0.06; 0.08)	-0.03 (-0.08; 0.03)	-0.05 (-0.12; 0.01)	-0.03 (-0.08; 0.02)	-0.08 (-0.14; -0.02)
Extended[b]	0.03 (-0.04; 0.10)	-0.02 (-0.07; 0.04)	-0.03 (-0.10; 0.03)	-0.03 (-0.08; 0.02)	-0.06 (-0.12; 0.00)
Extended-Plus[c]	0.03 (-0.04; 0.10)	-0.01 (-0.07; 0.04)	-0.03 (-0.10; 0.03)	-0.03 (-0.08; 0.02)	-0.06 (-0.12; 0.01)
L_{DEN} (dB[A])					
Discovery[a]	0.02 (-0.04; 0.07)	-0.02 (-0.06; 0.02)	-0.04 (-0.09; 0.01)	-0.03 (-0.07; 0.01)	-0.06 (-0.11; -0.02)
Extended[b]	0.03 (-0.02; 0.08)	-0.01 (-0.06; 0.03)	-0.03 (-0.07; 0.02)	-0.03 (-0.07; 0.01)	-0.04 (-0.09; 0.00)
Extended-Plus[c]	0.03 (-0.02; 0.08)	-0.01 (-0.06; 0.03)	-0.02 (-0.07; 0.02)	-0.03 (-0.07; 0.01)	-0.04 (-0.09; 0.00)

Abbreviations: IQR, interquartile range; $PM_{2.5}$, particulate matter with aerodynamic diameter ≤2.5 µm; PM_{10}, particulate matter with aerodynamic diameter ≤10 µm; PN_{AM}, accumulation mode particle number; NO_X, any nitrogen oxide; NO_2, nitrogen dioxide; $PM_{2.5abs}$, $PM_{2.5}$ absorbance; L_{night}, nighttime mean noise (10pm-6am); L_{DEN}, 24h mean noise; $Dist_{majroad}$, distance to the nearest major road; SD, standard deviation

[a] The Discovery Model was adjusted for age, sex, and education level.

[b] In addition to the variables included in the Discovery model, the Extended Model was adjusted for education level, alcohol consumption, smoking status, cumulative pack-years, environmental tobacco smoke, and weekly calorie expenditure by performing regular physical activity.

[c] In addition to the variables included in the Extended model, the Extended-Plus Model was adjusted for neighborhood unemployment rate.

Table S2. Estimates of the individual neurocognitive test models of the Attention and Executive Function Domain per IQR increase in mean exposure levels with increasing model adjustment among the Neuropsychological Tests group (n=615) of the 1000BRAINS study. From Nußbaum et al., 2019

Exposure / Adjustment Model	Cognitive Function					
	Attention		Executive Function			
	selective attention	processing speed	problem solving	figural fluency	concept shifting	susceptibility to interference
PM_{10}(µg/m^3)						
Discovery[a]	-0.01 (-0.06; 0.04)	-0.02 (-0.06; 0.03)	-0.01 (-0.05; 0.04)	-0.02 (-0.07; 0.02)	0.01 (-0.04; 0.06)	0.00 (-0.05; 0.05)
Extended[b]	-0.01 (-0.06; 0.04)	-0.02 (-0.06; 0.03)	-0.01 (-0.05; 0.04)	-0.02 (-0.07; 0.02)	0.01 (-0.04; 0.06)	0.01 (-0.04; 0.05)
Extended-Plus[c]	0.01 (-0.04; 0.07)	-0.03 (-0.08; 0.03)	0.02 (-0.04; 0.07)	-0.02 (-0.08; 0.03)	0.03 (-0.03; 0.08)	0.02 (-0.03; 0.08)
$PM_{2.5}$ (µg/m^3)						
Discovery[a]	-0.03 (-0.09; 0.02)	-0.03 (-0.08; 0.03)	0.00 (-0.06; 0.05)	-0.04 (-0.10; 0.01)	0.00 (-0.06; 0.06)	-0.01 (-0.07; 0.04)
Extended[b]	-0.03 (-0.09; 0.03)	-0.02 (-0.08; 0.04)	0.00 (-0.05; 0.06)	-0.04 (-0.09; 0.02)	0.01 (-0.05; 0.07)	0.00 (-0.06; 0.06)
Extended-Plus[c]	-0.01 (-0.08; 0.06)	-0.04 (-0.11; 0.03)	0.04 (-0.03; 0.10)	-0.04 (-0.11; 0.03)	0.02 (-0.04; 0.09)	0.02 (-0.04; 0.09)
$PM_{2.5abs}$ (10^{-5}/m)						
Discovery[a]	-0.01 (-0.06; 0.04)	0.01 (-0.04; 0.05)	-0.01 (-0.06; 0.03)	-0.01 (-0.06; 0.03)	0.00 (-0.05; 0.05)	-0.02 (-0.07; 0.02)
Extended[b]	0.00 (-0.05; 0.04)	0.01 (-0.03; 0.06)	-0.01 (-0.06; 0.04)	-0.01 (-0.06; 0.04)	0.01 (-0.04; 0.06)	-0.01 (-0.06; 0.04)
Extended-Plus[c]	0.02 (-0.04; 0.07)	0.01 (-0.04; 0.06)	0.01 (-0.04; 0.06)	-0.01 (-0.06; 0.05)	0.02 (-0.03; 0.07)	0.00 (-0.05; 0.06)
PN_{AM} (n/mL)						
Discovery[a]	-0.07 (-0.13; -0.01)	-0.04 (-0.10; 0.02)	0.02 (-0.04; 0.07)	-0.03 (-0.09; 0.03)	-0.01 (-0.07; 0.05)	-0.03 (-0.09; 0.03)
Extended[b]	-0.07 (-0.13; -0.01)	-0.03 (-0.09; 0.03)	0.03 (-0.03; 0.08)	-0.03 (-0.08; 0.03)	0.00 (-0.06; 0.06)	-0.01 (-0.07; 0.05)
Extended-Plus[c]	-0.06 (-0.12; 0.01)	-0.04 (-0.10; 0.03)	0.05 (-0.01; 0.11)	-0.02 (-0.09; 0.04)	0.01 (-0.05; 0.08)	0.00 (-0.06; 0.07)
NO_2 (µg/m^3)						
Discovery[a]	-0.02 (-0.07; 0.03)	0.01 (-0.04; 0.06)	0.00 (-0.04; 0.05)	0.00 (-0.05; 0.05)	0.01 (-0.03; 0.06)	-0.02 (-0.06; 0.03)
Extended[b]	-0.01 (-0.06; 0.04)	0.02 (-0.03; 0.06)	0.00 (-0.04; 0.05)	0.00 (-0.05; 0.05)	0.02 (-0.03; 0.07)	0.00 (-0.05; 0.05)
Extended-Plus[c]	0.00 (-0.05; 0.05)	0.01 (-0.04; 0.06)	0.02 (-0.03; 0.07)	0.00 (-0.05; 0.06)	0.03 (-0.02; 0.09)	0.01 (-0.04; 0.06)
NO_X (µg/m^3)						
Discovery[a]	-0.05 (-0.1; 0.01)	-0.02 (-0.07; 0.04)	0.01 (-0.04; 0.06)	-0.03 (-0.08; 0.03)	0.01 (-0.05; 0.06)	-0.01 (-0.06; 0.04)
Extended[b]	-0.03 (-0.09; 0.02)	-0.01 (-0.07; 0.04)	0.01 (-0.04; 0.06)	-0.02 (-0.08; 0.03)	0.02 (-0.04; 0.07)	0.01 (-0.05; 0.06)

Extended-Plus[c]	-0.02 (-0.08; 0.03)	-0.02 (-0.08; 0.04)	0.03 (-0.03; 0.08)	-0.02 (-0.08; 0.03)	0.03 (-0.03; 0.08)	0.02 (-0.04; 0.07)
$Dist_{majroad}$ (m) ≥100<200 vs ≥200						
Discovery[a]	0.02 (-0.18; 0.23)	0.20 (0.00; 0.40)	-0.01 (-0.20; 0.18)	0.09 (-0.11; 0.29)	0.18 (-0.02; 0.39)	-0.05 (-0.25; 0.15)
Extended[b]	0.03 (-0.17; 0.24)	0.21 (0.01; 0.41)	-0.01 (-0.20; 0.19)	0.09 (-0.12; 0.29)	0.19 (-0.02; 0.39)	-0.02 (-0.22; 0.18)
Extended-Plus[c]	0.04 (-0.16; 0.25)	0.21 (0.01; 0.41)	0.00 (-0.20; 0.19)	0.09 (-0.11; 0.29)	0.19 (-0.02; 0.39)	-0.01 (-0.22; 0.19)
$Dist_{majroad}$ (m) <100 vs ≥200						
Discovery[a]	0.04 (-0.19; 0.27)	0.19 (-0.03; 0.41)	0.11 (-0.10; 0.32)	0.22 (0.00; 0.44)	-0.07 (-0.30; 0.15)	-0.06 (-0.28; 0.16)
Extended[b]	0.03 (-0.20; 0.26)	0.20 (-0.02; 0.42)	0.10 (-0.12; 0.31)	0.19 (-0.04; 0.41)	-0.05 (-0.28; 0.18)	-0.05 (-0.27; 0.18)
Extended-Plus[c]	0.04 (-0.18; 0.27)	0.20 (-0.02; 0.42)	0.11 (-0.10; 0.33)	0.19 (-0.03; 0.41)	-0.04 (-0.27; 0.18)	-0.04 (-0.26; 0.19)
L_{night} (dB[A])						
Discovery[a]	0.03 (-0.06; 0.11)	0.00 (-0.09; 0.08)	-0.03 (-0.11; 0.05)	-0.02 (-0.1; 0.06)	-0.04 (-0.12; 0.05)	-0.01 (-0.10; 0.07)
Extended[b]	0.05 (-0.04; 0.13)	0.01 (-0.08; 0.09)	-0.03 (-0.11; 0.05)	-0.01 (-0.1; 0.07)	-0.03 (-0.12; 0.06)	0.01 (-0.08; 0.09)
Extended-Plus[c]	0.05 (-0.04; 0.14)	0.00 (-0.08; 0.09)	-0.03 (-0.11; 0.05)	-0.01 (-0.1; 0.07)	-0.03 (-0.11; 0.06)	0.01 (-0.08; 0.09)
L_{DEN} (dB[A])						
Discovery[a]	0.04 (-0.03; 0.10)	-0.01 (-0.07; 0.06)	-0.02 (-0.08; 0.04)	-0.02 (-0.08; 0.04)	-0.03 (-0.10; 0.03)	-0.02 (-0.08; 0.05)
Extended[b]	0.05 (-0.01; 0.12)	0.00 (-0.06; 0.07)	-0.02 (-0.08; 0.04)	-0.01 (-0.08; 0.05)	-0.03 (-0.09; 0.04)	0.00 (-0.06; 0.06)
Extended-Plus[c]	0.06 (-0.01; 0.12)	0.00 (-0.06; 0.07)	-0.02 (-0.08; 0.05)	-0.01 (-0.08; 0.05)	-0.02 (-0.09; 0.04)	0.00 (-0.06; 0.07)

Abbreviations: IQR, interquartile range; PM_{10}, particulate matter with aerodynamic diameter ≤10 µm; $PM_{2.5}$, particulate matter with aerodynamic diameter ≤2.5 µm; $PM_{2.5abs}$, $PM_{2.5}$ absorbance; PN_{AM}, accumulation mode particle number; NO_2, nitrogen dioxide; NO_X, any nitrogen oxide; $Dist_{majroad}$, distance to the nearest major road; L_{night}, nighttime mean noise (10pm-6am); L_{DEN}, 24h mean noise; SD, standard deviation

[a] The Discovery Model was adjusted for age, sex, and education level.

[b] In addition to the variables included in the Discovery model, the Extended Model was adjusted for education level, alcohol consumption, smoking status, cumulative pack-years, environmental tobacco smoke, and weekly calorie expenditure by performing regular physical activity.

[c] In addition to the variables included in the Extended model, the Extended-Plus Model was adjusted for neighborhood unemployment rate.

Table S3. Estimates of the individual neurocognitive test models of the Memory. Domain per IQR increase in mean exposure levels with increasing model adjustment among the Neuropsychological Tests group (n=615) of the 1000BRAINS study. From Nußbaum et al., 2019

Exposure / Adjustment Model	Cognitive Function – Memory		
	figural memory	verbal learning	verbal learning, delayed
PM_{10}(µg/m^3)			
Discovery[a]	-0.02 (-0.07; 0.02)	-0.02 (-0.07; 0.02)	-0.01 (-0.06; 0.04)
Extended[b]	-0.02 (-0.06; 0.02)	-0.01 (-0.06; 0.04)	0.00 (-0.05; 0.05)
Extended-Plus[c]	-0.02 (-0.07; 0.03)	0.00 (-0.05; 0.05)	0.01 (-0.05; 0.06)
$PM_{2.5}$ (µg/m^3)			
Discovery[a]	-0.05 (-0.10; 0.01)	-0.03 (-0.09; 0.02)	-0.01 (-0.07; 0.05)
Extended[b]	-0.04 (-0.09; 0.02)	-0.01 (-0.07; 0.04)	0.01 (-0.05; 0.06)
Extended-Plus[c]	-0.04 (-0.10; 0.02)	0.00 (-0.06; 0.07)	0.02 (-0.05; 0.09)
$PM_{2.5abs}$ (10^{-5}/m)			
Discovery[a]	-0.03 (-0.07; 0.01)	-0.04 (-0.08; 0.01)	-0.03 (-0.08; 0.01)
Extended[b]	-0.02 (-0.07; 0.02)	-0.02 (-0.07; 0.03)	-0.02 (-0.06; 0.03)
Extended-Plus[c]	-0.03 (-0.07; 0.02)	-0.01 (-0.06; 0.04)	-0.02 (-0.07; 0.04)
PN_{AM} (n/mL)			
Discovery[a]	-0.02 (-0.07; 0.03)	0.00 (-0.06; 0.06)	0.02 (-0.04; 0.08)
Extended[b]	-0.01 (-0.06; 0.04)	0.02 (-0.04; 0.07)	0.03 (-0.03; 0.09)
Extended-Plus[c]	-0.01 (-0.07; 0.05)	0.03 (-0.03; 0.09)	0.04 (-0.02; 0.11)
NO_2 (µg/m^3)			
Discovery[a]	0.00 (-0.05; 0.04)	-0.02 (-0.06; 0.03)	-0.02 (-0.06; 0.03)
Extended[b]	0.00 (-0.04; 0.05)	0.01 (-0.04; 0.05)	0.00 (-0.04; 0.05)
Extended-Plus[c]	0.01 (-0.04; 0.06)	0.01 (-0.04; 0.07)	0.01 (-0.04; 0.06)
NO_X (µg/m^3)			
Discovery[a]	-0.01 (-0.05; 0.04)	-0.01 (-0.06; 0.04)	0.00 (-0.06; 0.05)

Extended[b]	0.00 (-0.05; 0.05)	0.01 (-0.04; 0.07)	0.02 (-0.03; 0.07)
Extended-Plus[c]	0.01 (-0.05; 0.06)	0.03 (-0.03; 0.08)	0.03 (-0.03; 0.08)
$Dist_{majroad}$ (m) ≥100<200 vs ≥200			
Discovery[a]	-0.10 (-0.28; 0.08)	-0.11 (-0.31; 0.09)	-0.11 (-0.31; 0.09)
Extended[b]	-0.09 (-0.27; 0.10)	-0.07 (-0.26; 0.13)	-0.07 (-0.27; 0.13)
Extended-Plus[c]	-0.09 (-0.27; 0.10)	-0.06 (-0.26; 0.14)	-0.07 (-0.27; 0.13)
$Dist_{majroad}$ (m) <100 vs ≥200			
Discovery[a]	0.03 (-0.17; 0.23)	-0.01 (-0.23; 0.21)	-0.03 (-0.25; 0.19)
Extended[b]	0.02 (-0.18; 0.23)	0.02 (-0.20; 0.24)	0.00 (-0.22; 0.22)
Extended-Plus[c]	0.03 (-0.18; 0.23)	0.03 (-0.19; 0.25)	0.00 (-0.22; 0.23)
L_{night} (dB[A])			
Discovery[a]	-0.05 (-0.13; 0.02)	-0.04 (-0.12; 0.04)	-0.06 (-0.15; 0.02)
Extended[b]	-0.05 (-0.12; 0.03)	-0.01 (-0.09; 0.07)	-0.04 (-0.12; 0.05)
Extended-Plus[c]	-0.05 (-0.12; 0.03)	-0.01 (-0.09; 0.08)	-0.04 (-0.12; 0.05)
L_{DEN} (dB[A])			
Discovery[a]	-0.04 (-0.10; 0.02)	-0.03 (-0.10; 0.03)	-0.05 (-0.11; 0.01)
Extended[b]	-0.03 (-0.09; 0.02)	-0.01 (-0.07; 0.05)	-0.03 (-0.10; 0.03)
Extended-Plus[c]	-0.03 (-0.09; 0.03)	-0.01 (-0.07; 0.05)	-0.03 (-0.10; 0.03)

Abbreviations: IQR, interquartile range; PM_{10}, particulate matter with aerodynamic diameter ≤10 µm; $PM_{2.5}$, particulate matter with aerodynamic diameter ≤2.5 µm; $PM_{2.5abs}$, $PM_{2.5}$ absorbance; PN_{AM}, accumulation mode particle number; NO_2, nitrogen dioxide; NO_X, any nitrogen oxide; $Dist_{majroad}$, distance to the nearest major road; L_{night}, nighttime mean noise (10pm-6am); L_{DEN}, 24h mean noise; SD, standard deviation

[a] The Discovery Model was adjusted for age, sex, and education level.

[b] In addition to the variables included in the Discovery model, the Extended Model was adjusted for education level, alcohol consumption, smoking status, cumulative pack-years, environmental tobacco smoke, and weekly calorie expenditure by performing regular physical activity.

[c] In addition to the variables included in the Extended model, the Extended-Plus Model was adjusted for neighborhood unemployment rate

Table S4. Estimates of the individual neurocognitive test models of the Short Term/Working Memory Domain per IQR increase in mean exposure levels with increasing model adjustment among the Neuropsychological Tests group (n=615) of the 1000BRAINS study. From Nußbaum et al., 2019

Exposure / Adjustment Model	Cognitive Function – Short-Term/Working Memory				
	visual WM	visual spatial STM	visual spatial WM	verbal STM	verbal WM
PM_{10}($\mu g/m^3$)					
Discovery[a]	-0.02 (-0.07; 0.03)	0.05 (0.00; 0.10)	0.00 (-0.05; 0.05)	-0.03 (-0.08; 0.02)	-0.01 (-0.06; 0.04)
Extended[b]	-0.02 (-0.07; 0.02)	0.04 (-0.01; 0.10)	0.00 (-0.05; 0.05)	-0.03 (-0.08; 0.02)	-0.02 (-0.06; 0.03)
Extended-Plus[c]	-0.02 (-0.07; 0.03)	0.04 (-0.02; 0.10)	0.00 (-0.05; 0.06)	0.00 (-0.06; 0.06)	-0.01 (-0.06; 0.05)
$PM_{2.5}$ ($\mu g/m^3$)					
Discovery[a]	-0.03 (-0.09; 0.02)	0.06 (0.00; 0.12)	0.01 (-0.05; 0.07)	-0.06 (-0.12; 0.00)	-0.01 (-0.07; 0.04)
Extended[b]	-0.03 (-0.09; 0.03)	0.06 (0.00; 0.12)	0.02 (-0.04; 0.08)	-0.06 (-0.12; 0.00)	-0.01 (-0.07; 0.04)
Extended-Plus[c]	-0.02 (-0.09; 0.04)	0.06 (-0.01; 0.13)	0.03 (-0.04; 0.09)	-0.02 (-0.09; 0.05)	0.00 (-0.07; 0.06)
$PM_{2.5abs}$ (10^{-5}/m)					
Discovery[a]	-0.02 (-0.06; 0.03)	0.03 (-0.02; 0.08)	-0.01 (-0.06; 0.04)	-0.04 (-0.09; 0.01)	0.00 (-0.05; 0.04)
Extended[b]	-0.02 (-0.07; 0.03)	0.02 (-0.03; 0.07)	0.00 (-0.05; 0.04)	-0.03 (-0.08; 0.01)	0.00 (-0.05; 0.05)
Extended-Plus[c]	-0.01 (-0.06; 0.04)	0.01 (-0.04; 0.07)	0.00 (-0.06; 0.05)	-0.01 (-0.06; 0.05)	0.01 (-0.04; 0.07)
PN_{AM} (n/mL)					
Discovery[a]	-0.04 (-0.10; 0.02)	0.06 (0.00; 0.12)	0.03 (-0.03; 0.09)	-0.07 (-0.13; -0.01)	0.00 (-0.06; 0.06)
Extended[b]	-0.03 (-0.09; 0.03)	0.07 (0.01; 0.13)	0.04 (-0.02; 0.10)	-0.06 (-0.12; 0.00)	0.01 (-0.05; 0.07)
Extended-Plus[c]	-0.02 (-0.08; 0.04)	0.06 (0.00; 0.13)	0.05 (-0.01; 0.12)	-0.04 (-0.10; 0.03)	0.02 (-0.04; 0.08)
NO_2 ($\mu g/m^3$)					
Discovery[a]	-0.01 (-0.06; 0.03)	0.04 (0.00; 0.09)	0.02 (-0.03; 0.07)	-0.05 (-0.10; 0.00)	0.03 (-0.02; 0.08)
Extended[b]	-0.01 (-0.06; 0.04)	0.04 (-0.01; 0.09)	0.02 (-0.02; 0.07)	-0.05 (-0.10; 0.00)	0.04 (-0.01; 0.08)
Extended-Plus[c]	0.00 (-0.05; 0.05)	0.04 (-0.02; 0.09)	0.03 (-0.02; 0.08)	-0.03 (-0.08; 0.03)	0.05 (0.00; 0.10)
NO_X ($\mu g/m^3$)					
Discovery[a]	-0.04 (-0.09; 0.02)	0.06 (0.01; 0.12)	0.04 (-0.01; 0.10)	-0.06 (-0.11; 0.00)	0.03 (-0.03; 0.08)
Extended[b]	-0.03 (-0.08; 0.02)	0.06 (0.01; 0.12)	0.05 (-0.01; 0.10)	-0.06 (-0.11; 0.00)	0.03 (-0.02; 0.09)

Extended-Plus[c]	-0.03 (-0.08; 0.03)	0.06 (0.00; 0.12)	0.05 (0.00; 0.11)	-0.04 (-0.10; 0.02)	0.05 (-0.01; 0.10)
$Dist_{majroad}$ (m) ≥100<200 vs ≥200					
Discovery[a]	-0.08 (-0.28; 0.12)	-0.08 (-0.28; 0.13)	-0.09 (-0.29; 0.12)	-0.02 (-0.23; 0.19)	-0.13 (-0.33; 0.07)
Extended[b]	-0.06 (-0.26; 0.14)	-0.06 (-0.27; 0.15)	-0.08 (-0.29; 0.13)	-0.03 (-0.24; 0.19)	-0.14 (-0.34; 0.06)
Extended-Plus[c]	-0.05 (-0.25; 0.15)	-0.07 (-0.28; 0.14)	-0.08 (-0.29; 0.13)	-0.01 (-0.23; 0.20)	-0.13 (-0.33; 0.06)
$Dist_{majroad}$ (m) <100 vs ≥200					
Discovery[a]	0.22 (0.00; 0.43)	0.17 (-0.05; 0.40)	0.13 (-0.09; 0.36)	-0.02 (-0.25; 0.21)	0.09 (-0.13; 0.30)
Extended[b]	0.22 (0.00; 0.44)	0.15 (-0.08; 0.39)	0.12 (-0.11; 0.35)	-0.04 (-0.27; 0.20)	0.09 (-0.13; 0.31)
Extended-Plus[c]	0.23 (0.01; 0.45)	0.14 (-0.09; 0.38)	0.12 (-0.11; 0.35)	-0.01 (-0.25; 0.22)	0.10 (-0.12; 0.32)
L_{night} (dB[A])					
Discovery[a]	-0.08 (-0.16; 0.00)	-0.02 (-0.10; 0.07)	0.00 (-0.09; 0.08)	-0.03 (-0.12; 0.06)	-0.03 (-0.12; 0.05)
Extended[b]	-0.08 (-0.16; 0.01)	-0.02 (-0.11; 0.07)	0.00 (-0.09; 0.09)	-0.02 (-0.11; 0.07)	-0.03 (-0.11; 0.06)
Extended-Plus[c]	-0.08 (-0.16; 0.01)	-0.02 (-0.11; 0.06)	0 .00(-0.09; 0.09)	-0.02 (-0.11; 0.07)	-0.03 (-0.11; 0.06)
L_{DEN} (dB[A])					
Discovery[a]	-0.06 (-0.12; 0.00)	-0.02 (-0.09; 0.04)	-0.01 (-0.08; 0.05)	-0.03 (-0.10; 0.04)	-0.03 (-0.09; 0.03)
Extended[b]	-0.06 (-0.12; 0.01)	-0.03 (-0.09; 0.04)	-0.01 (-0.08; 0.06)	-0.02 (-0.09; 0.04)	-0.03 (-0.09; 0.03)
Extended-Plus[c]	-0.06 (-0.12; 0.01)	-0.03 (-0.09; 0.04)	-0.01 (-0.08; 0.06)	-0.02 (-0.09; 0.05)	-0.03 (-0.09; 0.04)

Abbreviations: IQR, interquartile range; WM, working memory; STM, short-term memory; PM_{10}, particulate matter with aerodynamic diameter ≤10 µm; $PM_{2.5}$, particulate matter with aerodynamic diameter ≤2.5 µm; $PM_{2.5abs}$, $PM_{2.5}$ absorbance; PN_{AM}, accumulation mode particle number; NO_2, nitrogen dioxide; NO_X, any nitrogen oxide; $Dist_{majroad}$, distance to the nearest major road; L_{night}, nighttime mean noise (10pm-6am); L_{DEN}, 24h mean noise; SD, standard deviation

[a] The Discovery Model was adjusted for age, sex, and education level.

[b] In addition to the variables included in the Discovery model, the Extended Model was adjusted for education level, alcohol consumption, smoking status, cumulative pack-years, environmental tobacco smoke, and weekly calorie expenditure by performing regular physical activity.

[c] In addition to the variables included in the Extended model, the Extended-Plus Model was adjusted for neighborhood unemployment rate.

Table S5. Estimates of the individual neurocognitive test models of the Language Domain per IQR increase in mean exposure levels with increasing model adjustment among the Neuropsychological Tests group (n=615) of the 1000BRAINS study. From Nußbaum et al., 2019

Exposure / Adjustment Model	Cognitive Function – Language				
	phonemic verbal fluency	+ concept shifting	semantic verbal fluency	+ concept shifting	vocabulary
PM_{10}(µg/m^3)					
Discovery[a]	-0.02 (-0.07; 0.03)	-0.01 (-0.06; 0.04)	-0.03 (-0.08; 0.02)	-0.04 (-0.09; 0.01)	-0.02 (-0.06; 0.03)
Extended[b]	-0.01 (-0.06; 0.04)	0.00 (-0.05; 0.05)	-0.03 (-0.07; 0.02)	-0.03 (-0.08; 0.01)	-0.01 (-0.05; 0.03)
Extended-Plus[c]	0.01 (-0.05; 0.06)	0.01 (-0.04; 0.07)	-0.02 (-0.07; 0.04)	-0.02 (-0.07; 0.04)	0.01 (-0.04; 0.06)
$PM_{2.5}$ (µg/m^3)					
Discovery[a]	-0.07 (-0.12; -0.01)	-0.05 (-0.11; 0.01)	-0.06 (-0.11; 0.00)	-0.06 (-0.12; 0.00)	-0.04 (-0.09; 0.01)
Extended[b]	-0.05 (-0.11; 0.01)	-0.03 (-0.08; 0.03)	-0.04 (-0.10; 0.02)	-0.04 (-0.10; 0.02)	-0.03 (-0.08; 0.02)
Extended-Plus[c]	-0.03 (-0.10; 0.04)	-0.02 (-0.08; 0.05)	-0.03 (-0.10; 0.03)	-0.02 (-0.08; 0.05)	0.00 (-0.06; 0.06)
$PM_{2.5abs}$ (10^{-5}/m)					
Discovery[a]	-0.04 (-0.09; 0.00)	-0.03 (-0.08; 0.02)	-0.03 (-0.08; 0.01)	-0.04 (-0.09; 0.00)	-0.04 (-0.08; 0.00)
Extended[b]	-0.03 (-0.08; 0.02)	-0.01 (-0.06; 0.03)	-0.02 (-0.07; 0.03)	-0.03 (-0.08; 0.02)	-0.03 (-0.07; 0.01)
Extended-Plus[c]	-0.01 (-0.07; 0.04)	0.00 (-0.06; 0.05)	-0.01 (-0.07; 0.04)	-0.01 (-0.07; 0.04)	-0.01 (-0.06; 0.03)
PN_{AM} (n/mL)					
Discovery[a]	-0.09 (-0.15; -0.03)	-0.06 (-0.12; 0.00)	-0.07 (-0.13; -0.01)	-0.05 (-0.11; 0.01)	-0.02 (-0.07; 0.03)
Extended[b]	-0.08 (-0.14; -0.02)	-0.04 (-0.10; 0.02)	-0.05 (-0.11; 0.01)	-0.03 (-0.09; 0.03)	-0.01 (-0.06; 0.04)
Extended-Plus[c]	-0.07 (-0.14; -0.01)	-0.04 (-0.10; 0.03)	-0.05 (-0.11; 0.02)	-0.01 (-0.07; 0.06)	0.01 (-0.04; 0.07)
NO_2 (µg/m^3)					
Discovery[a]	-0.04 (-0.08; 0.01)	-0.03 (-0.08; 0.02)	-0.04 (-0.09; 0.01)	-0.03 (-0.08; 0.02)	-0.01 (-0.05; 0.03)
Extended[b]	-0.02 (-0.07; 0.03)	-0.02 (-0.06; 0.03)	-0.02 (-0.07; 0.03)	-0.02 (-0.06; 0.03)	0.00 (-0.04; 0.04)
Extended-Plus[c]	-0.01 (-0.06; 0.04)	-0.01 (-0.06; 0.04)	-0.02 (-0.07; 0.03)	0.00 (-0.05; 0.05)	0.01 (-0.03; 0.06)
NO_X (µg/m^3)					
Discovery[a]	-0.04 (-0.10; 0.01)	-0.03 (-0.09; 0.02)	-0.06 (-0.11; -0.01)	-0.05 (-0.10; 0.01)	-0.01 (-0.06; 0.03)
Extended[b]	-0.03 (-0.08; 0.03)	-0.01 (-0.07; 0.04)	-0.05 (-0.10; 0.01)	-0.03 (-0.08; 0.02)	0.00 (-0.05; 0.04)
Extended-Plus[c]	-0.02 (-0.08; 0.04)	0.00 (-0.06; 0.05)	-0.04 (-0.10; 0.01)	-0.02 (-0.07; 0.04)	0.01 (-0.04; 0.06)

$Dist_{majroad}$ (m)					
≥100<200 vs ≥200					
Discovery[a]	0.03 (-0.18; 0.24)	-0.02 (-0.23; 0.18)	-0.16 (-0.36; 0.05)	-0.19 (-0.40; 0.01)	-0.02 (-0.20; 0.16)
Extended[b]	0.05 (-0.16; 0.26)	0.00 (-0.21; 0.20)	-0.14 (-0.34; 0.06)	-0.18 (-0.38; 0.02)	-0.02 (-0.20; 0.16)
Extended-Plus[c]	0.06 (-0.15; 0.26)	0.00 (-0.20; 0.21)	-0.14 (-0.34; 0.07)	-0.17 (-0.37; 0.03)	-0.01 (-0.19; 0.16)
$Dist_{majroad}$ (m)					
<100 vs ≥200					
Discovery[a]	-0.01 (-0.24; 0.22)	-0.04 (-0.27; 0.19)	0.12 (-0.11; 0.34)	0.15 (-0.07; 0.38)	-0.03 (-0.22; 0.17)
Extended[b]	-0.02 (-0.25; 0.21)	-0.08 (-0.30; 0.15)	0.10 (-0.12; 0.33)	0.13 (-0.09; 0.35)	-0.03 (-0.22; 0.17)
Extended-Plus[c]	-0.01 (-0.24; 0.22)	-0.07 (-0.29; 0.16)	0.11 (-0.11; 0.34)	0.14 (-0.08; 0.37)	-0.01 (-0.21; 0.18)
L_{night} (dB[A])					
Discovery[a]	-0.10 (-0.19; -0.02)	-0.05 (-0.13; 0.04)	-0.07 (-0.16; 0.01)	-0.05 (-0.14; 0.03)	-0.12 (-0.19; -0.05)
Extended[b]	-0.09 (-0.17; 0.00)	-0.02 (-0.11; 0.06)	-0.05 (-0.13; 0.04)	-0.03 (-0.11; 0.06)	-0.10 (-0.18; -0.03)
Extended-Plus[c]	-0.08 (-0.17; 0.00)	-0.02 (-0.11; 0.06)	-0.05 (-0.13; 0.04)	-0.03 (-0.11; 0.06)	-0.10 (-0.17; -0.03)
L_{DEN} (dB[A])					
Discovery[a]	-0.08 (-0.14; -0.01)	-0.04 (-0.11; 0.02)	-0.05 (-0.12; 0.01)	-0.04 (-0.11; 0.02)	-0.09 (-0.15; -0.04)
Extended[b]	-0.06 (-0.13; 0.00)	-0.02 (-0.09; 0.04)	-0.03 (-0.09; 0.03)	-0.02 (-0.08; 0.04)	-0.08 (-0.14; -0.02)
Extended-Plus[c]	-0.06 (-0.13; 0.00)	-0.02 (-0.09; 0.04)	-0.03 (-0.09; 0.04)	-0.02 (-0.08; 0.05)	-0.08 (-0.13; -0.02)

Abbreviations: IQR, interquartile range; PM_{10}, particulate matter with aerodynamic diameter ≤10 µm; $PM_{2.5}$, particulate matter with aerodynamic diameter ≤2.5 µm; $PM_{2.5abs}$, $PM_{2.5}$ absorbance; PN_{AM}, accumulation mode particle number; NO_2, nitrogen dioxide; NO_X, any nitrogen oxide; $Dist_{majroad}$, distance to the nearest major road; L_{night}, nighttime mean noise (10pm-6am); L_{DEN}, 24h mean noise; SD, standard deviation

[a] The Discovery Model was adjusted for age, sex, and education level.

[b] In addition to the variables included in the Discovery model, the Extended Model was adjusted for education level, alcohol consumption, smoking status, cumulative pack-years, environmental tobacco smoke, and weekly calorie expenditure by performing regular physical activity.

[c] In addition to the variables included in the Extended model, the Extended-Plus Model was adjusted for neighborhood unemployment rate.

Table S6. Estimates of IGI Models per IQR increase in mean exposure levels with increasing model adjustment among the MRI participant group (n=590) of the 1000BRAINS study. From Nußbaum et al., 2019

	IGI Regions					
	Left Hemisphere			Right Hemisphere		
Exposure / Adjustment Model	DLPFC	PCC/P	IPL	DLPFC	PCC/P	IPL
PM_{10} (µg/m^3)						
Crude[a]	-0.00 (-0.02; 0.01)	-0.01 (-0.03; 0.01)	0.00 (-0.01; 0.01)	-0.01 (-0.02; 0.01)	-0.02 (-0.03; 0.00)	-0.01 (-0.03; 0.00)
Base[b]	-0.00 (-0.01; 0.01)	-0.00 (-0.02; 0.01)	0.00 (-0.01; 0.01)	-0.01 (-0.02; 0.01)	-0.01 (-0.03; 0.01)	-0.01 (-0.02; 0.00)
Main[c]	-0.00 (-0.02; 0.01)	-0.01 (-0.03; 0.01)	-0.00 (-0.02; 0.01)	-0.01 (-0.02; 0.01)	-0.02 (-0.04; 0.00)	-0.02 (-0.03; 0.00)
$PM_{2.5}$ (µg/m^3)						
Crude[a]	-0.01 (-0.02; 0.01)	-0.01 (-0.03; 0.01)	0.00 (-0.01; 0.02)	-0.01 (-0.02; 0.01)	-0.01 (-0.03; 0.00)	-0.01 (-0.03; 0.00)
Base[b]	-0.00 (-0.02; 0.01)	-0.00 (-0.02; 0.02)	0.00 (-0.01; 0.02)	-0.01 (-0.02; 0.01)	-0.01 (-0.03; 0.01)	-0.01 (-0.03; 0.01)
Main[c]	-0.01 (-0.02; 0.01)	-0.01 (-0.03; 0.01)	-0.00 (-0.02; 0.01)	-0.01 (-0.03; 0.01)	-0.02 (-0.04; 0.00)	-0.02 (-0.04; 0.00)
$PM_{2.5abs}$ (10^{-5}/m)						
Crude[a]	-0.00 (-0.02; 0.01)	-0.01 (-0.02; 0.01)	0.00 (-0.01; 0.02)	-0.00 (-0.02; 0.01)	-0.01 (-0.03; 0.01)	-0.00 (-0.02; 0.01)
Base[b]	-0.00 (-0.01; 0.01)	-0.00 (-0.02; 0.01)	0.00 (-0.01; 0.02)	-0.00 (-0.02; 0.01)	-0.00 (-0.02; 0.01)	-0.00 (-0.01; 0.01)
Main[c]	-0.00 (-0.02; 0.01)	-0.01 (-0.03; 0.01)	0.00 (-0.01; 0.02)	-0.00 (-0.02; 0.01)	-0.01 (-0.03; 0.01)	-0.01 (-0.02; 0.01)
PN_{AM} (n/mL)						
Crude[a]	-0.01 (-0.02; 0.01)	-0.00 (-0.02; 0.02)	-0.00 (-0.02; 0.01)	-0.02 (-0.03; 0.00)	-0.01 (-0.03; 0.01)	-0.01 (-0.02; 0.01)
Base[b]	-0.01 (-0.02; 0.01)	-0.00 (-0.02; 0.02)	-0.00 (-0.02; 0.01)	-0.02 (-0.03; 0.00)	-0.01 (-0.03; 0.01)	-0.01 (-0.02; 0.01)
Main[c]	-0.01 (-0.03; 0.01)	-0.01 (-0.03; 0.02)	-0.00 (-0.02; 0.01)	-0.02 (-0.04; 0.00)	-0.01 (-0.04; 0.01)	-0.01 (-0.03; 0.01)
NO_2 (µg/m^3)						
Crude[a]	-0.01 (-0.02; 0.00)	-0.02 (-0.03; 0.00)	-0.00 (-0.02; 0.01)	-0.01 (-0.02; 0.01)	-0.02 (-0.04; 0.00)	-0.01 (-0.03; 0.00)
Base[b]	-0.01 (-0.02; 0.00)	-0.01 (-0.03; 0.01)	-0.00 (-0.01; 0.01)	-0.01 (-0.02; 0.01)	-0.01 (-0.03; 0.00)	-0.01 (-0.02; 0.00)
Main[c]	-0.01 (-0.02; 0.00)	-0.01 (-0.03; 0.00)	-0.00 (-0.02; 0.01)	-0.01 (-0.02; 0.01)	-0.02 (-0.04; 0.00)	-0.01 (-0.03; 0.00)
NO_X (µg/m^3)						
Crude[a]	-0.01 (-0.02; 0.00)	-0.02 (-0.04; 0.00)	-0.00 (-0.02; 0.01)	-0.01 (-0.02; 0.01)	-0.03 (-0.04; -0.01)	-0.02 (-0.03; 0.00)
Base[b]	-0.01 (-0.02; 0.01)	-0.01 (-0.03; 0.01)	-0.00 (-0.01; 0.01)	-0.01 (-0.02; 0.01)	-0.02 (-0.04; 0.00)	-0.01 (-0.03; 0.00)

Main[c]	-0.01 (-0.02; 0.01)	-0.02 (-0.04; 0.00)	-0.00 (-0.02; 0.01)	-0.01 (-0.02; 0.01)	-0.02 (-0.04; -0.01)	-0.02 (-0.03; 0.00)
$Dist_{majroad}$ (m) ≥100<200 vs ≥200						
Crude[a]	-0.01 (-0.07; 0.04)	-0.00 (-0.07; 0.07)	-0.05 (-0.10; 0.01)	-0.06 (-0.11; -0.01)	-0.06 (-0.13; 0.00)	-0.02 (-0.08; 0.04)
Base[b]	-0.01 (-0.06; 0.04)	-0.00 (-0.07; 0.07)	-0.05 (-0.10; 0.01)	-0.06 (-0.11; -0.01)	-0.07 (-0.14; 0.00)	-0.02 (-0.08; 0.03)
Main[c]	-0.01 (-0.06; 0.04)	0.00 (-0.07; 0.07)	-0.04 (-0.09; 0.01)	-0.06 (-0.12; -0.01)	-0.07 (-0.13; 0.00)	-0.02 (-0.08; 0.04)
$Dist_{majroad}$ (m) <100 vs ≥200						
Crude[a]	-0.05 (-0.10; 0.01)	-0.05 (-0.13; 0.03)	-0.01 (-0.06; 0.05)	-0.02 (-0.08; 0.03)	-0.03 (-0.11; 0.04)	-0.01 (-0.07; 0.06)
Base[b]	-0.04 (-0.10; 0.02)	-0.04 (-0.12; 0.04)	-0.01 (-0.06; 0.05)	-0.02 (-0.08; 0.04)	-0.02 (-0.09; 0.06)	-0.00 (-0.06; 0.06)
Main[c]	-0.03 (-0.09; 0.02)	-0.03 (-0.10; 0.05)	-0.00 (-0.06; 0.06)	-0.02 (-0.08; 0.04)	-0.01 (-0.09; 0.06)	-0.00 (-0.07; 0.06)
L_{night} (dB[A])						
Crude[a]	0.01 (-0.01; 0.03)	-0.02 (-0.05; 0.01)	0.01 (-0.01; 0.03)	0.02 (0.00; 0.05)	-0.02 (-0.05; 0.01)	0.01 (-0.02; 0.03)
Base[b]	0.01 (-0.01; 0.04)	-0.01 (-0.04; 0.01)	0.01 (-0.01; 0.03)	0.03 (0.00; 0.05)	-0.02 (-0.05; 0.01)	0.01 (-0.02; 0.03)
Main[c]	0.01 (-0.01; 0.04)	-0.01 (-0.04; 0.02)	0.01 (-0.01; 0.04)	0.03 (0.00; 0.05)	-0.02 (-0.05; 0.01)	0.01 (-0.02; 0.03)
L_{DEN} (dB[A])						
Crude[a]	0.01 (-0.01; 0.03)	-0.01 (-0.03; 0.01)	0.01 (-0.01; 0.02)	0.02 (0.00; 0.04)	-0.02 (-0.04; 0.00)	0.01 (-0.01; 0.02)
Base[b]	0.01 (-0.01; 0.03)	-0.01 (-0.03; 0.01)	0.01 (-0.01; 0.03)	0.02 (0.01; 0.04)	-0.01 (-0.03; 0.01)	0.01 (-0.01; 0.02)
Main[c]	0.01 (0.00; 0.03)	-0.01 (-0.03; 0.01)	0.01 (-0.01; 0.03)	0.02 (0.00; 0.04)	-0.01 (-0.03; 0.01)	0.01 (-0.01; 0.02)

Abbreviations: lGI, local Gyrification Index; IQR, interquartile range; DLPFC, dorsolateral prefrontal cortex; PCC/P, posterior cingulate cortex and precuneus; IPL, inferior parietal lobule; PM_{10}, particulate matter with aerodynamic diameter ≤10 µm; $PM_{2.5}$, particulate matter with aerodynamic diameter ≤2.5 µm; $PM_{2.5abs}$, $PM_{2.5}$ absorbance; PN_{AM}, accumulation mode particle number; NO_2, nitrogen dioxide; NO_X, any nitrogen oxide; $Dist_{majroad}$, distance to the nearest major road; L_{night}, nighttime mean noise (10pm-6am); L_{DEN}, 24h mean noise; SD, standard deviation

[a] The Crude Model included only the exposure variable.

[b] The Base Model was adjusted for age, sex, and education level.

[c] The Main Model was adjusted for age, sex, education level, alcohol consumption, smoking status, cumulative pack-years, environmental tobacco smoke, weekly calorie expenditure by performing regular physical activity, and neighborhood unemployment rate.

Danksagung

Diese Dissertation stellt das Ergebnis jahrelanger intensiver Arbeit dar. An dieser Stelle möchte ich mich bei jenen Menschen bedanken, die mich während dieser fordernden, aber auch außerordentlich bereichernden Phase meiner akademischen Laufbahn unterstützt haben.

Zu besonderem Dank bin ich meinen Professorinnen verpflichtet. Als erste und zweite Betreuerinnen haben mich Frau Prof. Svenja Caspers und Frau Prof. Barbara Hoffmann stets mit ihren Anregungen unterstützt. Doch auch Frau Dr. Christiane Jockwitz und Frau Sarah Lucht bin ich aufgrund ihrer Praxisanleitung sehr zu Dank verpflichtet.

Eine herausragende Stellung in jeglicher Hinsicht nehmen meine Familie und meine Freundin ein. Ohne Ihre liebevolle Fürsorge wäre diese Arbeit nicht zu dem Werk geworden, welches sie heute ist.

Letztendlich danke ich auch allen Probanden, die sich den Testungen unterzogen haben, auf denen meine Arbeit basiert. Nur durch Menschen wie sie, die sich freiwillig als Forschungssubjekte zur Verfügung stellen, ist wissenschaftlicher Fortschritt in der Medizin überhaupt erst möglich.